Space Radiobiology

10

Christine Elisabeth Hellweg, Carmen Arena, Sarah Baatout, Bjorn Baselet, Kristina Beblo-Vranesevic, Nicol Caplin, Richard Coos, Fabiana Da Pieve, Veronica De Micco, Nicolas Foray, Boris Hespeels, Anne-Catherine Heuskin, Jessica Kronenberg, Tetyana Milojevic, Silvana Miranda, Victoria Moris, Sébastien Penninckx, Wilhelmina E. Radstake, Emil Rehnberg, Petra Rettberg, Kevin Tabury, Karine Van Doninck, Olivier Van Hoey, Guillaume Vogin, and Yehoshua Socol

Learning Objectives

- To understand the difference between the origin and characteristics of Galactic Cosmic Rays, Solar Energetic Particles, and trapped radiation
- To understand the differences between the radiation environment in low Earth Orbit, in deep space, and on the surface of celestial bodies
- To understand the difference between deterministic codes and Monte Carlo codes for modeling radiation transport
- To understand the different steps in a Monte Carlo calculation for the radiation environment on a body
- To acquire awareness of human health issues associated with prolonged space missions
- To acquire an overview of possible acute, chronic, and late effects of space radiation
- To be able to list the organs that are mainly affected by space radiation
- To understand basic molecular mechanisms of biological effects induced by space radiation
- To learn about the importance as well as advantages and disadvantages of animal and cell culture models in space biology studies
- To consider the importance of plant models in space biology studies
- To get knowledge on existing ground facilities to simulate the space environment
- To get acquainted to the advantages and inherent limitations of ground facilities

Fabiana Da Pieve is currently employed by the European Research Council Executive Agency, European Commission, BE-1049 Brussels, Belgium. The views expressed are purely those of the authors and may not in any circumstances be regarded as stating an official position of the European Commission.

C. E. Hellweg
Radiation Biology Department, Institute of Aerospace Medicine, German Aerospace Center (DLR), Cologne, Germany
e-mail: christine.hellweg@dlr.de

C. Arena
Department of Biology, University of Naples Federico II, Naples, Italy
e-mail: c.arena@unina.it

S. Baatout
Institute of Nuclear Medical Applications, Belgian Nuclear Research Centre (SCK CEN), Mol, Belgium
e-mail: sarah.baatout@sckcen.be

B. Baselet
Radiobiology Unit, Belgian Nuclear Research Center (SCK CEN), Mol, Belgium
e-mail: bjorn.baselet@sckcen.be

K. Beblo-Vranesevic · P. Rettberg
Radiation Biology Department, Astrobiology, Institute of Aerospace Medicine, German Aerospace Center, Cologne, Germany
e-mail: kristina.beblo@dlr.de; petra.rettberg@dlr.de

© The Author(s) 2023
S. Baatout (ed.), *Radiobiology Textbook*, https://doi.org/10.1007/978-3-031-18810-7_10

N. Caplin
Human Spaceflight and Robotic Exploration, European Space Agency, Noordwijk, The Netherlands
e-mail: Nicol.Caplin@esa.int

R. Coos
Laboratory of Analysis by Nuclear Reactions, University of Namur, Namur, Belgium
e-mail: richard.coos@unamur.be

F. Da Pieve
European Research Council Executive Agency, European Commission, Brussels, Belgium

Royal Belgian Institute for Space Aeronomy, Brussels, Belgium
e-mail: fabiana.dapieve@aeronomie.be

V. De Micco
Department of Agricultural Sciences, University of Naples Federico II, Naples, Italy
e-mail: demicco@unina.it

N. Foray
Inserm Unit 1296 "Radiation: Defense, Health, Environment", Lyon, France
e-mail: nicolas.foray@inserm.fr

B. Hespeels
Namur Research Institute for Life Sciences, Institute of Life-Earth-Environment and Research Unit in Environmental and Evolutionary Biology, University of Namur (UNamur), Namur, Belgium
e-mail: boris.hespeels@unamur.be

A.-C. Heuskin
Namur Research Institute for Life Sciences, Laboratory of Analysis by Nuclear Reactions, University of Namur (UNamur), Namur, Belgium
e-mail: anne-catherine.heuskin@unamur.be

J. Kronenberg
Radiation Biology Department, Cellular Biodiagnostics, Institute of Aerospace Medicine, German Aerospace Center, Cologne, Germany
e-mail: jessica.kronenberg@dlr.de

T. Milojevic
Space Biochemistry Group, Department of Biophysical Chemistry, University of Vienna, Vienna, Austria
e-mail: tetyana.milojevic@univie.ac.at

S. Miranda · W. E. Radstake
Department of Molecular Biotechnology, Ghent University, Ghent, Belgium

Radiobiology Unit, Belgian Nuclear Research Center (SCK CEN), Mol, Belgium
e-mail: sfdsmira@sckcen.be; eline.radstake@sckcen.be

V. Moris
Research Unit in Environmental and Evolutionary Biology (URBE), University of Namur (UNamur-LEGE), Namur, Belgium

Research Unit in Molecular Biology and Evolution (MBE), Department of Biology, Université Libre de Bruxelles, Brussels, Belgium

S. Penninckx
Medical Physics Department, Hôpital Universitaire de Bruxelles (H.U.B.), Université Libre de Bruxelles, Brussels, Belgium
e-mail: sebastien.penninckx@bordet.be

E. Rehnberg
Radiobiology Unit, Belgian Nuclear Research Centre, SCK CEN, Mol, Belgium

Department of Molecular Biotechnology, Ghent University, Ghent, Belgium
e-mail: emil.rehnberg@sckcen.be

K. Tabury
Department of Biomedical Engineering, University of South Carolina, Columbia, SC, United States of America

Radiobiology Unit, Belgian Nuclear Research Centre, SCK CEN, Mol, Belgium
e-mail: kevin.tabury@sckcen.be

K. Van Doninck
Research Unit in Environmental and Evolutionary Biology (URBE), University of Namur (UNamur-LEGE), Namur, Belgium

Université Libre de Bruxelles, Molecular Biology and Evolution, Brussels, Belgium
e-mail: karine.van.doninck@ulb.be

O. Van Hoey
Research in Dosimetric Applications Unit, Belgian Nuclear Research Centre, SCK CEN, Mol, Belgium
e-mail: olivier.van.hoey@sckcen.be

G. Vogin
Centre Francois Baclesse, University of Luxembourg and Luxembourg Institute of Health, Luxembourg, Luxembourg
e-mail: Guillaume.vogin@baclesse.lu

Y. Socol (✉)
Jerusalem College of Technology, Jerusalem, Israel
e-mail: socol@jct.ac.il

10.1 Introduction

Experiments in space provided us with new insights into radiation biology. This chapter is organized as follows. First, we present a historical overview of the field that can be traced to the first experiments at the Eiffel tower. Then, we overview the space radiation environment and mathematical models used to describe it. Later in this chapter, we present a macroscopic picture of health effects in humans (observed or anticipated in the space environment). Afterward, we turn to a microscopic level and describe biomolecular changes introduced by space radiation. Then, we describe experimental evidence obtained from models—small animals, plants, eukaryotic cells, and extremophiles (organisms living under conditions extreme from a human point of view). Finally, we present an overview of ground-based facilities mimicking the space environment.

10.2 History of Space Radiation Studies and Space Radiobiology

10.2.1 From Earth Ground to the Eiffel Tower

Human space travels were very early the concerns of a number of scientists like Johannes Kepler who warned that extra-terrestrial trips would require ships fit to withstand the breezes of heaven [1]. The development of electroscopes manufactured by Pierre Curie made the assessment of local currents possible due to any particle crossing the two metallic plates [2]. The Italian physicist Domenico Pacini suggested in 1910 that the background noise measured with the Curie electroscopes was caused by radiation emitted from the Earth ground [3]. By performing some experiments with the Curie electroscope at the Eiffel tower, Theodor Wulf, a Jesuit priest, demonstrated that half of the radiation emitted by the Earth ground disappears at a height of 300 m. When the technology of balloons was safe, Victor Hess observed that the ionization density of the atmosphere progressively decreases up to 1000 m, but increases above 1800 m, suggesting the existence of two components of natural radiation: one from the Earth ground, the other from space, "cosmic rays" [4]. In 1936, Hess was awarded the Nobel Prize in physics for his discoveries [5].

10.2.2 From the Eiffel Tower to the Balloon Experiments

Between the 1930s and the 1940s, there were considerable advances in the technology of particle counters and in the knowledge of particle physics; thanks to balloon experiments, new clues were brought to support that cosmic rays consist of very energetic (10^8–10^{20} eV) particles. Furthermore, data hinted an unexpectedly high proportion of the iron-associated elements in the galactic cosmic radiation (GCR). The latter observation led to the hypothesis of the nucleosynthesis origin of cosmic rays [3]. Figure 10.1 shows the advances in space radiation biology since that period.

10.2.3 From the Balloon Experiments to Artificial Satellites

The pioneer works of William Gilbert, Carl Friedrich Gauss, and Henri Poincaré about magnetism suggested that charged particles may be influenced by the Earth's magnetism and that a ring current should exist around the Earth. At the end of the 1950s and overall in the 1960s, the number of artificial satellites increased drastically and permitted to verify these hypotheses. In 1958, James Van Allen and Louis A. Frank

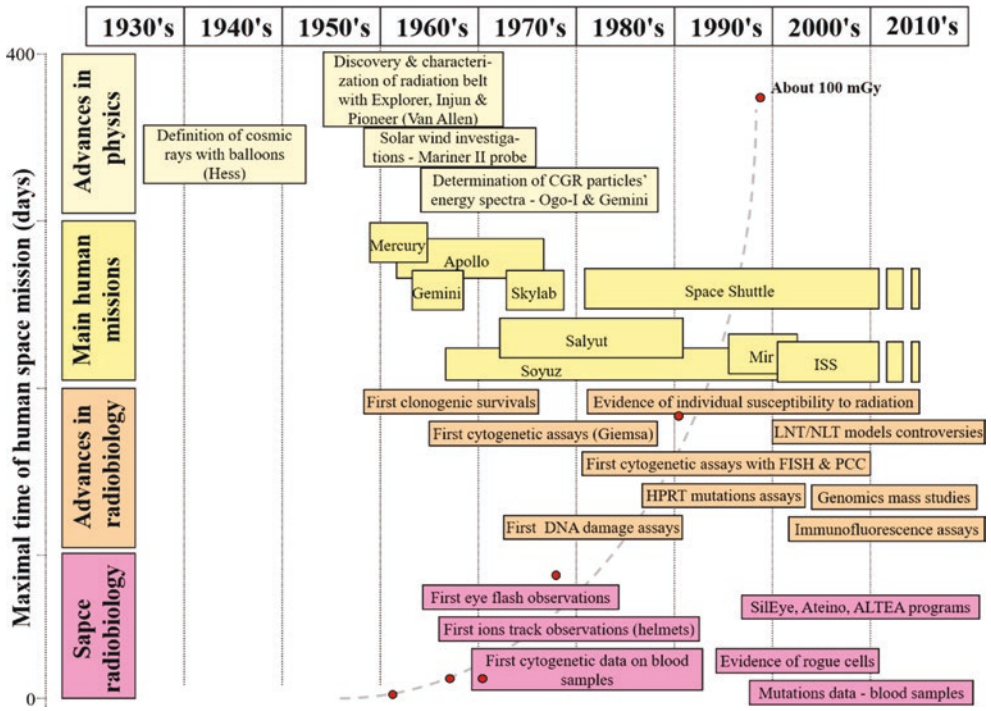

Fig. 10.1 Synopsis of advances in space radiation biology. The continuous increase of space mission duration up to 400 days is illustrated by the grey line on the left. For Mercury, Gemini, Apollo, Salyut, Skylab, and Mir missions, the maximum dose values are given as red dots [6]. *ALTEA* anomalous long-term effects on astronauts, *FISH* fluorescence in situ hybridization, *HPRT* hypoxanthine guanine phosphoribosyl transferase, *ISS* International Space Station, *LNT* linear no-threshold, *NLT* nonlinear threshold, *PCC* premature chromosome condensation, *SilEye* silicon eye. (Reprinted with permission from Maalouf et al. [6])

pointed out the existence of the Earth's radiation belt, based on data collected by the Explorer I and Pioneer IV satellites. Protons and electrons were found to be the major constituents of the Van Allen belt [7, 8]. In the same decade, Mariner II provided important data about the solar wind that permitted to document our knowledge on the radiation component from our Sun [9].

10.2.4 From Artificial Satellites to Manned Missions

During short-term (less than 2 weeks) missions in the 1960s at low Earth orbit (LEO), astronauts were exposed to several mGy at an average dose rate of about 0.17 μGy/min (245 μGy/mission day). This dose was delivered discontinuously as (1) the inner and outer zones of the Van Allen radiation belt contain protons and electrons of differing energy spectra that result in different secondary particles at dose rates different and energies; (2) the South Atlantic Anomaly (SAA), the area where the inner Van Allen radiation belt is the closest to the Earth surface, leading to an impressive flux of protons and electrons is passed about 15 times a day; here the dose rate can increase sixfold resulting in a significant contribution to the radiation exposure; and (3) unpredicted solar particle events (SPE) can increase the total dose, while the protection in LEO is still sufficient to prevent life-threatening acute radiation syndrome (see Sect. 10.6.2.1).

The characterization of individual heavy cosmic particles of high-energy and high atomic number—*Z*—(HZE) was performed with different physical radiation detectors (nuclear emulsions, plastics, silver chloride (AgCl) crystals, and lithium fluoride (LiF) thermoluminescence dosimeters) for the first time in space in the Biostack experiments flown aboard Apollo 16 and 17 (see Sect. 10.5). In parallel, their biological effects were examined in different biological objects such as bacterial spores, protozoa cysts, plant seeds, shrimp eggs, and insect eggs investigating various radiobiological end-points [10].

Examples of short-term experiments of up to 2 weeks in LEO combining radiation dosimetry and biological investigations were loaded on Space Shuttles (e.g., STS 9, 42, 45, 65), on free-flying satellites (e.g., LDEF, EURECA, BIOPAN 1–6) and on the MIR space station (Perseus mission). Later on, similar long-term experiments were performed on the International Space Station (ISS) (EXPOSE-E, -R, -R2) [11, 12].

"Cytogenetics observations revealed for the first time the major biological consequences of an exposure to space radiation: the yield of chromosome breaks seemed to increase after flight, but statistical significance was still needed (see Sect. 10.4.2.2). Data from eye flashes and helmets (see Sect. 10.4.2.3) suggested the existence of a certain "hidden part" of the heavy ions' component, probably due to secondary particles generated by the interaction of very high-energy particles with metallic materials. The contribution of these heavy ions to the total dose of radiation remained unknown at the end of the 1960s" [6].

10.2.5 From One Space Station to Another

Space experiments in combination with ground-based research (see Sect. 10.10) enabled a better understanding of the effects of space radiation and microgravity on human cells, microbes, and other biological models such as the roles of different complementary DNA repair mechanisms, the reactive oxygen species detoxification system and the intracellular accumulation of compatible solutes summarized, e.g., in Senatore et al. [13]. The modern picture of the space radiation dosimetry and its effects on human cells may be summarized as following [6]:

1. The energy spectrum of space particles and the dose spacecraft crews are exposed to can be quantified precisely by active and passive dosimetry. The dose delivered by secondary particles and countermeasures to reduce it require further investigations into the interaction of space radiation with a diversity of materials and in a complex spacecraft geometry.
2. Epidemiological studies for estimating hazards due to space radiation exposure are hampered by the small astronaut population, the individual radiation susceptibility, and radiation exposure history of each astronaut. International collaboration integrating different astronaut cohorts may help in overcoming these restrictions.
3. "Cytogenetic data undoubtedly revealed that space radiation exposure produces significant damage in cells. However, our knowledge of the basic mechanisms specific to heavy ion and low-dose and repeated exposures, and of adaptive responses is still incomplete. Furthermore, experiments about genomic instability and delayed mutagenesis may help in quantifying the risk of potential space radiation-induced cancer. The application of new radiobiological techniques may help in progressing in this field."

10.3 Space Radiation Environment

10.3.1 Origin and Nature of Space Radiation

Space is permeated with radiation, both electromagnetic radiation and particles with mass. Electromagnetic radiation in space spans many wavelengths, from long wavelength radio waves to very short-wavelength gamma rays. Gamma rays, X-rays, and some far/extreme ultraviolet (UV) waves, which can be generated for example during some transient

events on the Sun [14], are actually ionizing radiation. The wavelengths of UV, X-, and gamma rays are all shorter than those of visible light. The majority of these rays are absorbed by the Earth's atmosphere. The extraterrestrial solar UV radiation ranges from vacuum UV (wavelength <200 nm) to UVA (320–400 nm). The ozone layer absorbs some, but not all, of these types of UV radiation: UVA is not absorbed by the ozone layer, UVB (wavelength: 290–320 nm) is mostly absorbed by the ozone layer, but some does reach the Earth's surface, while UVC (wavelength: 100–290 nm) is completely absorbed by the ozone layer and atmosphere. Overall, the electromagnetic radiation reaching the Earth's surface encompasses radio waves, some microwaves, some infrared light, UVB and UVA radiation, and visible light. Of the light that reaches Earth's surface, infrared radiation makes up 49.4% while visible light provides 42.3%. UV radiation makes up just over 8% of the total solar radiation. UVA and UVB radiation contribute not only to premature aging of the skin but also to some serious health effects such as skin cancer, cataracts, and suppression of the immune system.

Generally however the expression "space radiation" mainly refers to radiation consisting of particles with a mass. There are three main radiation populations in space: galactic cosmic rays (intra- and extragalactic; GCR), solar radiation (including both the Solar Energetic Particles, SEP, and solar wind), and trapped radiation. A schematic representation of these radiation types and the environment which they can influence is given in Fig. 10.2.

10.3.1.1 Galactic Cosmic Rays (GCRs)

GCRs are constantly present highly energetic radiation in space. Their intensity is slowly varying and low with a few particles per second traversing an area of a cm^2 to a m^2 or more. They are nearly isotropic, meaning that they impinge from all directions. They originate from outside the heliosphere, most likely from deep space high-energy phenomena [16], such as supernova shock waves throughout the Galaxy, and also possibly from stellar wind termination shocks, pulsars, or other more exotic objects. They are composed of 98% baryons, of which 87% protons (hydrogen ions), 12% helium ions (α-particles), and 1–2% high-energy and highly charged ions, called High charge *Z* and Energy (HZE) particles, and 1% electrons and positrons [17]. HZE comprises ions from $Z = 3$ (Li) to $Z = 28$ (Ni). The most common elements are C, O, Mg, Si, and Fe ions (Fig. 10.3). Ions heavier than Ni can be encountered, yet these are very rare.

The spectrum of the GCRs is influenced by periodical, long-term, and short-term effects. Also, the Sun's behavior is periodical and follows an 11-year cycle which affects the interplanetary medium. The increased solar and heliospheric magnetic fields during the maximum phase of the solar cycle partially shield the solar system and decrease the low-energy portion of the GCRs flux, by preventing it from entering the inner heliosphere [18], while at solar minimum the reduced interplanetary magnetic field strength implies a more intense GCRs population [19]. The GCR flux is thus inversely proportional to the solar activity and decreases by a factor of 2–4 when moving from solar minimum to solar maximum,

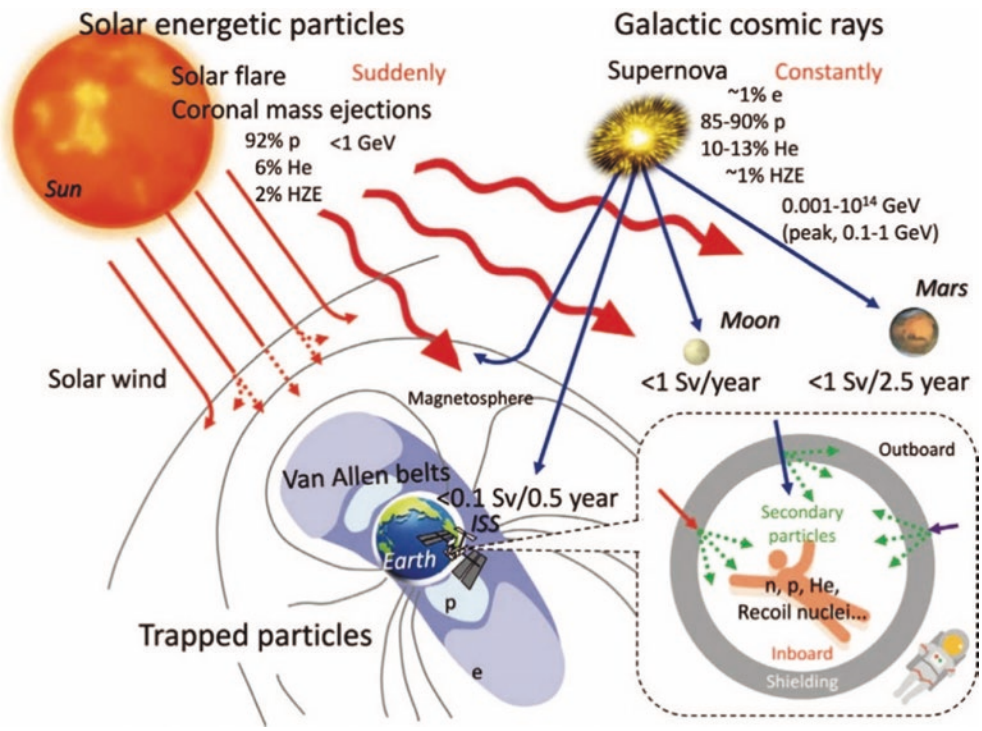

Fig. 10.2 Radiation environment during a space mission. (Image courtesy by ESA and reprinted from Chancellor et al. [15] with permission under Creative Commons Attribution-NonCommercial-NoDerivatives License: http://creativecommons.org/licenses/by-nc-nd/4.0/)

depending on the depth of the solar minimum and the intensity of the solar maximum [20, 21].

The modulation of the GCR flux for different ions is reported for the period of solar maximum and minimum. In the short term, GCRs can also be reduced by intense release of high-energy particles (mostly protons) during transient solar eruptions [22] (see Sect. 10.3.1.2). The energy spectrum of GCRs covers a huge range of energies: it commences at about 10^7–10^8 electron volt (eV) (10–100 MeV), and the most energetic *cosmic rays* reach up to 10^{20} eV (Fig. 10.4). A prominent feature is a so-called knee, with an energy of about 2.7–3.1 PeV (PeV = 10^{15} eV). This energy originated from the diffusive shock acceleration from the Galactic supernova remnants. The so-called anide or ankle, with an energy of about 5×10^{18} eV, is another characteristic of the energy spectrum. It is believed to mark the lower end of the energy of ultra-high energy GCRs, those that originate from extragalactic sources [24].

When traversing Earth's atmosphere, GCRs induce nuclear-electromagnetic-muon cascade reactions resulting in ionization of atmospheric molecules and generation of secondary particles [25, 26]. A small fraction of the initial primary particles, together with secondary particles of sufficient energy, reaches the ground. The maximum in secondary particle energy release (Pfötzer maximum) occurs at altitudes of 15–26 km depending on latitude and solar activity level. The radiation reaching the Earth's surface has levels similar to other low levels of radiation that humans are frequently exposed to. The average yearly exposure of a person is around 3.5 millisieverts (mSv). About half of this dose can be attributed to artificial sources (X-ray, computer tomography (CT) scan, mammography), while the other half originates from natural sources, including around 10% from cosmic radiation.

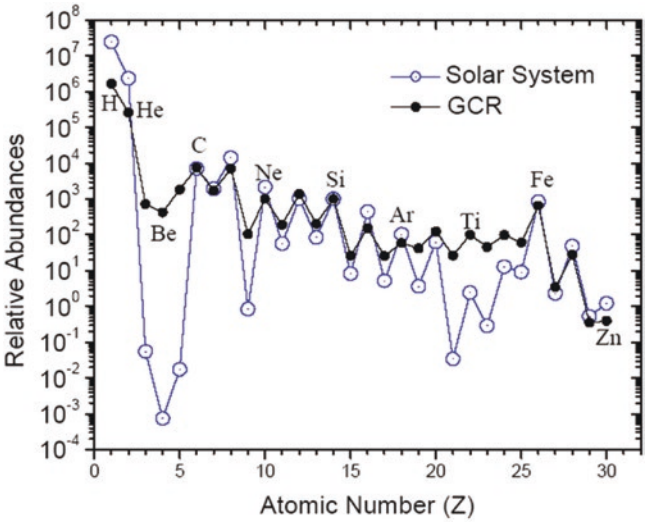

Fig. 10.3 GCR composition, as based on data from NASA's Advanced Composition Explorer (ACE) spacecraft. (Reprinted with permission from http://www.srl.caltech.edu/ACE/ACENews/ACENews83.html)

10.3.1.2 Solar Energetic Particles (SEPs)

SEPs originate from transient events on the Sun and come as massive injections of mostly protons and electrons (and to lesser extent helium (~4%) and heavier ions), with typical energies from ten to hundreds of MeV [27]. These transient events are Sun eruptions such as flares and Coronal Mass Ejections (CMEs). Characteristically, a flare lasts only minutes to hours and is the result of an explosive energy release from the Sun's coronal magnetic field. Also, the electromag-

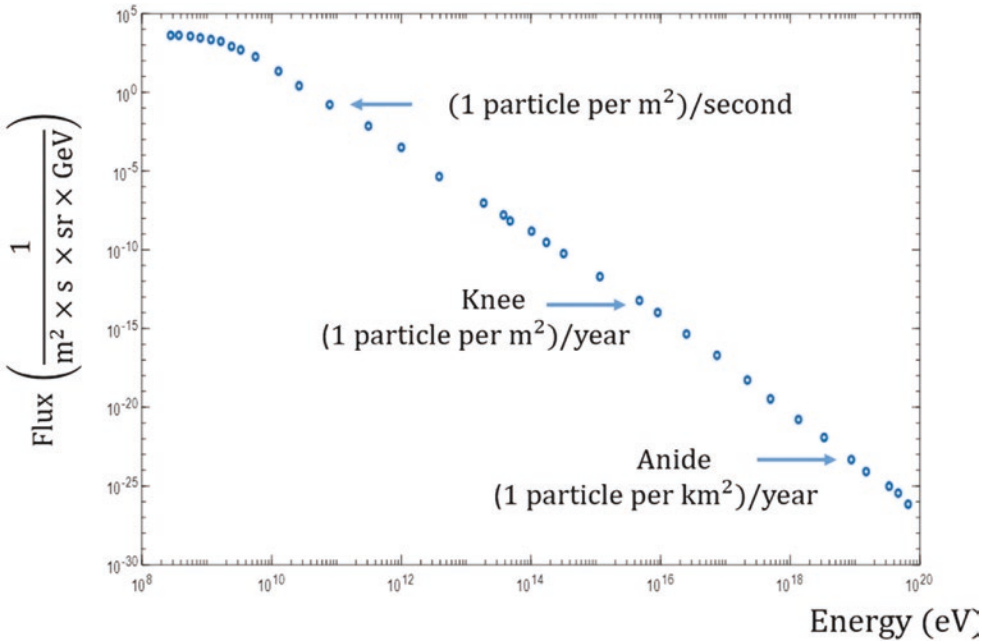

Fig. 10.4 GCR overall average fluxes versus energy. (Data from Beatty et al. [23])

netic flux increases, particularly in the short-wavelength (Extreme ultraviolet—XUV, gamma ray) range, and also in the radio regime. Usually originating in active regions, CMEs are large-scale plasma-magnetic structures with high speeds (up to thousands of km/s) associated with prominence eruptions and flares.

The likelihood of CME events increases with the power and size of the related flare event, although not all CMEs are associated with flares. Such events extend from several hours to a few days, and they have a higher likelihood of occurring during solar maximum. The level of the Sun's activity is fairly described by the number of sunspots, which provides an indication of the phases of the cycle. The number of spots increases toward the solar maximum, while during solar minimum the Sun's surface is almost spotless. Nevertheless, such SEPs events are hardly predictable and can also occur during solar minimum. Examples of an active region, an initial flare, and then a prominent eruption initiating a CME is shown for the 28/10/2003 event as part of the "Halloween Storms of 2003" in Fig. 10.5, with the related sudden increase in proton flux as detected by the Geostationary Operational Environmental Satellite (GOES) satellite (Fig. 10.6a). Examples of fluences (integral of the flux over the period of the event) related to major SEP events are shown in Fig. 10.6b.

A classification exists between Impulsive SEP events, which are short (≤1 day), numerous (~1000/year in periods of high activity), and of low intensity, and gradual events, which are long (several days at energies of a few MeV/nucleon), rather rare (a few tens per year), characterized by orders of magnitude higher protons fluences than impulsive events and ascribed to acceleration by CME-driven shocks as they propagate through the heliosphere. There is however some debate about the role played by "flare acceleration" in these events [29, 30].

Contrary to GCRs, SEP events can be considered mostly inducing deterministic effects (Sects. 10.4.2 and 10.6.2). Deterministic effects are those certainly occurring once a specific threshold dose has been overpassed. The high-intensity SEP flux can significantly increase the absorbed dose to astronauts, for example, during extravehicular activities (EVA) at the ISS, or eventually, if the event is characterized by a "hard" spectrum with a strong high-energy component, also during both interplanetary mission or missions on thin atmosphere such as Mars. Acute radiation syndrome (ARS), sickness, or, in extreme cases, death after a lethal dose can occur [31].

A comparison between GCR and SPE can be found in Table 10.1 (adapted from NASA Space Flight Human System Standards—NASA Standard 3001).

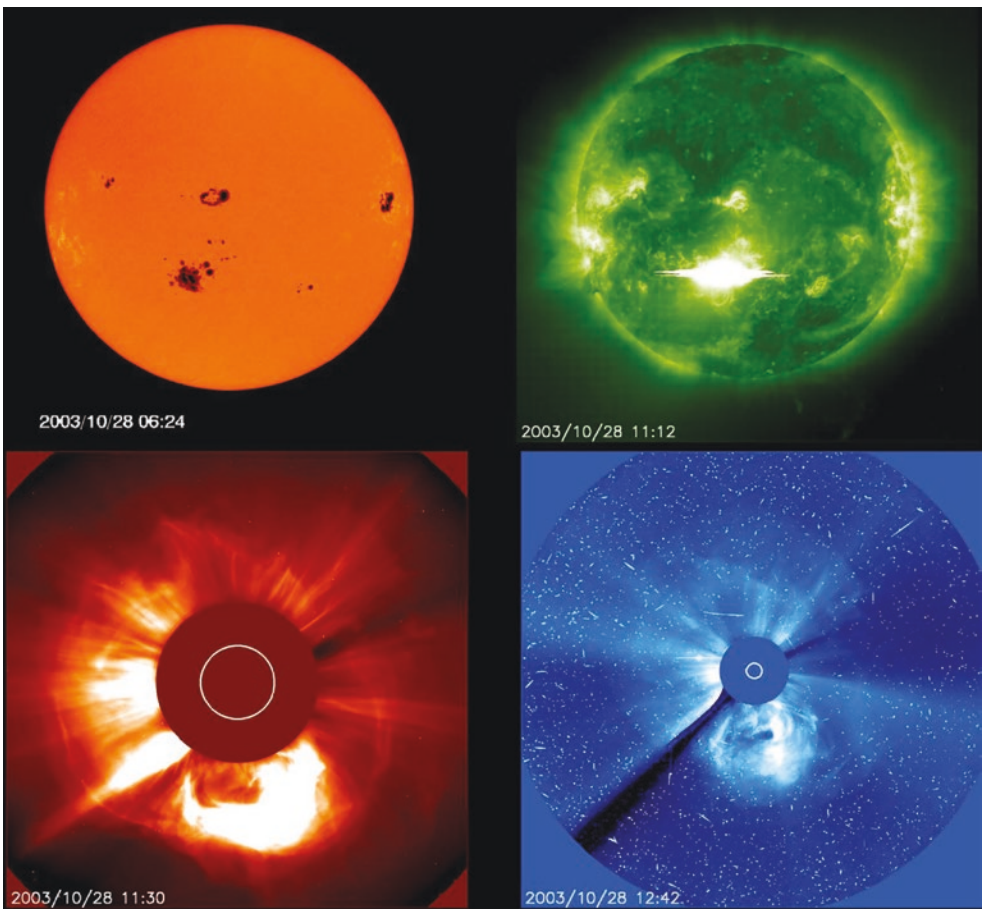

Fig. 10.5 The active regions (upper left), solar flare (upper right), and coronal mass ejections (CME, lower left and right) of the 28/10/2003 event captured by the Solar and Heliospheric Observatory (SOHO) satellite. The CME was imaged by the Large Angle and Spectrometric COronagraph (LASCO) instrument by blocking the light from the solar disk. (Courtesy of SOHO/EIT and SOHO/LASCO consortium. SOHO is a project of international cooperation between ESA and NASA)

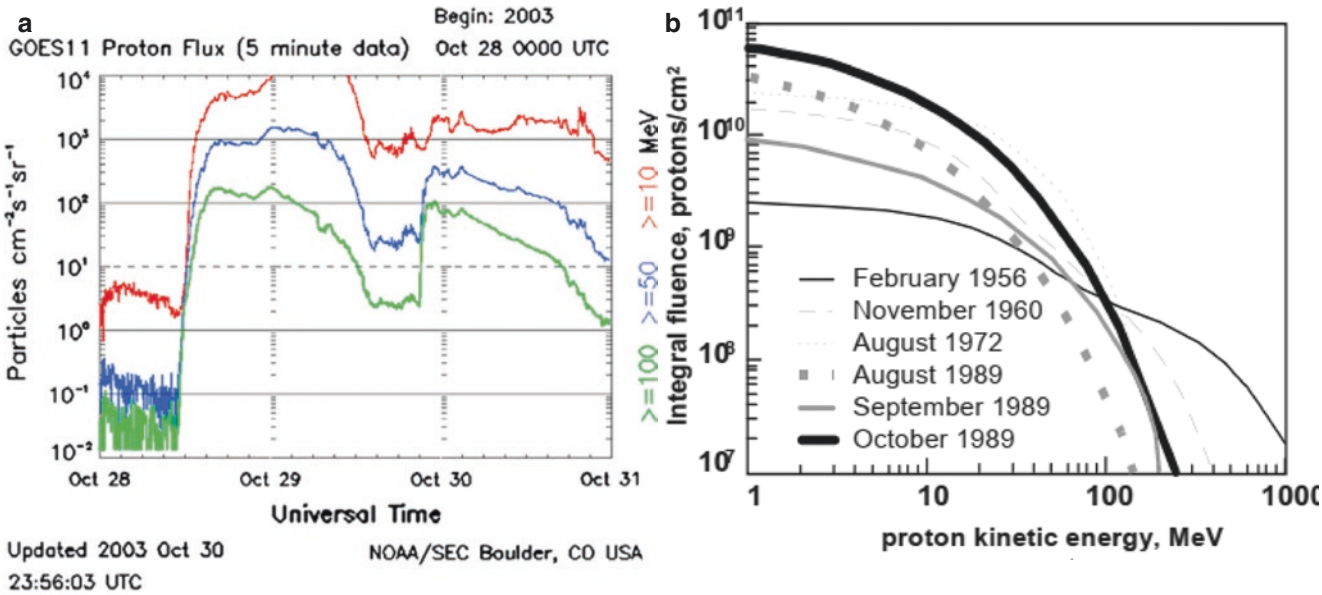

Fig. 10.6 (**a**) Proton flux between 28 and 31 October 2003. The 5-min averaged integral proton flux for energy thresholds of >10 (red line), >50 (blue line), and >100 MeV (green line) was measured by the primary Geostationary Operational Environmental Satellite (GOES) satellite of the Space Weather Prediction Center (SWPC). *CO* Colorado, *MeV* Mega electron volt, *NOAA* National Oceanic and Atmospheric Administration, *s* second, *sr* steradian, *UTC* Coordinated Universal Time. Reprinted with permission under terms of the Creative Commons Attribution License [28]. (**b**) Distribution in the energy of proton fluences for major past SEPs events (free space). (Reprinted with permission from: The space radiation environment: an introduction. Schimmerling W. https://three-jsc.nasa.gov/concepts/SpaceRadiationEnviron.pdf. Date posted: 2-5-2011)

Table 10.1 Comparison of GCR and SPE

	GCR	SPE
Spatial distribution	Isotropic beyond terrestrial influence (no preferred direction of arrival)	Non-isotropic at onset, later becoming diffused through the solar system
Composition	Protons (~87%) and helium ions (~12%) with the remainder consisting of HZE (1–2%)	Mostly protons
Temporal variations	Chronic	Acute
Energy	Extending to at least 10^{17} eV in some cases (much greater maximum than solar particles)	About 10^{10} eV highest recorded
Origin	Theories only; supernova explosions, neutron stars, pulsars, or other sources	Active regions of flares on the Sun, CMEs
Flux density	Relatively low: about 2 particles/cm²/s of all energies	Very high: may be as high as 10^6 particles/cm²/s
Biological effects	Primarily genotoxic and mutagenic with some vital cell destruction	Primarily acute damages, possible sudden illness, incapacitation, or death

Adapted from https://msis.jsc.nasa.gov/sections/section05.htm#_5.7_RADIATION

10.3.1.3 Solar Wind

The solar wind is a continuous flow of plasma from the Sun's corona, mainly consisting of protons, electrons with a small percentage of He ions, with kinetic energies between 0.5 and 10 keV. There are also some trace amounts of heavy ions and atomic nuclei such as C, N, O, Ne, Mg, Si, S, and Fe. Their energy results from the high temperature of the Sun's corona and allows them to escape the Sun's gravity. The flux of the solar wind varies over time, solar longitude and latitude, together with its temperature, density, and speed. At distances of more than a few solar radii from the Sun, the solar wind reaches supersonic speeds of 250–750 km/s [32]. At much greater distances, about 75–90 astronomical units (1 au is the distance Sun-Earth), the so-called "termination shock," interactions of the local interstellar medium with the solar wind slow it down to subsonic speed.

There are different classes of solar wind [30]:

(a) The long-lived solar wind high-speed streams, representatives of the inactive or "quiet" Sun. Sources for such streams are coronal holes usually located above inactive parts of the Sun, where "open" magnetic field lines prevail, e.g., around activity minima at the polar caps;

(b) A slow wind stream from more active near-equatorial regions on the Sun, often associated with "closed" magnetic structures. Sharp boundaries exist between these two solar wind streams (in longitude as well as in latitude),

and their main properties differ significantly according to the location and magnetic properties at the source;

(c) Another slow solar wind stream emerging during high solar activity, from active regions distributed over large parts of the Sun, in a highly turbulent state. It is highly variable and usually contains a significant fraction (about 4%) of alpha particles;

(d) The solar wind disturbances superimposed on the ambient solar wind in case of CMEs. They exhibit unusually high percentages of alpha particles (up to about 30%).

The Earth's magnetosphere deflects the solar wind, causing most of the solar wind to flow around and beyond us. Nevertheless, a small number of particles from the solar wind reach the upper atmosphere and ionosphere. This may produce phenomena such as aurora and geomagnetic storms, the latter occurring when large inflation of the magnetosphere, due to an increased pressure of the contained plasma, distorts the geomagnetic field.

In space missions, the solar wind has no impact on astronauts, as it is efficiently stopped by the spacecraft shielding and also by appropriate astronaut suits, because of the small range in a matter of the low speed-solar wind particles. However, if not appropriately shielded, the solar wind particles may affect the human body during eventual EVAs in deep space or on the surface of airless bodies, such as the Moon.

10.3.1.4 Trapped Radiation

Trapped radiation particles are produced mainly by the interaction of GCRs and SEPs with the Earth's atmosphere and are trapped by its magnetic field into the Van Allen radiation belts. These comprise:

(a) A stable inner belt of trapped protons and electrons with energies between some keV and 100 MeV that is centered at a height between 300 and 1000 km above the Earth and reaches up to a height of around 10,000 km.

(b) A less stable outer electron belt, comprising mainly high-energy (0.1–10 MeV) electrons and which extends from an altitude of about 10,000–40,000 km (see Fig. 10.7 for a schematic representation).

In the radiation belts, the energetic particles move along Earth's magnetic field lines, via the combination of three types of motion: a fast rotation (or "gyration") around magnetic field lines, typically thousands of times each second; a back-and-forth bouncing along the stronger magnetic fields in the northern and southern hemispheres, typically lasting 1/10 s; a slow drift around the magnetic axis of the Earth (the drift is eastward for electrons and westwards for ions), such drift is from the current field line to its neighbor, with the particle keeping roughly the same distance from the axis. A typical time to complete a full circle around the Earth is a few minutes.

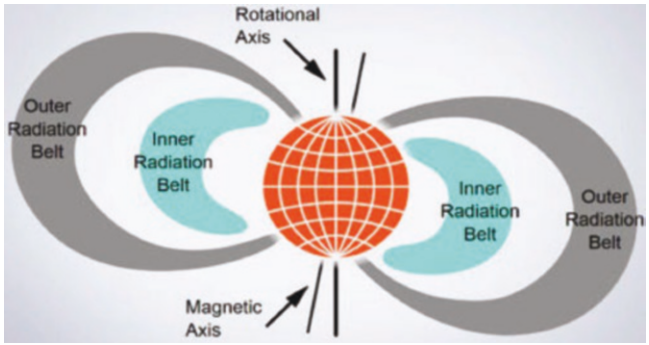

Fig. 10.7 Radiation belts of the Earth. (Figure from Van Allen radiation belt. Reprinted with permission from Wikipedia. Author Booyabazooka at English Wikipedia, https://commons.wikimedia.org/wiki/File:Van_Allen_radiation_belt.svg)

In the area above the southeastern part of South America and the South Atlantic, the inner radiation belt approaches the surface of Earth down to a few hundreds of kilometers (South Atlantic Anomaly, SAA). This is caused by the tilt and shift of the axis of the dipole-like magnetic field of the Earth with respect to its axis of rotation [33]. The dip of magnetic lines leads to an increased particle flux within this region.

The dose rate experienced by the astronauts on the ISS has a considerable contribution from trapped protons in the inner Van Allen belt because the ISS orbit with an altitude of about 400 km passes through this belt at the SAA (roughly 50% of the total dose rate) [34].

10.3.2 Radiation Environment in Low Earth Orbit (LEO)

A low Earth orbit (LEO) is an Earth-centered orbit close to our planet with an altitude ranging from 160 to 2000 km. Thus, the ISS, which flies at an altitude of around 400 km, is also in such an orbit, with an orbital inclination (the tilt of the orbital plane with respect to the equatorial plane, which helps to understand an orbit's orientation with respect to the equator) of 51.6° and an orbiting period of 90–93 min. Consequently, in 24 h the ISS makes 16 orbits of Earth and travels through 16 sunrises and sunsets. The environment of these altitudes is extreme and characterized by microgravity, high vacuum, meteoroids, extremes of temperature, ionospheric plasma, space debris, and UV as well as ionizing radiations.

The radiation sources are GCR, trapped radiation, and SEP events. The GCR environment accounts for about 50% of the total dose rate, the other 50% being induced by trapped protons of the inner belt, the only component of the inner belts that reaches energies and intensities to be important for effects on astronauts inside the ISS [35]. Other orbits, such

as Medium Earth Orbits (2000–35,786 km), Geostationary orbits (35,786 km), and High Earth Orbits (over 35.786 km), are exposed to different sub-components of the trapped radiation, some may not pose any danger. On board the ISS, astronauts encounter SPE events as a transient increase in dose rates. As mentioned above, the GCR flux is modulated by the solar cycle. At the ISS altitude, the GCR flux is also modified by the geomagnetic field, besides the modulation due to the solar activity. This field removes particles with lower energies (~few GeV/nucleon), but particles of higher energies are unaffected [36]. At low altitudes, the trapped radiation is also modulated by solar activity: at solar maximum, because of the increase in UV radiation, the upper atmosphere expands, leading to the loss of trapped protons at low altitudes. Furthermore, the inner radiation belt is mainly filled by decaying neutrons created by incoming GCR particles and the GCR flux is inversely proportional to solar activity [37]. Therefore, at solar maximum, a lower proton flux is present, leading to a smaller radiation hazard compared to the solar minimum [36, 38].

The interaction of energetic protons and HZE nuclei with spacecraft structures produces an additional intravehicular radiation field. This secondary radiation includes mainly, protons, neutrons, photons (X-rays and gamma rays), leptons (e.g., electrons and positrons), mesons (e.g., charged pions) and a great number of lighter and heavier nuclear isotopes (ions) [39, 40]. This happens in LEO and is of high concern in particular for the deep Space phase of a mission (see below), as the spacecraft would not be protected by the Earth's atmosphere and magnetic field.

10.3.3 Radiation Environment Beyond LEO (Deep Space, Moon, Mars)

10.3.3.1 Deep Space

Radiation challenges for astronautic missions beyond LEO, such as travel to the Moon or Mars, come from SEP events, GCR and intravehicular secondary radiation (Fig. 10.2). The solar wind particles, also constantly present in deep Space, do not contribute to the radiation dose induced in crews inside a spacecraft, as they are efficiently stopped even by thin shielding thicknesses.

Similar to the case of the LEO scenario, most GCRs are not efficiently stopped by regular depths of spacecraft shielding. The intravehicular radiation field is constituted by the ensemble of secondary radiation mentioned above. Adding more shielding would increase to a considerable extent the weight at launch and would not reduce the GCR-induced absorbed dose to zero. As the only modulation of GCR in deep space is provided by the shielding of the heliospheric field during solar maximum, the idea of carrying out missions to Mars during solar maximum has been considered a viable option. If one considers that during a 180-day trip at the solar maximum peak a crew would also likely receive a total SEP-contributed dose equivalent, a round trip to Mars would result in a total dose equivalent of 560 ±180 mSv,[1] higher than the estimation based on the data from the Radiation Assessment Detector (RAD) onboard the Mars Science Laboratory NASA mission [41] which was on cruise during solar minimum [42]. The above estimate for the radiation exposure is substantially lower than the accepted safe upper limit for 30–60-years old nonsmoking females and males (above 1500 mSv—see Fig. 10.8). However, inaccuracy and limitations of the models and unpredictability of SEP events must be considered.

10.3.3.2 Airless Bodies: The Moon

The Moon is about 380,000 km away from Earth and is the next endeavor for space missions beyond LEO. Although some areas of the Moon have a weak magnetic field, the Moon does not have a global magnetic field like on Earth and no atmosphere. Consequently, its surface is not shielded from radiation. The solar wind particles get stopped in the first millimeters or, maximally, centimeters of the lunar regolith, while GCR and SEP can impact the lunar surface also resulting in the production of backscattered secondary particles. The total amount of radiation that astronauts will be exposed to is influenced strongly by solar activity, their whereabouts on the Moon surface with respect to local magnetic fields, and the type and amount of radiation shielding used in spacecraft, Moon vehicles, and habitats. Recently, the Lunar Lander Neutrons and Dosimetry experiment aboard China's Chang'E 4 lander revealed that radiation levels on the Moon's surface are 200–1000 times more than that on Earth's surface and 2.6 times more than what astronauts onboard the ISS are exposed to Zhang et al. [44]. Efficiency of the radiation shielding by lava tubes on the Moon appears promising to reduce the dose rates considerably [45].

10.3.3.3 On Mars

Mars does not possess a global magnetic field, and it has only a thin atmosphere with its surface pressure less than 1% of that at Earth's surface. Therefore, high-energy GCRs can reach the surface, although still a considerable portion of them will induce hadronic-electromagnetic-muon cascades in the atmosphere, causing fragmentation/spallation and ionization showers of downward secondaries. All these particles can then induce further reactions in the planet's regolith, which generate a backscattered, albedo radiation component,

[1] Sievert (Sv) denotes the equivalent dose as measure for biological and medical relevant quantification of dose in radiation protection. For a detailed explanation please refer to Chap. 2.

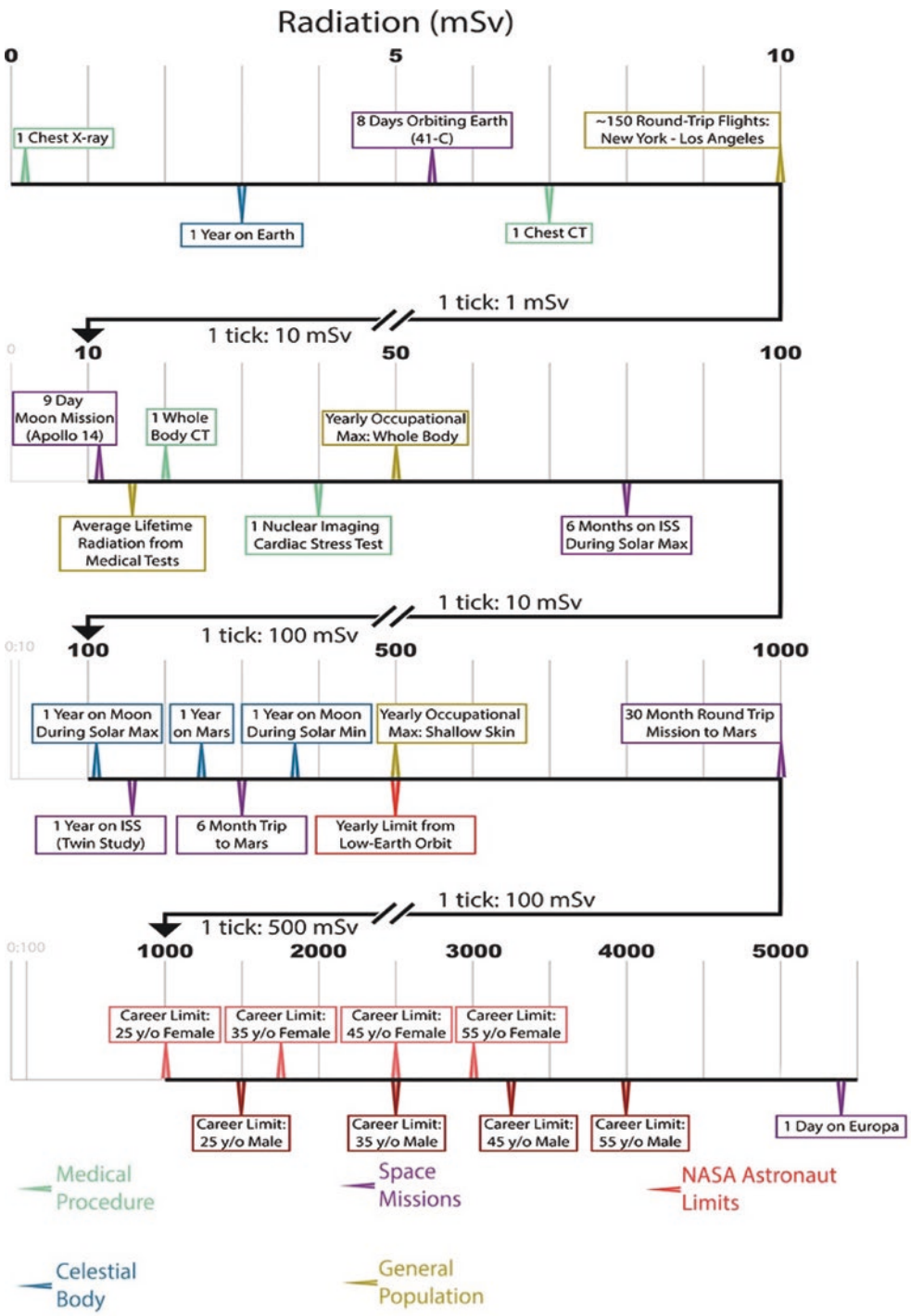

Fig. 10.8 Relative radiation exposure of varying duration during medical procedures (green), specific space missions (purple), and on various celestial bodies (blue). The astronaut yearly and career limits are given in red boxes. For comparison, some facts on radiation exposure of the general population and occupational exposure limits (US) are indicated (gold). (Reprinted with permission from Iosim et al. [43])

giving overall complex spectra including both primaries and (downward and upward) secondaries at the surface [46–48].

SEP events can increase the dose rate and dose equivalent at the Martian surface and constitute a danger for EVA on Mars. Only protons impinging the top of the atmosphere with energy above ~200 MeV do actually reach the ground, and thus SEPs events with high flux contribution at high energy constitute the biggest hazard for explorers on Mars if they are not in a habitat or otherwise sufficiently shielded. For the solar wind, despite the thin character of Mars' atmosphere, the upper layers of the latter are able to stop such radiation. Underground solutions for Mars habitats, shielded from the radiation by the regolith, are being investigated [49].

Overall, to contextualize radiation doses in space, a comparison of these doses to doses received during medical interventions is shown in Fig. 10.8. It is important to emphasize that being exposed to a hefty radiation dose within a

short time (minutes to hours) will be more health-threatening than the same dosage over a longer duration of months of years. Yet, although the health effects of acute radiation exposure are well studied, less is known about the effects of chronic exposure.

10.3.4 Space Radiation Shielding

Ionizing radiation exposure is one of the most critical health risks for astronauts. Inside the ISS, astronauts are exposed to an effective dose rate of the order of 20 μSv/h, which is about 100 times higher than on the Earth's surface. Beyond LEO in deep space, the protection of the Earth's atmosphere and magnetic field disappears, leading to an effective dose rate of the order of 75 μSv/h. Also, on the surface of the Moon or Mars, there is only limited protection and astronauts are exposed to respectively about 30 and 25 μSv/h. It is estimated that astronauts will accumulate during a Mars mission a total effective dose of the order of 1 Sv, leading to an extra risk for cancer of the order of a few percent up to more than 10% depending on sex and age [50]. Furthermore, on their way through deep space or on the surface of the Moon or Mars, astronauts can receive such high doses during intense solar storms that immediate health effects or even a deadly outcome are possible (see Sect. 10.4.2). Therefore, it is clear that astronauts need to be protected against ionizing radiation in space.

The only technology that can currently be used in practice to reduce the radiation level in spacecraft is to use shielding materials for stopping part of the radiation. The heavy ion impinging on the shielding material is the projectile, and the shielding material is the target. A multitude of interactions can occur when the projectile hits the target, including fragmentation of the projectile or target. For comparison of different materials, the area density as mass per unit area in g/cm^2 is used (for example, an 1 cm thick plate of Al with the density of 2.7 g/cm^3 has an area density of 2.7 g/cm^2). In current spacecraft, one makes most use of constructive materials such as aluminum. Unfortunately, such materials are not the most efficient for radiation shielding in space (see Chap. 4). The interaction of energetic GCRs with heavier elements such as aluminum results in the breakup of these heavier elements and the creation of secondary cosmic radiation such as energetic heavy ions and neutrons. Therefore, when using aluminum for shielding, the effective dose rate first increases as function of the shielding thickness before it starts to decrease and this decrease is quite flat as attenuation of heavy ions is nearly in balance with the build-up of light particles (Fig. 10.9 Left).

Materials consisting of lighter elements such as hydrogen have a higher stopping power per unit of mass for charged radiation particles as they attenuate their fluence via projectile fragmentation. They also minimize the build-up of neutrons and other target fragments. Radiation protection of astronauts can thus be further optimized by making use of

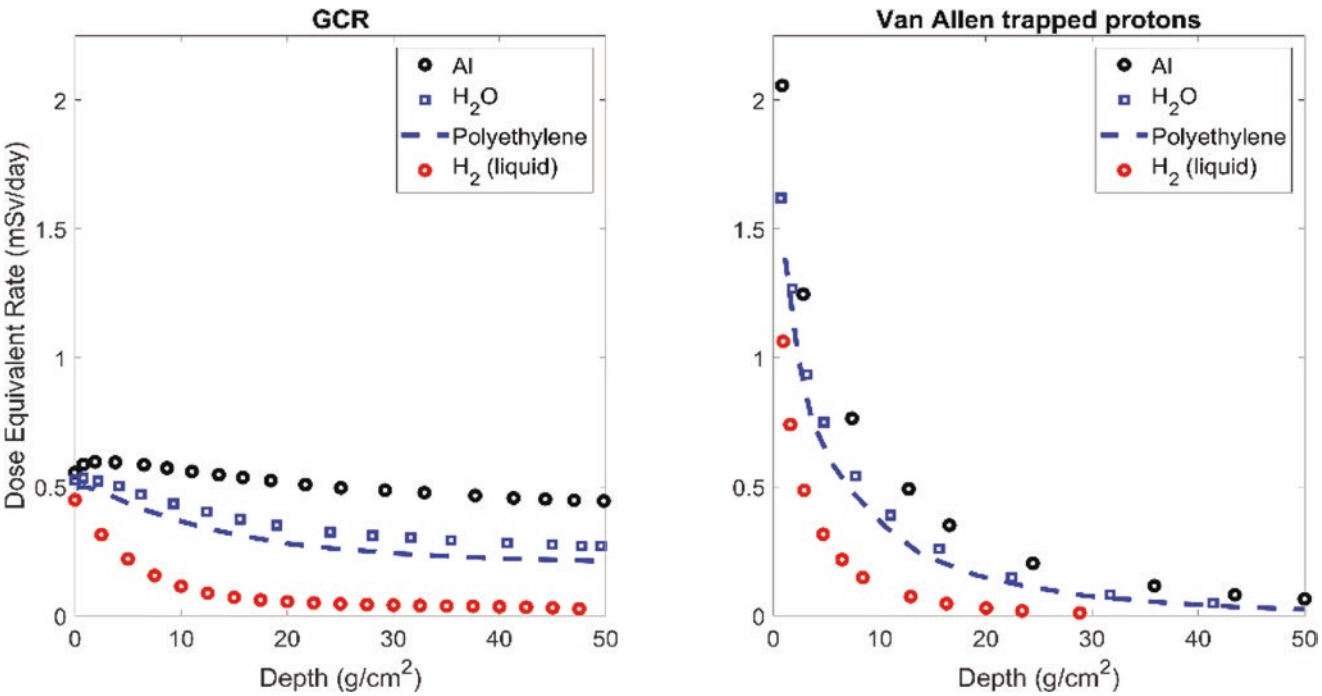

Fig. 10.9 Calculated dose equivalent rate in LEO (51.6° inclination, 390 km altitude) as a function of shielding thickness given as area density for different shielding materials: (left) GCR, (right) Van Allen trapped protons. (Data used with permission from Dietze et al. [37])

lighter shielding materials or, for instance, also by making strategic use of the necessary stock of water as additional shielding. Figure 10.9 shows the calculated dose equivalent rate for a LEO orbit similar to that of ISS (51.6° inclination, 390 km altitude) as a function of shielding thickness for different shielding materials. At standard temperature and pressure, based on a density of 1000 kg/m^3, the water column required to reach an area density of 20 g/cm^2 would have a height of 20 cm. For 20 g/cm^2 aluminum, a material thickness of 7.4 cm is derived from the density at room temperature of 2.7 g/cm^3. At the same area density of 20 g/cm^2, the shielding effect of water is much more pronounced than the one of aluminum. The thickness of the two materials is different, but they would contribute to the same extent to the mass budget of the spacecraft which is critical for leaving the Earth surface during launch. The left and right plots show the results for respectively GCRs and Van Allen protons. These plots clearly show that hydrogenous materials are much more efficient for radiation shielding in space.

In spacecraft it is unfortunately not possible to reduce the effective dose rate to the dose rate on Earth's surface. With limited shielding, a large part of the energetic protons and electrons from SEPs and the Van Allen protons can be stopped. However, GCRs have such high energies that about 1000 g/cm^2 of shielding is required to reduce the effective dose rate to the level on Earth's surface. Due to mass constraints in spacecraft, only shielding of the order of a few 10 g/cm^2 is possible. In spacecraft, astronauts can thus be protected against sudden very high and potentially deadly doses from solar storms, but they will be unavoidably chronically exposed to the ever-present GCRs leading to an increased risk for late effects.

It is clear that with current technology additional radiation exposure in spacecraft is unavoidable. However, for future manned missions to the Moon or Mars during which astronauts will stay on the surface for a longer time it will be necessary to strongly reduce their radiation exposure during their stay. This is possible because on the surface of the Moon or Mars, we can make use of the present soil material to provide adequate shielding. A few meters of soil material should suffice to reduce the effective dose rate level to similar levels as on Earth's surface. This can be done by building igloos or by living in caves or lava tubes.

Besides shielding by using materials to block the radiation, it is in principle also possible to make use of strong electromagnetic field for shielding. Several research groups are investigating this possibility. However, the required mass and energy consumption of such systems makes the concept practically impossible with current technology (Box 10.1).

Box 10.1 Highlights

(a) GCRs are the constantly present highly energetic radiation in space, they are mostly constituted by protons, with a smaller contribution from alpha particles and HZE particles. They generate particle showers in the atmosphere, although a small portion of direct GCRs can eventually reach the ground.
(b) SEP events are more probable during solar maximum, but they can actually also occur during solar minimum.
(c) Trapped radiation is constituted by GCRs and solar protons trapped in the Van Allen belts. Trapped radiation is a concern for ISS-like missions, especially because of the flux accumulated during different orbits in the SAA, or also missions on other orbits crossing one or the other belt.

10.3.5 Mathematical Modelling the Space Radiation Environment and Induced Doses

10.3.5.1 Transport of Radiation Through Matter: Deterministic and Monte Carlo Methods

The modeling of the radiation environment at or inside a spacecraft, at different altitudes in the atmosphere or at the surface/subsurface of a planet, a moon, or a small body allows to obtain the relevant dosimetric quantities for the assessment of the health risks incurred by humans due to radiation [51–53], as well as to estimate the half-lives of biomolecules in search-for-life studies [54, 55].

The transport of radiation through matter is described by the time-independent Linear Boltzmann Transport Equation, which allows to treat atomic and nuclear collisions. The Boltzmann transport equation (10.1) describes the flux $n_i(\boldsymbol{r}, E, \Omega, t)$ of several types of particles i, possessing different energies E, and moving in different directions Ω by considering the particle balance in a small volume V. It thus gives the average space-time distribution of the expected energy-momentum behavior of the particle beam, transported and scattered across the target, where each interaction is characterized by its own differential cross-section $\frac{d^2\sigma}{d\Omega dW}$. The Boltzmann equation reads as follows:

$$\int d\boldsymbol{r}\frac{\partial n_i\left(\boldsymbol{r},E,\Omega,t\right)}{\partial t}=\underbrace{-\oint_S dA\boldsymbol{j}\left(\boldsymbol{r},E,\Omega,t\right)\cdot\hat{\boldsymbol{a}}}_{\text{unscattered particles}}\underbrace{-N\int_V d\boldsymbol{r}n_i\left(\boldsymbol{r},E,\Omega,t\right)v\left(E\right)\sigma\left(E\right)}_{\text{particles scattered out}}$$

$$\underbrace{+N\int_V d\boldsymbol{r}\int dE'\int d\Omega' n_i\left(\boldsymbol{r},E',\Omega',t\right)v\left(E'\right)\frac{d^2\sigma}{d\Omega'' dW''}}_{\text{particles scattered in}} \tag{10.1}$$

$$\underbrace{+N\int_V d\boldsymbol{r}\int dE'\int d\Omega'\sum_j n_j\left(\boldsymbol{r},E',\Omega',t\right)v\left(E'\right)\frac{d^2\sigma_{\text{sec},i}}{d\Omega'' dW''}}_{\text{production of secondaries}}+\underbrace{\int_V d\boldsymbol{r}\,Q_{\text{source}}\left(\boldsymbol{r},E,\Omega,t\right)}_{\text{source}}$$

In this equation:

- the first term is the time-dependent flux change, due to particles escaping from the system boundaries, or disappearing by an absorption reaction or radioactive decay;
- on the right-hand side, the unscattered term represents the flux change due to translation without change of energy and direction (free flight);
- the particles scattered out are those exiting a "cell" (a unit volume in the phase space, the latter comprising both space and time variables);
- the particles scattered in are those entering a "cell" from a "cell" at a previous point in the phase space;
- the production of secondaries represents the effect of collisions;
- the source term can be external (e.g., a particle beam irradiating the target volume), or internal (e.g., neutrons from fission reactions in the volume).

In particular for high-energy particles, the number of interactions that must be described in order to find the solution to this equation is daunting, including ionization, excitation, spallation/fission/fragmentation, production of positron-emitting nuclei, and de-excitation through gamma rays. A solution to the problem can be attained via two different approaches:

1. **Deterministic methods**. These are deterministic approaches based on approximations to the Boltzmann equation and often on the reduction to a 1D problem via the use of the straight-ahead approximation, according to which the secondary particles from nucleon-nucleus collisions are emitted in the direction of the incident nucleon [37]. They rely on models for the relevant quantities in the transport calculation and use the continuous slowing down approximation (CSDA). Deterministic codes such as NASA's HZETRN [56] and BRYNTRN [57] follow such an approach and require relatively low computational resources to perform calculations and the calculation time is relatively short. This is due to the fact that deterministic codes do not consider all products of reactions and neglect their correlation, e.g., the coefficients used in the Boltzmann equation are related to relatively simple one-particle quantities. Thus, correlations on event-by-event basis are not considered and particle scattering at an angle is ignored [58]. Last, such methods can only be applied to restricted geometries and restricted interaction models.
2. **Monte Carlo method**. Monte Carlo (MC) is a stochastic method, exploiting random numbers to (a) "generate" an initial particles' "cocktail"; (b) track them in arbitrary geometries; (c) accumulate the contribution of each track to a statistical estimator of the desired physical observables [59]. Step-by-step particles' transport is simulated according to the statistical model of their interactions. Quantities (such as step lengths, event type, energy losses, and deflections) are sampled via generation of random values according to a given probability distribution. Indeed, in MC codes, the MC method deals with sampling from suitable stochastic distributions, with large samplings allowing to solve the integrations of multidimensional integrals.

In the context of space environment, the main interest is in high-energy particles whose scattering is generally low-angle. Therefore, it is reasonable to approximate multiple scatterings by a single continuous step, taking into account overall energy loss and direction change. This approach is known as the condensed-history technique. For example, ionization and excitation energy losses are described as continuous processes, i.e., they are continuously distributed along a particle step, if the loss is lower than a chosen threshold, together with their fluctuations.

Several MC codes are used nowadays throughout the world, such as Geant4 [60], FLUKA [61], and PHITS [62]. MC codes provide a detailed treatment of the three-dimensional transport of ions and neutral particles (see Chap. 4).

10.3.5.2 Practical Steps in the Modelling of the Space Radiation Environment and Induced Doses

An overview of the different steps for calculation of the radiation environment of a celestial body is given in Fig. 10.10.

Input Spectra

The input spectrum for GCRs can be chosen among different existing models that account for the variations of GCR particle fluxes due to variations in solar activity and in the large-scale heliospheric magnetic field throughout the solar cycle. The ISO 15390 model (ISO-15390 2004) [63] accounts for solar cycle variations in the GCR intensities on the basis of 12-month averages of the sunspot number. Changes in the large-scale heliospheric magnetic field are usually taken proportional to the corresponding changes in the Sun's magnetic field, considering also solar cycle. More accurate models describe the spectra of GCR beyond the heliospheric modulation region. The CREME96 [64] and its updated version CREME2009 (https://creme.isde.vanderbilt.edu/) are based on a semi-empirical model [65] where the particle spectrum is calculated as a product of a function describing the LIS and a function describing the modulation according to solar activity. GCR particle spectra are described in the energy range from 10 to 10^5 MeV/nucleon, from H up to Ni nuclei from the year 1760 to present. The Badhwar–O'Neill 2010 (BON2010) [66] uses, instead of an empirical description of the modulated GCR.

As in the CREME model, a physical approach to describe the GCR propagation in the heliosphere due to diffusion, convection, and adiabatic deceleration. The BON2010 model exploits data from the International Sunspot Number (ISN) and considers time lag of GCR flux relative to the solar activity. The ISN is calibrated with GCR measurements from the Advanced Composition Explorer (ACE) and the Interplanetary Monitoring Platform-8 (IMP-8). The Burger-Usoskin model [67] is limited to GCR He and H ions assuming a constant ratio of the two types of ions. The reconstruction of the modulation parameter is based on neutron monitor count rates. The DLR model by Matthia et al. [68] describes the GCRs spectra of nuclei based on a single parameter, which is derived from measurements of the ACE spacecraft and from Oulu neutron monitor count rates for different solar modulation conditions.

SEP proton spectra are often considered from historical events, then parameterized by double power law fits in kinetic energy to event-accumulated integral fluence measured by the Geostationary Operational Environment Satellites and/or ground-based neutron monitor data [69].

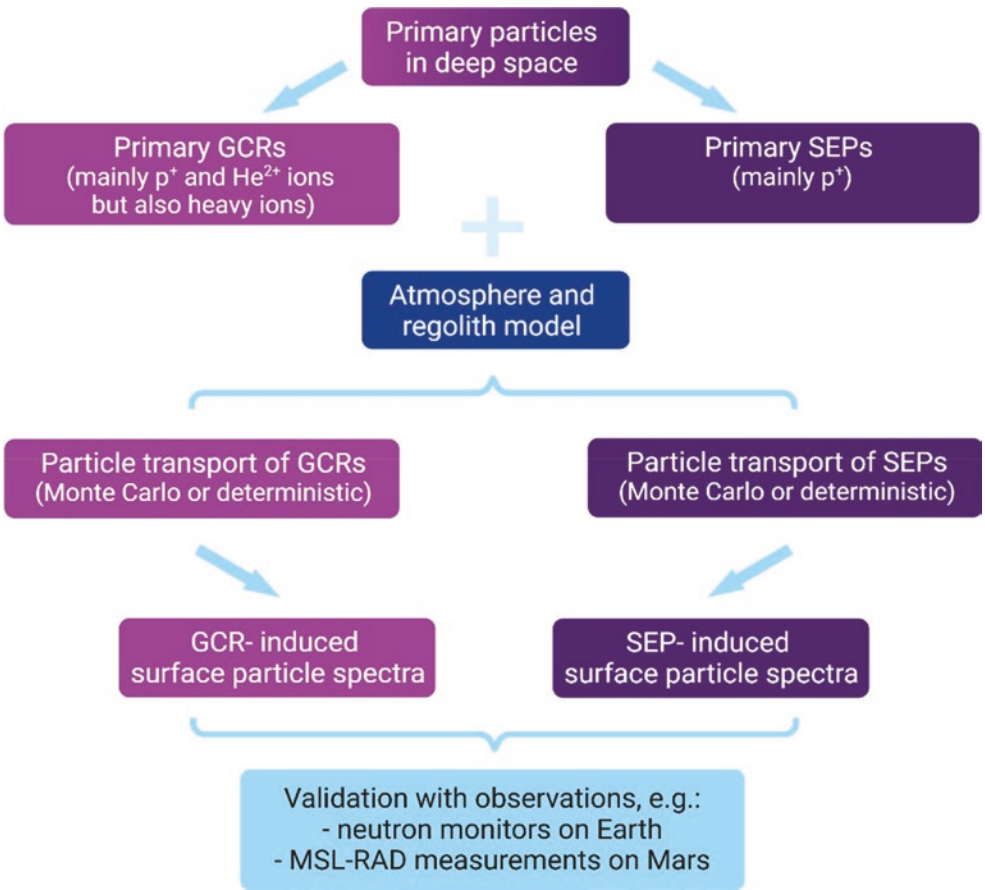

Fig. 10.10 Scheme for Monte Carlo (MC) calculations of the radiation environment at a planet/celestial body, here in particular Mars. *GCRs* galactic cosmic rays, *SEPs* solar energetic particles, p^+ protons, He^{2+} *ions* helium ions

Input spectra for both GCR and SEP events can often be retrieved via user-friendly tools, such as the SPENVIS online tool (https://www.spenvis.oma.be/) that is actually a collection of modules that allow for calculations of the radiation environment and radiation-induced effects via MC simulations in Geant4, or the On-Line Tool for the Assessment of Radiation in Space (OLTARIS) which operates on top of the deterministic code HZETRN (https://oltaris.nasa.gov/).

Atmospheric Model

For Earth, more than 99.99% of its atmosphere's mass is contained in the lower atmospheric layers below about 100 km. This region is mainly composed of N_2, O_2, and Ar which account for about 75%, 23%, and 1.3% by mass, respectively. The exact mass fraction of each constituent depends on the altitude. The water content in the atmosphere is highly variable but small, with the hydrogen fraction only reaching the order of $10^{-5\%}$ even in cloudy conditions [70]. Composition, density, temperature, and pressure vertical profiles can be obtained, for example, from the empirical atmospheric model 1 NRLMSISE-00 [71], which includes total mass density from satellite accelerometers and from orbit determination covering 1981–1997. For Mars, vertical profiles for pressure, density, temperature, and chemical composition of the atmosphere are often constructed exploting databases like MCD (Mars Climate Database http://www-mars.lmd.jussieu.fr) [46, 49]. Data can be extracted for specific locations, a specific day/night time, and season. The surface elevation and topology are extracted from the Mars Orbiter Laser Altimeter (MOLA) aboard Mars Global Surveyor. The fields (temperature, wind, density, pressure, radiative fluxes, etc.) are stored on a 5° × 5°, longitude-latitude grid from the surface to 120 km (and above) are averaged and stored 12 times a day, for 12 Martian "seasons."

Surface and Subsurface

For Earth, the soil is often considered to consist of $50\%_{Vol}$ solids (of which $75\%_{Vol}$ SiO_2 and $25\%_{Vol}$ Al_2O_3) and a scalable amount of H_2O. Studies show that the neutron environment strongly depends on soil moisture (and air humidity) [72]. The composition of the surface and subsurface of Mars can either be chosen to model specific scenarios, for example, a default basaltic composition (SiO_2 51.2%, Fe_2O_3 9.3%, H_2O 7.4%) [73] or more/less hydrated compositions to study the possibility of underground shielding habitats [49], or it can be taken from data from the Gamma Ray Spectrometer aboard Mars Odyssey [46]. The dosimetric quantities at the Martian surface do not depend strongly on the regolith composition, although some differences due to hydration and Fe-content can affect neutrons and gamma rays spectra [49].

Propagation

MC particle transport codes strongly rely on the availability of physics models and database of cross sections. A schematic view of the downward and upward main particles that need to be considered is shown in Fig. 10.11. In the open source Geant4 code [60], hadronic models are: (1) data-driven, which mainly deals with the detailed transport of low-energy neutrons and isotope production, (2) parametrized models which include fission, capture, elastic, and inelastic scattering reactions; (3) theoretical models for high energies, above several 10–100 MeV, where experimental cross-section data are scarce. For electromagnetic physics, the basic processes for electrons, positrons, photons, and ions, such as Compton scattering, photoelectric effect, pair production, muon-pair production for photons, ionization, δ-electron production, Bremsstrahlung, Čerenkov radiation, and annihilation, are considered. Additionally, processes involving the atomic shell structure such as Rayleigh scattering are also considered. Special process classes handle muon interactions like Bremsstrahlung, capture, and annihilation. Multiple scattering models provide corrections for path lengths and lateral displacements of multiple scattered charged particles. In order to decrease the computational time and resources, a certain production cutoff in the range is set for electrons, positrons, and photons, which is translated to energy below which the particle then loses its remaining kinetic energy continuously along the track and no secondary particles are produced.

Target

In principle, the proper approach to calculate the absorbed dose and dose equivalent rates is to use. Such standardized phantom has been defined by the International Commission on Radiation Units (ICRU) and it is given by the ICRU sphere, a 30 cm-diameter sphere with a density of 1 g/cm^3 and a mass composition of 76.2% O, 11.1% C, 10.1% H, and 2.6% N,

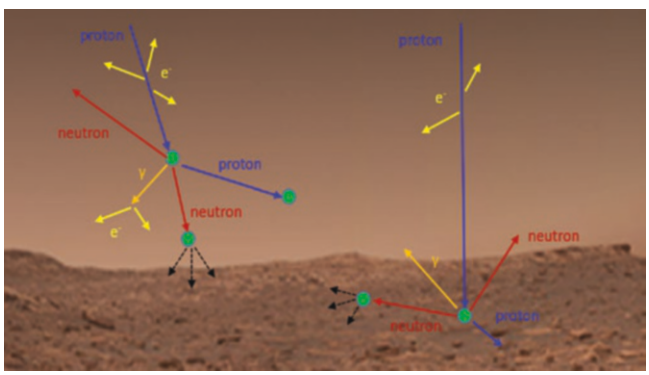

Fig. 10.11 Schematic view of the particle showers (main particles are plotted here) generated in the downward propagation of primary GCRs particles through the Martian atmosphere and of the backscattered particles [74]

which reflects the composition of tissue. Still, in recent times more human-like phantoms have been used [75]. However, such complexity is not always necessary, and sometimes other spheres of water or water slabs have been used [76].

Apart from running the MC (or deterministic) codes in standalone mode, several tools such as the previously mentioned SPENVIS online system (https://www.spenvis.oma.be/), OLTARIS (https://oltaris.nasa.gov/), and the EXPACS/PARMA code (https://phits.jaea.go.jp/expacs/) based on PHITS can be used to run a combination of the steps described above, resulting in a punctual estimation of doses at a specific location on a body or altitude in an atmosphere or in radiation maps covering several regions.

For human exploration of Mars and other bodies, the quantities of interest are the absorbed dose corrected by the relative biological effectiveness (RBE) factor (to estimate the risk for acute effects or death due to high doses for Solar Energetic Particle events) and the Effective Dose and Dose Equivalent to respectively estimate the risks to long-term effects induced by exposure to GCRs and to compare with measurements from radiation detectors. Space Agencies implement the ALARA principle [77] which ensures that mission operations are designed to keep the radiation risks as low as reasonably achievable. Although the different agencies use common limits for deterministic effects on the ISS, different career radiation exposure limits (for stochastic effects) for astronauts in LEO missions exist and no specific limits for interplanetary missions are issued (only those for LEO exist).

10.3.5.3 Harmonization of Risk Models for Stochastic Effects: The Problem of Radiation Quality Factors

Harmonization of risk models requires improvements in modeling radiation sources, in the accuracy of radiation transport codes, and the development of new realistic quality factors based on the features of the variegated radiation field in Space.

As already mentioned in Chap. 2, the approach commonly used for estimating risk from high linear energy transfer (high-LET) radiations is based on multiplying the induced absorbed dose (in units of *gray*) by a so-called *quality factor*, or *RBE factor* (always greater than one, usually below 20) representing the enhancement of effectiveness of the high-LET radiation. Such increased effectiveness comes from available evidence on the RBE of the radiations from both laboratory and theoretical studies (Sects. 10.4 and 10.5). As previously shown, RBE varies with LET. It depends also on other factors and may be different, e.g., for particular chromosome aberrations, mutations, or different tumor types. Also, RBE may vary in different biological systems. Furthermore, low-LET dose response is usually nonlinear while high-LET response tends to be more linear.

However, for radiation protection purposes, the use of RBE for low-dose exposure to radiation with different LET was superseded by the adoption of radiation weighting factor, w_R, by the International Commission on Radiological Protection (ICRP) [78], to convert absorbed dose (measured in Gy) to equivalent dose (measured in Sv) in a tissue and to effective dose (measured also in Sv) in the body. ICRP recommends $w_R = 1$ for photons of all energies, electrons, and leptons. The value $w_R = 2$ is recommended for protons and charged pions, and $w_R = 20$ for α-particles, heavy charged particles, and fission fragments [78] (see Table 10.2). However, the adoption of specific values for such weighting factors, based on the judgment from the available data on RBE, was accompanied by a recognition of the simplistic description and of the limited accuracy that the systematic application of this set of values for w_R would have brought. Thus, quality factors, Q(LET), defined as a continuous function of the LET of the radiation, were later introduced in order to give broadly similar results for measured radiation fields [78] (see Table 10.2). Such quality factors are nowadays used in the risk assessment model by the European Space Agency and were also used in the previous risk assessment model by NASA.

Nevertheless, this specification of Q in terms of the LET alone suffers from the limitations already highlighted in Chap. 1, about the fact that the sole LET cannot fully describe the effectiveness of radiation in inducing biological damage. Indeed, even simply from the perspectives of the first-stage radiation-induced effects, without mentioning the complex dependencies of the RBE on phenomena related to the chemi-

Table 10.2 Radiation weighting factors and quality factors

Radiation type	Radiation weighting factor (w_R)	Quality factor (Q(LET))
Photons	1	
Electrons and muons	1	
Protons and charged pions	2	
Alpha particles, fission fragments, heavy ions	20	
Neutrons	A continuous function of neutron energy	
For LET < 10 keV/μm		1
For 10 ≤ LET ≤ 100 keV/μm		$Q = 0.32L^{-2.2}$
For LET > 100 keV/μm		$Q = 300L^{-1/2}$

cal and biological steps, it remains the fact particles with different charge and different velocity may have the same LET and still inducing different final biological effects. The variation in the effectiveness of radiation in inducing different final biological effects has thus its root in the differences in track structures between particles that have the same LET but different charge and velocity, as highlighted in Chap. 1. Differences can be particularly large for the HZE particles encountered in space, methods used on Earth are inadequate for space travel, as, among other reasons, the ICRP radiation quality description does not represent HZE radiobiology correctly.

The key difference between (a) the quality factor used by NASA [79] for the projection of risk from space exposures and (b) the quality factor recommended by the ICRP (Q(LET)) for operational radiation protection on Earth is consideration of track structure (Box 10.2).

Box 10.2 Modeling

(a) The Boltzmann equation describes the transport of radiation in matter; it can be solved via analytical (deterministic) or via numerical (Monte Carlo) methods.

(b) The different steps for setting up a calculation of the radiation environment are input radiation spectra, definition of the parameters describing the atmosphere, with dependence on the altitude, definition of the regolith composition, definition of the physics model to be used according to the different energy ranges, definition of the target where the scoring of the absorbed dose will be done.

10.4 Human Health and Organs at Risks for Space Travel

The space environment is hostile to the health of astronauts in several ways. The confinement in the restricted space of spacecraft for shorter or longer periods exposes the crew to sometimes severe behavioral problems. Microgravity can lead to osteoporosis, a modification of the electrolyte compartments, sarcopenia, cardiac arrhythmias, dysthemeral rhythm disorganization, vestibular deconditioning, relative immunosuppression, and postural hypotension on return [80]. Finally, the space radiation environment is very different and much more hostile than that encountered on Earth. Add a temperature amplitude of 300 °C on the spacecraft's surface and the almost absolute vacuum conditions that astronauts must consider during extravehicular excursions. Finally, let us point out the disturbances secondary to the return to the ground: neurological, vestibular, cardiovascular reconditioning, etc.

10.4.1 Radiation Exposure During Space Missions

The constant flux of galactic cosmic rays (GCR) causes astronauts' chronic low-dose whole-body exposure during space missions. The primary GCR particles interact with the spacecraft hull, so that astronauts are—like patients—exposed to secondary radiation from nuclear interactions between the incident radiation and the shielding of the spacecraft. Due to mass limitations for launching spacecraft, complete shielding of GCR is not feasible. Compared to an astronaut suit for extravehicular activities, the shielding of the spacecraft by aluminum and other materials strongly reduces the skin dose and also, but to a much lower extent, the whole-body dose. On the microscopic level, due to the physical characteristics of particle radiation, very high doses can be reached, leading to permanent damage (see Sect. 10.4).

In LEO, traversal of the SAA of the inner radiation belt contributes to the accumulated dose during, e.g., a mission on the ISS. Human phantom experiments on the ISS (MATROSHKA experiment series) allowed the quantification of the effective dose rate which was 690–720 μSv/day during extravehicular activities and lower inside the ISS amounting to 550–570 μSv/day [81, 82]. Therefore, astronauts accumulate effective doses of around 100 mSv during a 6-months ISS mission. The variations of the accumulated dose depend on solar activity and the flight altitude of ISS, with higher doses during lower solar activity and increasing flight altitude. For a 1000-day Mars mission, a total effective dose of galactic cosmic radiation of about 1 Sv is expected [83, 84], which is quite considerable and exceeds terrestrial lifetime radiation exposure limits, which amount to 400 mSv in the European Union. Risks of cancer and degenerative diseases are associated with this chronic GCR exposure (Fig. 10.12).

Solar Particle Events (SPE) emanating from the Sun (Sect. 10.3.1.2) result in increased proton fluxes that may reach the spacecraft or a celestial body surface. In LEO, protection by the Earth's magnetic field is still sufficient to protect from deadly SPE, but in free space or on planets or moons without magnetic field and atmosphere, high doses might be accumulated within hours or days in situations of insufficient shielding, e.g., in a spacesuit. Above a certain threshold, acute effects will occur (Fig. 10.12). In contrast to GCR, shielding of SPE protons is feasible in special compartments of the spacecraft, which can be surrounded by more material. Astronauts can protect themselves from an SPE in such a radiation shelter until the proton flux normalizes.

10.4.2 Acute Effects

Deterministic effects appear for acute global exposures classified as medium, high, and very high (0.2 to more than 10 Sv) by UNSCEAR [85].

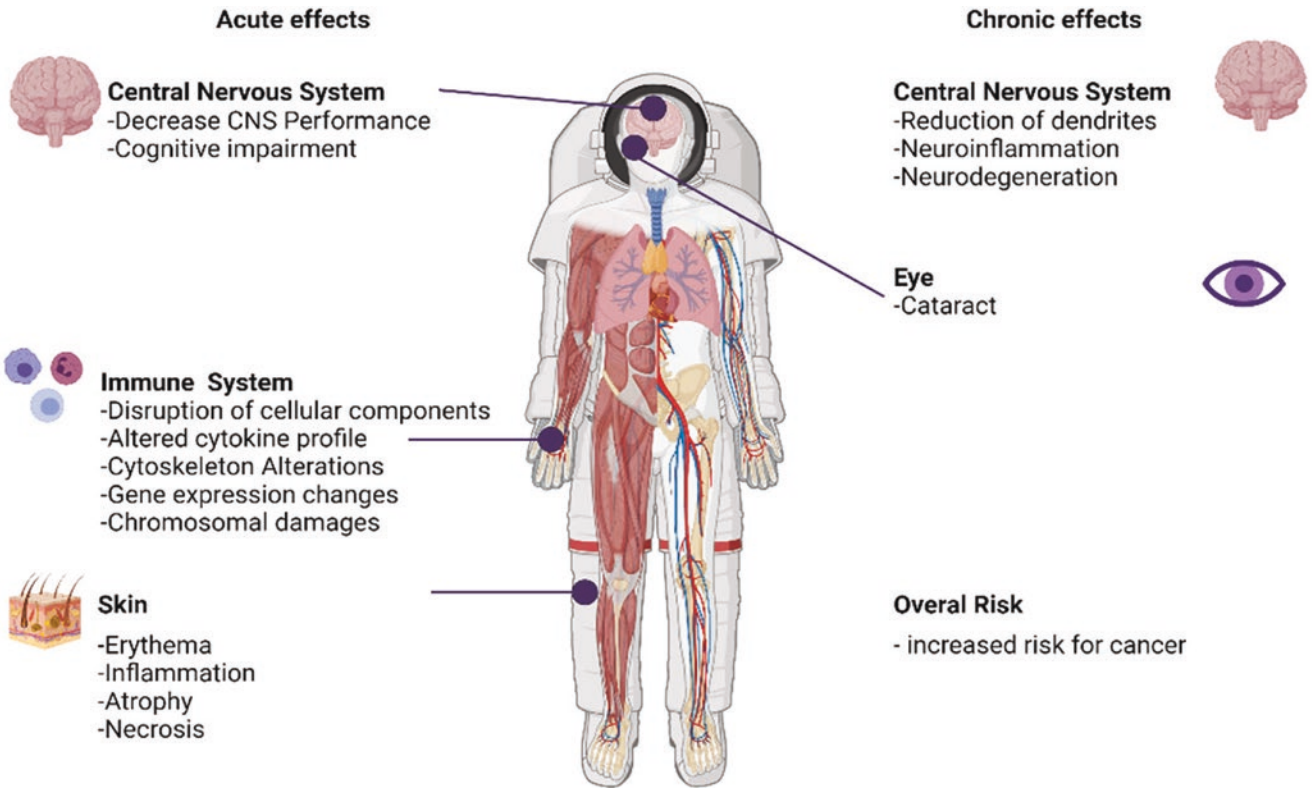

Fig. 10.12 Possible health effects of space radiation exposure

Under exceptional conditions of insufficient shielding during spaceflight, the exposure to mostly protons during a large solar particle event (SPE), the whole-body dose can reach several Gy or the skin dose even tens of Gy and thereby cause the acute radiation syndrome (ARS, see Chap. 2, Sect. 2.7.2). Such situations in the event of a solar flare of exceptional intensity can occur in LEO in areas of weakness of the Van Allen belts, extravehicular exit, and exit on extraterrestrial soil in a spacesuit or an insufficiently shielded vehicle. The total dose is delivered over a short period of time: generally, instantaneously but by definition over less than 4 days.

The acute effects affect rapidly renewing tissues which are particularly radiosensitive (bone marrow, digestive epithelium, germ cells, skin). The classic "radiation sickness" or prodromal syndrome (headache, dizziness, nausea, bone marrow hypoplasia) occurs for an exposure of 0.5–1 Gy. A dose of 3–4 Gy kills 50% of exposed individuals in 1 month [86]. Unlike the desired partial exposure of patients undergoing radiotherapy, solar flares are unpredictable, which seriously complicates mission planning for astronauts.

10.4.2.1 Chronic and Late Effects: Cancer and Degenerative Diseases

For several decades, NASA has collected data concerning acute and chronic morbidity and mortality in US astronauts in the NASA's Longitudinal Study of Astronaut Health [87]. One main aim is to determine whether astronauts' occupational space radiation exposure is associated with an increased risk of cancer or other diseases. The cohort is made up of 312 astronauts selected by NASA since 1959. Employees at the NASA Johnson Space Center in Houston, Texas, served as the control group. In January 2003, just before the explosion of the Columbia shuttle, 29 deaths (9.3%) were counted in the group of astronauts versus 17 (1.8%) in the control group. Note 20 accidental deaths among astronauts (versus 2 in the matched group). No other cause reached the threshold of significance.

Compared to the control group at matched age, astronauts had a higher specific mortality rate (SMR) from cancer. This difference was not significant. However, both groups had a lower specific mortality rate than the general population. Fourteen cases of cancer have been described in astronauts (not counting 33 cases of non-melanoma skin cancer), which represents a relative risk of 1.59 compared to the Air Force pairings but of 0.54 compared to the cohort of NCI (general population), which ultimately remains insignificant. A later study found that standardized mortality rates for astronauts were significantly below US white male population rates [88].

During a Mars exploration mission, each cell nucleus of an astronaut would be crossed by a proton or a secondary electron every 2 days, and by a heavier ion every month [89].

Due to their strong ionizing power, these ions appear to be the main vector of carcinogenic risk despite their low fluence.

The interval between irradiation and tumor appearance has been shown in rats to be shortened compared to conventional radiation [90, 91]; fewer events would be needed in the promotion of carcinogenesis induced by high-LET particles. Particle mass, energy, and charge can influence the cancer risk of an HZE particle.

The linear no-threshold (LNT) model used to predict the risk of cancer mortality in astronauts sent on interplanetary missions relies on data from atomic bomb survivors extrapolated to this particular population, to these types of particles, and to the dose rates encountered in the space environment. Though nearly universally used by public bodies to assess cancer risk, LNT is far from being a scientific consensus and its application for low dose rates is rather controversial—see Chap. 2. For cancer risk estimation, age at exposure, attained age, sex- and tissue-specific mortality and incidence, and latency has to be considered. Also, an important question is whether the additional cancer risk induced by space radiation exposure is independent of other cancerogenic events (excess absolute risk, EAR), or whether the risk depends on other cancer risks (excess relative risk, ERR).

Table 10.3 summarizes the LNT-estimated carcinogenic risk under different exposure conditions. The confidence interval includes epidemiological, physical, and biological uncertainties. The maximum acceptable risk for an astronaut dying from cancer is typically set at 3% [50].

Besides the calculated increased cancer risk for astronauts, cataracts might be triggered or promoted by space radiation exposure. Astronauts exposed to a dose of more than 8 mSv exhibit earlier and more frequent cataracts (in a study that identified 295 astronauts paired with as many US Air Force pilots) [92].

Table 10.3 Doses and LNT-based estimates for cancer mortality risk following space missions

	Absorbed dose (Gy)	Effective dose (Sv)	Risk of death by cancer (%) [$IC_{95\%}$]	
			Male 40 y.o.	Female 40 y.o.
Moon Mission (180 days)	0.06	0.17	0.68 [0.20–2.40]	0.82 [0.24–3.00]
Mars Orbit Mission (600 days)	0.37	1.03	4.00 [1.00–13.50]	4.90 [1.40–16.20]
Mars Mission (1000 days)	0.42	1.07	4.20 [1.30–13.60]	5.10 [1.60–16.40]

10.4.2.2 Chromosomal Aberrations and Biodosimetry

Due to the densely distributed ionizations around a heavy ion's path through a cell nucleus, severe DNA damage (Sect. 10.5.3) possibly leading to chromosomal aberrations (Sect. 10.5.2) can be induced. Therefore, chromosome damage induced in vivo was identified early as a sensitive biodosimeter [93, 94] that integrates radiation exposure in quality and quantity and also the individual radiosensitivity [95]. Peripheral blood lymphocytes are accessible by venipuncture and the chromosomal aberration test can be performed with these cells before and after flight.

In order to determine the effects of space radiation on astronauts, chromosomal aberrations were quantified already in Gemini astronauts before and after the spaceflight [96]. In some astronauts, a small increase was observed after the flight which did not correlate with flight duration (1–14 days), extravehicular activities, or diagnostic radioisotope injections [96]. Missions with a duration of up to 3 weeks did not result in an increase of the aberrations above background; after missions of 6 months or longer, a rise was clearly observed [95, 97–104], but dose estimation based on the cytogenetic analysis varied strongly [95]. Here, the inter-individual variability of the translocations' half-life in peripheral blood lymphocytes has to be considered [105]. Also, the basal aberration frequency and the reaction toward ionizing radiation varies from individual to individual [106–108]. Furthermore, the effects of multiple space missions might not be additive [109, 110]. Prediction of dicentrics frequencies for a Mars mission assume values 10–40× above background in peripheral lymphocytes [111].

For detection of reciprocal translocations, multicolor fluorescence in situ hybridization (mFISH) was first applied to members of the Mir-18 crew [112]. In search of a specific marker of heavy ion exposure, complex chromosome interchanges were suggested and analyzed in blood lymphocytes of astronauts [113, 114]. High-resolution multicolor banding (mBAND) of chromosome 5 can visualize intrachromosomal exchanges—long-term missions to the ISS did not increase this parameter [115]. Such inversions were only recently found in three astronauts during a 6-months ISS mission [116]. Complex chromosomal rearrangements occur very rarely in astronauts therefore their use as biomarker is limited [93]. Over the years, different cytogenetic or chromosomal signatures that allow reconstruction of absorbed dose and radiation quality were suggested, such as insertions [117], inversions [118], and complex chromosome interchanges, but up to now, no consensus for a biomarker of exposure to high-LET radiation has been reached [119] (see Sect. 8.7).

The relevance of the telomere elongation that was first observed during the 1-year ISS mission and its fast shortening after return to Earth [120], which was now also found during 6-months missions [116], for assessment of space

radiation risk is currently unclear. The telomere changes are considered as an integrative biomarker for effects of the spaceflight environment [121].

10.4.2.3 Light Flashes

Before the first human went to space, in 1952, Professor Cornelius A. Tobias made the famous prediction that cosmic radiation can cause unusual light sensations by interaction with the visual system. The Apollo-11 astronaut Edwin (Buzz) Aldrin was first reported to have perceived light flashes during the Moon mission [122]. This initiated a series of investigations already during the following Apollo missions [123], and later on Mir, Skylab, Apollo-Soyuz Test Project (ASTP), Shuttle missions, and on the ISS. They started with observation sessions and nuclear emulsion plates (Apollo light flash moving emulsion detector, ALFMED). The observations were later combined with sophisticated particle detectors in the Silicon Eye (SilEye-1 and -2) experiments on Mir [124], and Alteino-SilEye-3 and Anomalous Long-Term Effects on Astronauts (ALTEA) experiments on ISS, which included also an electroencephalograph.

The observations of the Apollo astronauts resulted in an average event rate of one light flash event in ~3 min [123]. In LEO, when passing through the SAA, the light flash rates are very high [125], and outside the SAA, light flash frequency is higher in the polar parts of the orbit than in equatorial latitudes [126]. The number of light flashes perceived in LEO varies on average between one every minute up to one every 7 min on Mir [127] or every 20 min [128, 129] dependent on the orbital height, the inclination, the shielding of the spacecraft and solar activity [130].

So, in conclusion, contrarily to the usual statement that we have no senses to perceive ionizing radiation, when closing their eyes, most space travelers can "see" the exposure to galactic cosmic rays and trapped radiation as mostly colorless light flashes or phosphenes in the form of spots, stars, streaks, or diffuse clouds of light [125]. About 15–20 min of dark adaptation is required [123] so that they are usually perceived before falling asleep.

This light flash phenomenon is explained by a visual sensation that is produced by the interaction of highly energetic heavy ions with the retina of the eye [131, 132] or possibly with visual centers in the brain or the optic nerve after penetration of the spacecraft walls and the eye or head. The interaction might be direct or indirect via Cherenkov radiation in vitreous humor which is emitted as light when the charged particle passes through it with a velocity higher than the speed of light in the vitreous humor [133]. The probability of a heavy ion to cause a light flash has been estimated to be around 1%—with increasing probability with increasing LET—and for protons to be below 0.001% in LEO [127]. A deleterious effect of the flashes on vision is not suspected, but some astronauts report that their sleep was disturbed by light flashes.

10.5 Biomolecular Changes Induced by Space Radiation

Ionizing radiation, which exists primarily in the form of high-energy, charged particles make up space radiation. The radiation environment in space is characterized by a high complexity due to different sources and a higher number of particle species, and a broad energy range. Galactic cosmic radiation (GCR), solar particle events (SPE), and, in LEO, trapped radiation are the naturally occurring sources of space radiation.

The exposure to GCR occurs at a low dose rate on the organismal level, but strong cellular effects might be triggered in case of a "hit" by an energetic particle, especially high Z and high energy (HZE) particles or heavy ions. HZE particles make up only 1% of GCR therefore only small hit frequencies are expected in the human body that could be responsible for late effects [134]. First evidence of biological effects of HZE particles was found in mice after a high-altitude balloon flight when the coat of black mice locally turned grey [135]. Single particle effects on different dormant biological systems under spaceflight conditions were proven by means of the Biostack experiments on the Apollo-16 and -17 missions [10, 136]. In this experimental system, biological systems and detector foils were stacked onto each other to allow assignment of heavy ion hits to the biological systems. Heavy ion hits were detected in plastic foils (cellulose nitrate, polycarbonate), silver chloride crystals, and nuclear emulsions. The biological systems were immobilized on the foils with water-soluble polyvinyl alcohol and included *Bacillus subtilis* spores, seeds of the thale cress *Arabidopsis thaliana*, roots of the field bean *Vicia faba*, eggs of the brine shrimp *Artemia salina*, insect eggs (stick insect, *Carausius morosus* and rice weevil, *Tribolium confusum*), and protozoa cysts (*Colpoda cucullus*). The outgrowth of *B. subtilis* after germination was significantly reduced after an HZE particle hit [137, 138]. During the development of brine shrimp eggs that were hit by a single particle, abnormalities appeared at the extremities, the thorax, and the abdomen [139] and the eggs showed the most sensitive reaction toward HZE particles compared to the other biological systems in Biostack [137, 140]. Developmental abnormalities were also found in hit insect eggs [141]. The total dose for the Biostack experiments was quite low (5.8–7.5 mGy), and ~0.03 mGy was allocated to the HZE particles, whereby it has to be considered that the local dose in a hit cell can be much higher than the total dose.

These experiments were continued in LEO using the Free Flyer Biostack Experiment (LDEF—Long Duration Exposure Facility) [142], EURECA—European Retrievable Carrier [143–146], and the biosatellites COSMOS 1887 and 2004 [147, 148] and refined, so that synergistic effects of

HZE particle hits and microgravity in the developmental disorders of *C. morosus* were revealed.

These intriguing results showing strong deleterious effects of single particle traversals and even an enhancement by other spaceflight environmental effects initiated a multitude of biological experiments in space and at heavy ion accelerators (see Sect. 10.9) in order to quantify the biological effectiveness of HZE particles, to understand the underlying mechanisms and to develop countermeasures. A variety of experimental models are used for these experiments (see Sects. 10.5–10.7, and 10.8.2). The uncertainties in risk assessment for cancer and non-cancer effects in the central nervous system and other organ systems for astronauts are still unacceptably high therefore further investigations into the biological effects of HZE particles are necessary. The experimental approaches shown in Box 10.3 below take the low dose rate but strong biological effects in case of a particle hit into account.

Box 10.3 Experimental Approaches for HZE Particle Effects

Natural GCR exposure

- Correlation of biological effects with single particle hits by combination of biological model and detector foil, e.g., Biostack; can be combined with 1xg reference centrifuge to determine contribution microgravity effects
- Correlation of light flashes with HZE particles that traverse astronauts' eyes
- Dose accumulation over weeks or months by storing dormant or freeze-dried or deep-frozen cells or small organisms in space, subsequent reactivation and measurement of radiation damage or response
- Determination of spaceflight effects by exposure of, e.g., fruit flies, rodents, or other organisms on satellites or high-altitude balloons

Exposure to selected HZE particles

- Exposure of a variety of biological systems at heavy ion accelerators or microbeam facilities to selected heavy ions (singe particle at defined energy or mixture of particles of defined energies) and analysis of the biological response

10.5.1 Cellular Survival, Cell Death, and Proliferation

As described in Chap. 2, radiation quality is an important factor influencing the cell death response. It can affect the extent and mode of cell death. A stronger cell killing of human cells by alpha particles with an LET up to 100 keV/µm was already observed in the 1960s [149], indicating an RBE for cell killing up to 7. Since then, survival data after heavy ion exposure were collected for many mammalian cell types including primary cells and tumor cell lines using the colony forming ability (CFA) test which is described in Chap. 2. This was less driven by space radiation research but by tumor therapy research to identify suitable ions and to determine the cell killing RBE for treatment planning. The shoulder observed in the dose response curves for cell killing by low-LET radiation disappears in high-LET survival curves, resulting in purely exponential dose–effect relationships and indicating the lack of repair capacity after heavy ion exposure [150] (Fig. 10.13).

Clonogenic cell survival data for more than 1100 experiments comparing the effects of ion irradiation to photon irradiation are available in a database established by the GSI biophysics group [151]. The database is called Particle Irradiation Data Ensemble (PIDE, www.gsi.de/bio-pide). The maximal RBE for cell killing (10% survival level) was observed in the LET range of 100–200 keV/µm with values of 2–7 [151]. This large variation in RBE is explained by the influence of particle species and energy in addition to LET, of cell type and other experimental factors. At LETs above ~200 keV/µm, more energy is deposited in a cell traversed by a particle than is required to kill the cell and more hits per cell cannot produce more cell death as any hit will kill the cell, resulting in a decrease of RBE that is called "overkill effect."

The clonogenic survival data integrate cell death by various modes such as mitotic catastrophe, apoptosis, necrosis,

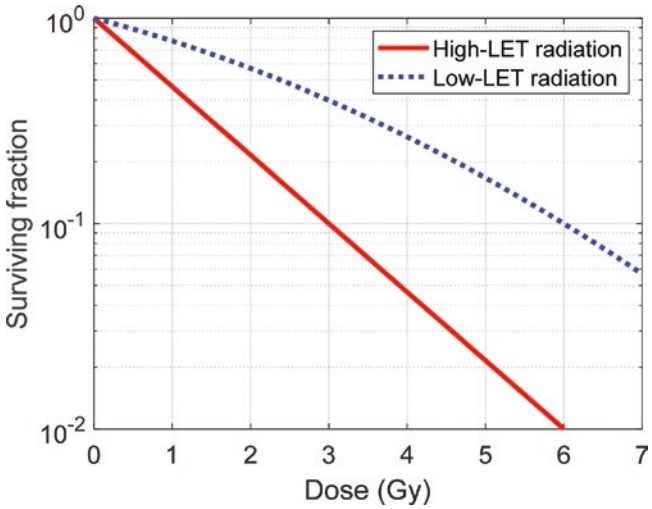

Fig. 10.13 Survival of mammalian cells after exposure to low linear energy transfer (LET) and high-LET radiation. Low-LET radiation includes photons, electrons, positrons, protons, and more. High-LET radiation encompasses heavy ions, and, depending on energy, also He ions and neutrons

autophagy, and other mechanisms (see Chap. 2) and permanent cell cycle arrest, possibly accompanied by cellular senescence. As for low-LET radiation, it depends on the cell or tissue type whether a cell population is prone to ionizing radiation-induced apoptosis [152]. Apoptosis might occur at higher rates after high-LET radiation exposure compared to low-LET irradiation with a maximum at a LET of ~100 keV/µm [153].

The consequences of heavy ion-induced cell death for the organism can be that transformation of a heavily damaged cell is prevented thereby protecting from cancer. This effect also limits the number of cells with mutations (see Sect. 10.5.4) or chromosomal aberrations at a LET >200 keV/µm (see Sect. 10.5.2) and cellular transformation (see Sect. 10.5.5). On the other hand, deleterious effects might occur such as depletion of stem cell pools or loss of terminally differentiated cells with no or low regeneration potential that might affect the functionality of a tissue or organ.

For some microorganisms, growth and viability were measured during space missions. A 14-days exposure of *Escherichia coli* on the Space Shuttle or 140-d exposure on Mir did not result in any differences in viability and mutations frequencies in comparison to ground controls [154, 155]—the same was the case in *Saccharomyces cerevisiae* [156]. Using repair-deficient *E. coli* mutants, DNA polymerase, and 3′→5′ exonuclease were identified as the most important enzymes for GCR-induced DNA damage in *E. coli* [157]. Also, the slime mold *Dictyostelium discoideum* did not grow differently and did not show differences in the mutation frequency in the spores during a 7-days Shuttle flight [158, 159], but the number of spores per fruiting body was reduced [160].

10.5.2 Chromosomal Aberrations

Chromosomal aberrations are alterations in DNA structure that become microscopically visible after following a chromosome staining protocol [161] (see Chap. 2). They can result from mis-rejoining of DNA ends from ionizing radiation-induced DNA double strand breaks (DSB), from lack of repair leading to terminal deletions and incomplete exchanges or from chromosome mis-segregation [162, 163]. They are exquisitely and quantitatively sensitive to ionizing radiation. Symmetrical resolution of the DNA DSB can lead to chromosomal interchanges resulting in translocations which are usually nonlethal. Asymmetrical resolution produces among other dicentrics (chromosomes with two centromeres) and acentric fragments, mostly contained within micronuclei; also, during the repair process, DNA sections can be lost, producing a deletion [164]. Ionizing radiation can also induce quadriradials (U-type by asymmetrical resolution, X-type by symmetrical resolution). Complex and asymmetric aberrations such as dicentrics usually lead to cell death (lethal aberrations) [163].

They are determined during metaphase or by chemically induced Premature Chromosome Condensation (PCC, see Chap. 2) during interphase [165], usually in lymphocytes or fibroblasts, providing data on a cell-by-cell basis. Their dose–response relationship follows a curvature. While dicentrics and acentric fragments can be detected with a GIEMSA staining, mFISH is required for interchromosomal translocations and mBAND for intrachromosomal translocations (see Sect. 10.3.4). Inversions can be detected by Directional Genomic Hybridization (dGH) [166].

Chromosomal aberrations are of high interest in space radiation biology as they are an early-stage effect and regarded as a surrogate endpoint for cancer risk as many human cancers are linked to them and all "clastogens[2]" are both mutagenic and carcinogenic.

For carcinogenesis, the surviving cells with chromosomal aberrations are relevant. The fraction of these cells depends on LET, track structure, and fractionation (Box 10.4).

HZE particles have a very high efficiency in inducing chromosomal aberrations—the RBE in comparison to low-LET radiation was estimated to reach 30–35 during interphase [163, 167, 168]. Furthermore, high-LET α-particles at low fluences (1 track per cell nucleus) were more efficient in inducing complex aberrations in human peripheral blood lymphocytes than X-rays [117]. Complex chromosome aberrations are defined as aberrations that involve three or more breaks in at least two chromosomes. Here, the particle track structure comes into play [169]. Delta rays move out of the primary particle track, producing further ionizations that can induce damage. This damage might interact with other breaks generated by either a separate track or delta rays emanating from it (intratrack action). The range of the delta rays is proportional to the specific energy of its corresponding primary particle. Higher energy particles would have a greater chance of track interaction than their lower energy

Box 10.4 Factors Influencing Induction of Chromosomal Aberrations by Ionizing Radiation

Dose rate
Fractionation
Linear energy transfer (LET)
Track structure
Cell nuclear geometry (e.g., spherical or flat)

[2]A "clastogenic" agent directly causes DNA strand breaks or disturbs normal DNA-related processes resulting in insertion, deletion, or rearrangement of chromosome sections.

counterparts because of the longer range of the delta rays where breaks can be close in space and time at high doses and dose rates as they are produced by multiple tracks (inter-track action). The breakpoints induced by delta rays add up to those produced in the primary particle track. Hence, the number of exchange breakpoints and their spatial arrangement are important determinants for the formation of complex exchanges. For example, the number of breakpoints per cell was higher for ^{56}Fe ions (1.1 GeV/n) and α-particles (0.9 MeV/n) in comparison to ^{137}Cs γ-rays. In spherical cell nuclei, one particle traversal is sufficient to produce two breakpoints, e.g., in a lymphocyte [170, 171]. In summary, HZE particles produce more breakpoints per track and more highly complex exchanges compared to low-LET radiation [118] (Fig. 10.14). These complex aberrations partly disappear between the first and second cell division after radiation exposure, but some are transmissible and might be stable through several cell generations.

10.5.3 DNA Damage and Repair Kinetics

As other radiation qualities, protons, α-particles, and HZE particles can induce various types of DNA damage by direct ionization or indirectly through radiolysis of intracellular water (see Chap. 2). Among base damage, loss of bases, DNA-DNA and DNA-protein crosslinks, single strand breaks (SSBs), and double strand breaks (DSBs), DNA DSBs are the most severe DNA lesion. Unrepaired DNA DSBs are at the center of biological effects such as cell killing and chromosomal aberrations and are trailblazers of the majority of early and late effects induced by ionizing radiation exposure [163, 172, 173].

What makes particle radiation special is the multitude of ionizations localized along the particle's path through the cell. The spatial distribution of direct DNA damage differs strongly for low- and high-LET radiation, with a diffuse distribution for the former and clusters for the latter. Such clusters of different damage (base lesions, abasic sites, SSB, DSB, etc.) within a few helical turns of DNA are called complex DNA damage (Fig. 10.15) (formerly: multiply damaged sites or clustered DNA damage) [164, 174, 175].

Although the contribution of direct action to the biological effectiveness of high-LET radiation is larger than indirect action [176], reactive oxygen species (ROS) generated by radiolysis can also play a part in the overall radiation effects. As the lifetime and diffusion range of ROS are small, only radicals produced in DNA's vicinity are relevant for DNA damage induction and increase in its complexity. With increasing LET, the contribution of direct effects rises, and the indirect effects drop. Low-LET radiation and endogenous ROS rarely induce complex DNA damage [163].

The detection of GCR-induced DNA damage succeeded in HeLa cells during the Shuttle and Mir missions [177–179]. In human lymphoblastoid cells that were stored at –80 °C for

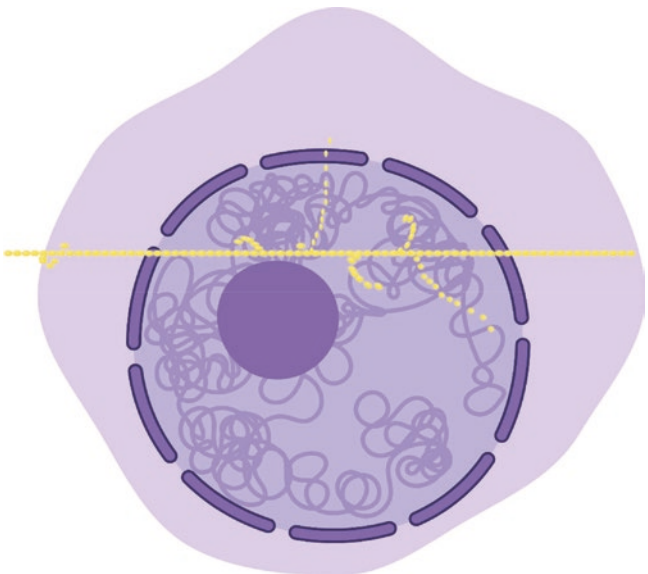

Fig. 10.14 As a heavy ion travels through a mammalian cell nucleus, a multiple of ionizations is produced, damaging a chromosome arranged in its nuclear territory several times. Delta rays emanating from the primary track can induce further damage. Therefore, traversal of high-LET radiation through a cell nucleus can produce many breakpoints in chromosomes

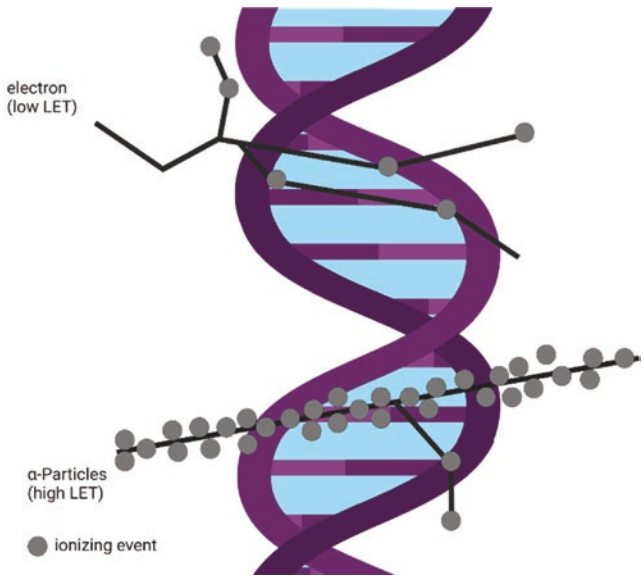

Fig. 10.15 Comparison of ionizations (grey dots) in a DNA molecule that are induced by electrons as an example of low-LET radiation and by a high-LET α-particle. The ionizations produced by the α-particle are located densely along the track, with some secondary electrons (δ rays) generated while traversing the cell. This spatial distribution goes along with a higher probability of simultaneously breaking both DNA strands thereby producing a double strand break (DSB), and also further damage to bases and single strand breaks (SSB) in close proximity which is then called complex DNA damage

several months on ISS—in total 134 days at an average dose rate of 0.7 mSv/day, one particle track per 100 cells was detected by means of immunofluorescence staining of γH2AX after return to the ground (see below) [180]. Such tracks were also observed in human fibroblasts that were cultivated for 14 days on the ISS [181].

10.5.3.1 Repair of HZE Particle-Induced Double Strand Breaks and Complex Damage

Various DNA damage repair pathways ensure genome integrity and stability in uni- and multicellular organisms. The current understanding is that multiple repair pathways have to be coordinated to repair complex DNA damage making it very challenging, that short fragments might be lost during repair and that multiple breakpoints in the DNA ribose-phosphate backbone can favor complex genomic rearrangements [164, 182]. The damage might still persist at DNA replication because of repair delays that were observed after HZE particle exposure. If repair of complex lesions is completed, its fidelity might be lower when compared to simple DNA damage [183–185]. After ^{56}Fe ion (1 GeV/n) exposure, 14% of the damage remained unrepaired compared to 5% after γ-ray or α-particle exposure [171]. In vivo, persistent DNA DSBs were found even 1 month after exposure to iron ions [186]. Growth arrest, cell death, or senescence are possible consequences of such unrepaired DNA damage [164], while mutations and chromosomal aberrations are key steps in cellular transformation and tumorigenesis.

DSBs are mainly repaired by nonhomologous end joining (NHEJ) and homologous recombination (HR) in eukaryotes (see Chap. 2). DNA DSB repair follows biphasic kinetics with a faster velocity in the beginning and lower speed at later timepoints. The phosphorylated form of the histone variant H2AX (γH2AX) [187, 188] as a marker of DNA DSB is often applied to microscopically visualize DSB induced by high-LET radiation exposure, sometimes in combination with antibodies binding to 53BP1 or other DSB repair proteins or to oxidative base damage [189]. After immunofluorescence staining, fluorescent foci indicate γH2AX and 53BP1 accumulation around DNA DSB. Ground-based experiments performed at heavy ion accelerators allow quantification of DNA damage induction and DNA repair by one ion with a specific energy or, since lately, several ion species with specific energies hitting the cells from one direction (see Sect. 10.10.4). They are usually performed additionally with low-LET radiation for comparison.

For example, in human fibroblasts, repair of DSB induced by carbon ions was slower than those induced by proton or helium ion irradiation and the size of the repair foci increased with increasing LET [190]. Larger repair foci that persist longer are a common finding when exposure to heavy ions and X-rays are compared [191, 192]. One day after exposure to 1 GeV/n iron ions, 30–40% of the 53BP1 and γH2AX foci still remained indicating the extent of residual damage [193]. The slow repair kinetics and incompleteness of repair of DNA damage induced by high-LET radiation [190, 191, 194] are consistent findings of experiments with mammalian cells at heavy ion accelerators. Also, there are some hints that high-LET radiation inhibits c-NHEJ and shifts toward error-prone alternative nonhomologous end joining repair and microhomology-mediated end joining, resulting in a lowered fidelity of repair for days or weeks [195]. Other studies have shown that the repair of complex DNA requires DNA resection for processing at the DNA ends in G1 and G2 cells and forces the pathway choice toward resection-dependent HR [196, 197].

As mentioned above, to repair complex DNA damage, other repair pathways might be involved such as base excision repair (BER) and/or nucleotide excision repair NER [198]. Oxidative base damage such as 8-oxoguanine can be restituted by BER starting with damage recognition and removal by a DNA glycosylase and final steps by polymerase and ligase proteins [172]. NER is responsible for the repair of larger helix-distorting lesions.

In summary, DNA damage complexity increases with increasing LET, resulting in less effective DNA repair, a higher rate of residual lesions, genomic instability, and enhanced cell killing [174].

10.5.3.2 Effects of Other Spaceflight Environmental Factors Such as Microgravity on DNA Repair

The results of the Biostack experiments raised the question of whether microgravity or other spaceflight environmental factors affect DNA repair processes, as explained hereinafter. The advanced Biostack experiments included an inflight 1*g* control on a centrifuge, allowing the separation of effects of microgravity and of all other environmental factors. In this experiment, eggs of the stick insect *Carausius morosus* were exposed in space and the HZE particle hits were traced back to the eggs by means of particle track detector foils. Back on Earth, the insects were allowed to hatch. When the eggs were hit by an HZE particle under microgravity, more abnormalities were observed compared to hits during centrifugation at 1*g*, indicating additive or even synergistic damaging effects of cosmic radiation and microgravity [144].

Therefore, DNA repair and radiation response under microgravity were examined in further spaceflight experiments using a 1*g* centrifuge inflight control and in ground-based simulation using clinostats or random positioning machines. For determining subtle differences in DNA repair capacity or kinetics, a high level of DNA damage has to be induced. For this purpose, the dose rates of GCR in LEO on the Space Shuttle or on ISS are too low; therefore, DNA damage has to be induced by irradiation on ground in a metabolically inactive state, by irradiation in space using an arti-

ficial radiation source brought in LEO or by incubation with chemicals. When radiation damage was already induced on ground using a radiation source, cooled cells were brought to space and activated there to repair their DNA under microgravity [199, 200]. Alternatively, DNA DSB were induced by bleomycin [201] or restriction enzymes [202] during spaceflight. Often, no or only small interactions were found [203, 204]. In yeast however DNA DSB repair was delayed under microgravity, suggesting additive effects of radiation and microgravity [205, 206]. In human fibroblasts and *Bacillus subtilis*, microgravity did not influence the repair of DNA SSB and DSB [200, 207]. Also, ligase activity [204] and DNA replication [208] were not affected. The expression of genes involved in the DNA damage response was altered under microgravity [209–211]. Besides these gene expression changes, a growth-stimulating effect of microgravity was observed in many ground-based and space experiments that might contribute to the microgravity effects on the DNA damage response [209]. In ground-based experiments, limitations of various microgravity simulators have to be considered [212], especially the generation of shear forces [213] as possible confounders. For microorganisms, such as bacteria, it has also to be considered whether they are motile because of, e.g., flagella or not, and the effect of microgravity can be most likely attributed to changes in the medium surrounding the microbes [214].

Animal experiments addressing the question of DNA repair under spaceflight conditions are scarce. After a 14-day spaceflight, the level of the tumor suppressor p53, which acts as a transcription factor in the DNA damage response, was increased in the muscle of mice compared to ground control mice [179]. Experiments with the nematode *Caenorhabditis elegans* during the Shenzhou-8 mission revealed changes in the expression of four microRNAs and of 4.2% of the genes involved in the DNA damage response after 16.5 days of microgravity when compared to the inflight 1*g* control [215]. Hindlimb unloading is used in rodent models to simulate on ground the head-ward fluid shift that occurs in microgravity. After 21 days of hindlimb unloading and low-dose irradiation of mice, some genes involved in DNA repair, chromatin organization, and cell cycle were differentially expressed in the spleen compared to control mice [216].

10.5.3.3 Future Space Experiments

Space experiments are the only way to unambiguously identify the effects of real microgravity on biological systems, here the enzymatic repair of radiation-induced DNA damages. The opportunities to perform experiments with actively metabolizing organisms in space are rare and usually have a long lead time from the acceptance of an experiment proposal to the execution of the experiment in space.

The Biolab facility in the Columbus module of the ISS provides many possibilities for biological experiments on microorganisms, cells, tissue cultures, small plants, and small invertebrates in LEO (https://www.esa.int/Science_Exploration/Human_and_Robotic_Exploration/Columbus/Biolab). However, experiments on the ISS are subjected to limitations such as up- and download mass, up- and download temperature conditions, availability of a suitable facility in space, data downlink, number of sample replicates, appropriate control experiments in space and on ground. The Biolab facility will be used for LUX-in-Space (ESA AO LSRA-2014-026, Team Coordinator: P. Rettberg), the first space experiment where the whole series of events from DNA damage induction in metabolically active cells to the different steps of enzymatic repair reactions will take place in real microgravity and the repair kinetics will be monitored by optical measurements in situ. The effects of microgravity will be clearly separated from other spaceflight factors by comparison with parallel samples on an onboard 1*g* centrifuge in the Biolab facility and in a parallel ground control experiment with identical samples in flight-identical hardware. Due to safety issues, ESA decided to apply UV radiation for DNA damage induction. It causes defined types of DNA damage, e.g., cyclobutane pyrimidine dimers, which are among those also induced by ionizing radiation. Bacteria serve as model organisms possessing the same type of nucleotide excision repair as all other living organisms including humans. The capability of bacterial cells to counteract radiation damage by activating genes involved in DNA repair will be assessed using a bioluminescent reporter gene operon under the control of the SOS regulon, known as the SOS LUX assay. The DNA repair kinetics will be followed by bioluminescence and optical density measurements. For the space experiment, TripleLux Part C preparatory work was already performed successfully to adapt the SOS LUX assay to the space conditions provided by the Biolab facility on the ISS. This experiment was canceled later by ESA due to a lack of available resources at that time and it is a predecessor of LUX-in-Space [217, 218]. The launch of LUX-in-Space is scheduled for 2023/2024.

Biosentinel will be the first deep-space experiment investigating the repair of DNA damage induced by space radiation (Principal Investigator: Sharmila Bhattacharya). It is a further development of NASA's biological CubeSats, small satellites with different payloads that were already flown successfully in LEO. Biosentinel will first follow a trajectory of cis-lunar flyby and, for 6–12 months, enter a heliocentric orbit. The organism under investigation is the budding yeast *Saccharomyces cerevisiae*. These eukaryotic cells are robust, desiccation resistant, were already flown in space before, and have similarities to cells of higher organisms such as humans. Cells from a radiation-resistant yeast wildtype strain and a radiation-sensitive Δrad51D mutant will be uploaded in a dry form. After different periods of time, during which the cells will accumulate radiation-induced DNA damage, the

cells will be activated by the addition of nutrient medium and their growth and metabolic activity will be measured optically. In parallel, another Biosentinel payload will be flown in the ISS, in addition to the corresponding ground reference experiment. The launch is scheduled for 2022 as a secondary payload of NASA's Artemis-1 mission [219, 220].

10.5.4 Mutagenesis

Mutations as a deleterious outcome of erroneous repair of space radiation-induced DNA damage are of special interest in radiation risk assessment as they can initiate the multi-step carcinogenic process [163, 182] and they can be responsible for genetic effects in the offspring if they occur in the germline. Mutations can be detected in cells that survived irradiation and are, as chromosomal aberrations, late endpoints of radiation-induced DNA damage. For improving space radiation risk assessment, the dependence of mutation induction by radiation of different linear energy transfer (LET) was examined in different biological systems: Mutation induction by heavy ions was determined in many organisms including bacteria (*E. coli*, *B. subtilis*), yeast (*S. cerevisiae*), *Neurospora*, *Drosophila*, *C. elegans*, *M. musculus*, plants, and mammalian cell systems including human fibroblasts and lymphoid cells. These were mostly ground-based experiments at heavy ion accelerators.

The hypoxanthine guanine phosphoribosyl transferase (HPRT, EC 2.4.2.8) gene (mutations on the single copy X-chromosome in male-derived cells) in human diploid fibroblasts was used in early studies of LET dependency of mutation induction. A maximum of around 7 times more mutations compared to low-LET radiation was observed for helium ions or heavier ions with a LET of 100–300 keV/µm [221]. The number of mutations per single track through a mammalian cell nucleus increases with LET, reaching saturation at around 100 keV/µm [222]. The induction of mutations in the X-linked HPRT locus in Chinese hamster cells by accelerated heavy ions reached a local maximum in the LET range of 80–100 keV/µm [223].

Studies on mutation induction in autosomes became possible by means of A_L human-hamster hybrid cells having one copy of human chromosome 11. In these hybrid cells, neutrons of various energies were more efficient in inducing mutations in the a1 locus on chromosome 11 compared to gamma rays; the RBE reached up to 30 at the 0.1% survival level [224]. The autosomal thymidine kinase gene (TK1) locus in human cells allowed investigation of the loss of heterozygosity (LOH) which can occur via deletion or allelic recombination and it revealed a higher peak of mutations at a lower LET (~50–100 keV/µm) compared to the HPRT mutations (up to 15× compared to ~5×). As for other biological endpoints, LET is not the only determinant of the biological efficiency of an HZE particle. The track structure means the energy deposition pattern varies for different ion species of the same LET. Such an effect of ion species was observed for mutation induction at the HPRT locus in human fibroblast-like cells—the RBE for mutation induction determined in this system was between 3.6 and 7 for carbon and neon ion beams in the LET range of 60–120 keV/µm compared to ^{137}Cs gamma rays [225].

Besides mutations observed in the direct hit cells, bystander mutagenesis can contribute to the overall mutation rate after particle exposure as it was observed, for example, after alpha particle exposure [226].

An experiment on the ISS designed to detect mutations in human cells that were induced by natural galactic rays made use of the frozen storage as described in Sect. 10.5.3. Frozen human lymphoblastoid TK6 cells were stored for 134 days in the Kibo module of the ISS and accumulated a dose of 72 mSv. After analysis on ground, a tendency for higher mutation frequency at the TK locus was observed in the flight samples compared to ground control [227]. Earlier experiments on Mir for 40 days with a model system based on *Saccharomyces cerevisiae* and *Escherichia coli* also revealed two to threefold higher mutation frequencies in some flight samples compared to ground samples, with a predominance of large deletions that might be caused by high-LET radiation [228].

10.5.5 Transformation

If mutations occur in tumor suppressor genes and inactivating them, or proto-oncogenes and activating them, cells can be transformed and lose growth control including anchorage-dependent growth. It can be seen as a surrogate marker for the carcinogenic potential of a radiation quality in question. Transformation can only occur in cells that survived the radiation exposure. In vitro, transformation of mammalian cells is determined by their ability to grow anchorage independently in soft agar. The soft agar test was applied to different cell types after exposure to HZE particles at heavy ion accelerators in order to determine their potential for transformation, usually in comparison to low-LET radiation.

Already in the 1980s, it was shown that HZE particles are more effective in transforming mammalian cells than low-LET radiation: In mouse embryonic cells (C3H10T1/2), the effectivity of transformation increased up to 10 with a LET ~200 keV/µm [229] while Hei et al. observed a plateau at LETs of 80–120 keV/µm [230]. In Golden hamster embryo cells, ^{14}N ions (LET 530 keV/µm) and ^{4}He ions (36 and 77 keV/µm) were ~3× more effective in inducing cellular transformation than gamma or X-rays [231]. Later, a maximal RBE for neoplastic transformation was found at a LET of ~100 keV/µm, reaching a maximum of seven [232]. In

human bronchial epithelial cells, iron and silicon ions (LET 151 and 44 keV/µm, respectively) were more efficient in inducing transformation than gamma rays from a ^{137}Cs source especially when these cells were oncogenically progressed by stable transfection of mutant oncogenes [233].

10.5.6 Cell Cycle Changes

Cell cycle arrests play a central role in the DNA damage response of dividing cells. Before the cell enters the next cell cycle phase, e.g., from G1 to S phase or from S to G2/M phase, they allow repair of damaged DNA (Chap. 2). They can therefore protect from cell death, mutations or chromosomal aberrations. Concerning the special radiation qualities present in space that are prone to induce complex DNA damage which might persist longer, stronger, or longer cell cycle arrests might be induced in comparison to low-LET radiation. Early experiments observing mitotic delay by time-lapse microscopic cinematography already gave hints that accelerated neon ions produce a stronger delay compared to Co-60 gamma rays [234]. High-LET radiation produces stronger and more persistent blocks in the G2 phase of the cell cycle than low-LET radiation [235]. In synchronous V79 Chinese hamster cells, the cell cycle delays per particle traversal increased with increasing LET and were primarily due to blocks in S and G2/M phase of the cell cycle [236]. Permanent arrest in the G1 phase can also be induced by high-LET radiation [237]. The relative biological efficiency of heavy charged particles with a LET in the range of 100–330 keV/µm for inducing cell division delays was 3.3–4.4 [236] and the percentage of mitotic cells as indication of an arrest at the early G2/M checkpoint decreased with increasing LET [238]. The cell cycle regulating protein p21 (CDKN1A) accumulates in nuclear foci rapidly after heavy ion exposure of fibroblasts [239]. Besides this, expression levels of cell cycle regulatory proteins might be affected to a higher extent by high-LET radiation compared to low-LET radiation [237], for example, after iron ion exposure p21 expression was much higher compared to gamma rays and persisted 10 days after irradiation [193].

10.5.7 Gene Expression

Similar to studies with low-LET radiation, gene expression studies after high-LET radiation developed from a focus on single genes (mRNA and protein level by Northern Blot, RT-PCR, real-time RT-qPCR, Western Blot) to arrays of multiple genes, microarrays [240] and detection of the levels of all mRNAs present in cell populations or even single cells by RNA sequencing. After exposure to ionizing radiation, signal transduction pathways can result in the activation of transcription factors. These transcription factors bind to binding sites in their target genes' promoters which are specific for them (usually short palindromic DNA motifs) [241]. Also, besides promoter or enhancer activation via transcription factor binding, epigenetic mechanisms can be responsible for (persistent) gene expression changes and are therefore the focus of mechanistic research (see Sect. 10.5.9).

In addition to spaceflight experiments, a huge amount of gene expression data from ground-based exposure to neutrons, protons, and different heavy ions for different experimental model systems exists. NASA GeneLab (https://genelab.nasa.gov/) offers a repository for space-related omics data, among others transcriptomics and proteomics from experiments with model organisms, cells, cell lines, and tissues. Currently, a comprehensive picture of gene expression changes is difficult to paint due to the multiple influencing factors that range from the model system (e.g., gut epithelial cells and human bronchial epithelial cells, tissue, animal model) to the methods, cell cycle phase, radiation qualities, doses, kinetics of exposure, timepoint after exposure, and additional spaceflight environmental factors (such as simulation of microgravity effects by hindlimb unloading). The interpretation of the data is complicated by the fact that in the majority of the heavy ion accelerator experiments, the dose is acutely applied within minutes, while exposure during long-term space missions is protracted over several months.

The emerging view is that heavy ions, especially iron ions are capable to induce a stress response persisting for several weeks in addition to an early transient response. This early response can encompass p38MAPK and TP53 activation and expression of its target genes, whereby the cell cycle regulator gene CDKN1A can also be expressed TP53-independently. In tissues, long-term changes in the expression of genes involved in inflammatory and free-radical scavenging pathways occur after iron ion exposure and these changes involve transcription factors such as signal transducer and activator of transcription 3 (STAT3), GATA binding protein 4 (GATA4), Nuclear Factor κB (NF-κB) and nuclear factor of activated T cells 4 (NFATc4) [242]. In human cells, NF-κB was strongly activated by heavy ions, its activation depended on LET [243] and the expression of several chemo- and cytokines was increased [244].

10.5.8 Telomeres and Aging

HZE particles are potent inducers of senescence, more potent than gamma rays. Senescence-associated changes in the tumor microenvironment may induce invasion and stemness of tumor cells. Senolytics can be applied to eliminate senescent cells and thereby deplete senescent stromal

cells with tumor supportive roles. Shortening of telomeric sequences can lead to telomere fusions and contributes the chromosome instability after heavy ion exposure [245]. Furthermore, accumulation of short telomeres eventually triggers apoptosis or senescence. Unlike normal somatic cells, germline, stem, and tumor cells avoid the latter through a high expression of telomerase. Due to natural telomere shortening during cell division, telomere length is highly linked to aging [246]. Considering the environmental radiation exposure during spaceflight, with higher levels of HZE particles compared to on Earth, NASA investigated the effect of spaceflight on telomere length in the twin study. The twin study examined molecular- and physiological differences of twin astronauts, one spending a year onboard the ISS and the other on Earth [120]. Telomere lengths of peripheral blood mononuclear cells (PBMCs), collected from peripheral blood samples taken preflight from both twins were of similar length. However, during spaceflight, the space twin's telomere length increased significantly, while the Earth twin's telomers remained stable during the study. Once returning to Earth, the increased telomere length diminished within 48 h and the number of short telomeres increased compared to preflight [116]. While an unexpected finding, increased telomere length has recently been associated with other biological functions such as DNA damage response, cell cycle kinetics, and mitochondrial stress [247]. Indeed, chromosome aberrations (inversions and translocations) were more frequent during spaceflight and inversion frequencies of the space twin remained elevated postflight, consistent with ionizing radiation exposure inflight. Furthermore, DNA damage repair pathways were upregulated in several circulating immune cells, suggesting increased genomic instability due to ionizing radiation during spaceflight [121]. Similar results (increased telomere length and chromosomal aberrations) were also seen in astronauts during a 6-month spaceflight mission. While telomerase activity likely is responsible for the increased telomere length inflight, the actual contributing mechanism is still unknown. However, astronauts returning from 1 year and 6 month missions showed elevated telomerase activity upon return to Earth [116].

10.5.9 Epigenetics

Persistent gene expression and functional changes induced by space radiation exposure could be caused by changes in the epigenome. Changes in the DNA methylation profile and in the histone code encompassing methylation and acetylation of histones could therefore contribute to high-LET carcinogenesis and degenerative diseases and could represent possible prophylactic or therapeutic targets.

For example, in immortalized human bronchial epithelial cells, hypermethylation at CpG sites occurred early after Fe-56 ion exposure and persisted a long time [248]. Long-term epigenetic reprogramming after such exposure was also observed in hematopoietic progenitor and stem cells [249].

High levels of DNA methylating enzymes were also found in the hippocampus of Si-28 ion irradiated mice that developed cognitive impairment [250].

In addition to heavy ion exposure experiments, combined exposure to simulated microgravity and chronic low-dose irradiation or spaceflight experiments using small animals or cell cultures and astronaut data reveal alterations in the methylome and histone modification status after combined exposure to spaceflight environmental factors such as microgravity and space radiation. The lasting imprint of high-LET radiation exposure on the epigenome might allow monitoring the cumulative biological impact of space radiation exposure [248].

10.6 Small Animal Experimental Models and Biological Changes of Space Radiation

10.6.1 Importance of the Use of Animals in Research and Their Particular Use in Space

The use of small animal models in research is debatable, but still essential to provide general information on cellular and molecular mechanisms, to develop new drugs and treatments. They are mainly used in fundamental scientific research, for the advancement and development of new diagnostic tests and treatment for diseases, for education of researchers as well as in safety assessments of drugs and chemicals.

Animals are a useful research subject for a variety of reasons. Only in living organisms, it is possible to study complex physiological processes. Furthermore, the environment of the experiment can be perfectly controlled (e.g., diet, light, housing, etc.). Also, they have a shorter life cycle so studies can be conducted throughout a whole lifespan or across generations. Animals are biologically very similar to humans and often suffer from similar health problems. In fact, mice share more than 85% of protein-encoding genes with humans—Why Mouse Matters, from the National Human Genome Research Institute (https://www.genome.gov/10001345/importance-of-mouse-genome).

Animal experiments can cause harm to the animal thus ethical review processes have been established around the world [251]. With respect to this, the 3R´s principle by [252] ensure the reduction of animal numbers, refining the test methods to lower the harm to the animal to a minimum and

replace animal experiments with alternative methods, when possible (Box 10.5).

Box 10.5 Russell and Burch's The Principles of Humane Experimental Technique was First Published in 1959

The aim of the principle is to improve the treatment of laboratory animals and at the same time advance the quality of scientific studies.

Replacement: Includes methods that avoid or replace the use of animals such as computer/mathematical models (in silico), cell culture models (in vitro), or relative replacement (e.g., invertebrates, such as fruit flies and nematode worms).

Reduction: With improved experimental design, modern imaging, or sharing data and resources, the total number of animals needed can be minimized.

Refinement: Modification in the experiment, which minimize pain, suffering, and distress and allow general improvement of animal welfare (e.g., improvement in the research animal housing conditions, analgesia, and anesthesia for pain relief).

The animals that are most used for terrestrial research are mice, fish, and rats. Since the beginning of space exploration also animals have been used in space programs. Similarly, to how microgravity and cosmic radiation can affect human health, animals are also affected. This is why during an early space mission, at the beginning of 1940, animals were used to investigate various biological processes and the effects of space flights on living organisms. On the 20th of February 1947 the first living organism, fruit flies, were sent to space with the V2 rocket. The dog Laika was the most famous and first mammal which was sent to an orbital spaceflight around the Earth (Fig. 10.16) onboard of the Soviet Spacecraft Sputnik 2 on 3rd November 1957 [253]. Since then, a variety of animals have been sent into space including rodents, ants, cats, monkeys, spiders, and jellyfishe. Nowadays the effect of space conditions on animals, including microgravity and radiation, can also be studied to a certain degree on Earth with the help of clinostats, particle accelerator, and X-ray machines. However, all factors of the complex space environment cannot be simulated simultaneously on Earth.

Fig. 10.16 On 3 November 1957 Laika was the first living mammal that was sent to space onboard the satellite Sputnik 2

10.6.2 Acute Effects

10.6.2.1 Acute Radiation Syndrome

In case of a large SPE and insufficient shielding, the acute radiation syndrome (ARS, see Chap. 2) might be induced, endangering astronauts' health and mission success. To understand the pathogenesis of ARS induced by protons and develop therapeutic approaches for space missions, experiments with different animal models including rodents, minipigs, and non-human primates were performed. Whole-body doses up to 2 Gy are expected when astronauts are exposed to large SPE in free space with insufficient shielding. In this dose range, effects on the immune system (see Sect. 10.6.2.3) dominate the syndrome. As the skin dose can be 5–10 higher, the skin might be damaged (see Sect. 10.6.2.2).

10.6.2.2 Skin Effects

Forming the barrier between the outside environment and the inside of the body, the skin is a vital organ. Different skin layers provide the skin with tensile strength and keep a proper barrier function to prevent body water loss, regulate the immune defense and temperature, and protect against ultraviolet damage. The outermost layer, the epidermis, is built mostly out of layers of keratinocytes that differentiate and migrate toward the skin surface. A balance between the proliferation of keratinocytes and shedding of dead cells at the surface of the skin regulates the thickness of the epidermal layer. Below the epidermis lays the dermal skin layer which is mostly composed of connective tissue. Skin's tensile strength and elasticity are provided by Collagen type I and III, and elastic fibers. Fibroblasts are the major provider synthesizing these proteins. Furthermore, they play a major part in skin wound healing by migrating to the side of the wound, recruiting other cells, and remodeling the extracellular matrix (ECM) to restore the injured skin [254].

The skin receives greatest dose and greatest number of stopping particles, particularly during solar flares [255]. SPE events during EVA could lead to higher skin dose than to internal organs. Furthermore, simulations of SPEs has shown

that the total skin dose for astronauts performing EVAs is estimated to be up to 32 Gy (for SPE simulation of August 1972) [31].

Radiation-induced skin injuries can be distinguished by several phases depending on the condition of exposure [256]. Early skin reaction is shown by erythema within a few hours after irradiation. After several weeks, inflammatory damage, erythema, loss of epidermal cells, moist desquamation, hyperpigmentation, edema/hyper-proliferation, and epilation can be observed. Late effects can develop after several months and include dermal atrophy, necrosis, and problems related to the deterioration of the skin vasculature. Skin problems, such as burns and slower wound healing, combined with a deprived immune system increase the risk of infections and hinder recovery from ARS [31].

Because of morphological similarities between (mini) pigs and human skin, these animals have been widely used to better understand the skin reaction to ionizing radiation. Furthermore, rodent models such as mouse, rat, or guinea pig have also been studied for ionizing radiation effects on skin.

Using porcine models, researchers have been able to indicate skin toxicity after exposure to a simulated SPE radiation resembling the energy and fluence profile of a SPE documented in 1989 [257]. Hyperpigmentation of minipig irradiated skin was observed 7 days after irradiation and lasted throughout the entire observation period. These observations were supported by an increase in melanin deposition found in the stratum granulosum. Further observations of increased proliferation, parakeratosis (an accelerated keratinocytic turnover) and increased amount of melanophages, are thought to be an indication of an inflammatory skin response after irradiation.

Other studies exposed minipigs to doses ranging from 5 to 25 Gy of electrons [258]. In agreement with previous mentioned study, a dose-dependent hyperpigmentation of the skin was observed as well as an increase in melanin deposition. Furthermore, in the highest dose exposed group of 25 Gy, skin wounds and ulcers developed 19 days after irradiation on body parts that received the highest dose (tail, ears, and legs). In addition, hair loss in the form of alopecia was observed along the dorsum of these pigs.

Low dose rate exposure of skin to low doses of photons, seem to mostly induce oxidative stress and ECM alterations as observed in a mouse model [259]. Skin gene expression changes related to oxidative stress and extracellular matrix (ECM) have been found after whole-body γ-ray exposure. At low dose rates, genes involved in the formation of reactive oxygen species (ROS) were significantly upregulated at doses of 0.25 Gy. Furthermore, dose rate effects were also found in ECM gene expression profiles. Enhanced expression of genes encoding ECM structural components were found after low dose rate exposure.

10.6.2.3 Acute Effects of Proton Radiation Exposure in the Immune System

The immune system consists of a variety of cells, processes, and chemicals that combine efforts to protect the body from foreign microbes, viruses, cancer cells, and toxins [260].

Dysfunction of the human immune system has been shown during [261] and even after space flight [262]. Among the causes of this immune dysfunction, an altered distribution of the cellular components and altered cytokine profiles [263], as well as cytoskeleton alterations and gene expression dysregulation [264] has been shown in many immune cells. When human lymphocytes are subjected to simulated cosmic radiation in vitro they show chromosomal damage, depending on the type of radiation shielding.

The adverse effects of space radiation on the immune system is one of the major concerns for space flight. The vast majority of the cellular components that constitute the immune system are highly sensitive to ionizing radiation [265]. It is still not clear if space radiation has a synergistic effect in combination with microgravity, principally in long duration missions and in the context of the immune system.

As mentioned, in vitro models have been widely used for studying the effects of space radiation on several cellular types. However, the complexity of most systems—such as the case of the immune system—require approaches that will better mimic physiologic conditions, either in ground-based studies or inflight campaigns. Several animal models that recreate some of the conditions of space flight have been developed for use on Earth. For immunology studies, murine models remain one of the most commonly used small animal model in space radiobiology. Rats exposed to 56-Fe (5 GeV/n) to total doses of 0, 1, 2, and 4 Gy showed a decrease in their lymphocytes, particularly B cells. In another study, mice were irradiated with total (single) doses of 0, 0.5, 2, and 3 Gy with 56-Fe ions. Red blood cell (RBC) counts diminished proportionally to the dose. All three major types of leukocytes also decreased [266].

Sanzari et al. [267] directed a series of radiation experiments using Yucatan minipigs. The animals were exposed to beams comprised of Solar Particle Events (SPE)-like protons, 155 MeV, and electrons, 6 and 12 MeV, with dose profiles that mimic SPE radiation. Their findings suggest that, based on the magnitude of the decrease and the time required to reach the lowest leukocyte counts after irradiation, the proton SPE radiation had more impact on the count than electron SPE radiation, with lymphocytes being the most sensitive type of leukocytes. After proton SPE radiation at skin doses >5 Gy, certain populations of leukocytes (neutrophils) had lasting effects following the irradiation (up to 90 days) [267].

For studying the intricate function of the immune system and how it responds to acute exposures of space radiation, small animal models are essential since they can showcase the network of phenomena. Adding up to the already chal-

lenging task of pinpointing the alterations occurring in the irradiated immune system we must find a way of adding the following to the equation: isolation, altered circadian rhythms, psychologic stress, and, of course, altered gravity levels.

Chronic and late effects of space radiation exposure encompass increased cancer risk, early cataract formation, and a possibly increased risk for degenerative diseases of several organ systems such as the cardiovascular and the central nervous system).

10.6.2.4 Cancer

Animal models of cancer induction by space radiation play a crucial role in the determination of the radiation risk associated with a space mission.

Firstly, they provide with information about the RBE of different space radiation components such as HZE particles for cancer induction in different organs when compared to a low-LET radiation quality, such as gamma rays or X-rays. The Radiation Quality Factor is derived from the RBE data for cancer induction by HZE particles to scale from gamma radiation to the mixed field of GCR in space radiation cancer risk models. If the RBE is above 1, a higher cancer risk can be assumed for space radiation compared to well-known terrestrial low-LET radiation qualities.

Secondly, experiments with high and low dose rates are the basis to estimate the dose and dose rate effectiveness factor (DDREF) to scale from acute to chronic radiation exposure and thereby account for dose rate effects. As animal experiments with exposure at low dose rates are rarely feasible at heavy ion accelerators because of restricted beam time access, dose-rate effect experiments were performed so far at neutron facilities.

Furthermore, animal models give insight into the mechanisms of cancerogenesis by HZE particle exposure, e.g., the role of non-targeted effects, and thereby allow to identify potential molecular targets for effective countermeasures (Box 10.6).

Box 10.6 Mouse strains

Inbred mouse strains are produced by at least 20 generations of brother-sister mating and they are traceable to a single founding pair. The individuals of an inbred strain are genetically nearly identical to each other and experimental results are highly reproducible. Examples: CBA mouse (cross of Bagg albino and DBA), C57BL/6 mouse (with black coat), BALB/c (Bagg albino) mouse.

Outbred strains provide genetic diversity and are effectively wildtype in nature with as little inbreeding as possible.

Mating of at least two strains led to the generation of the **first filial generation (F1) hybrid mice**.

The first animal experiment with HZE particles to determine cancer induction by single ion exposure used mice and focused on the induction of tumors of the exocrine Harderian gland which is located between eye and ear [268–271]. In these experiments, tumor prevalence was determined by sacrificing mice at a predetermined timepoint after exposure and the number of mice with tumors was counted or the number of tumors per mouse was counted. As this gland does not exist in humans, other animal models were developed and applied. Two different approaches predominate: either wild-type rodents, e.g., inbred, F1 hybrid, or outbred mice, or genetically altered rodent models are exposed to HZE particles at a heavy ion accelerator. Multiparent outbreeding strategies can reduce the strong effects of the genetic background that limit gene-environment interactions in studies with inbred, genetically homogeneous animals [272]. To consider sex-specific cancer types, optimally, both sexes are included [272]. After whole-body irradiation of wild-type rodents, they were followed up over the lifespan of the animals for tumor induction. Alternatively, rats were followed up by palpation until first tumor (time-to-cancer incidence), with an additional follow-up until death. After necropsy, histology was performed to determine the number and types of cancer, e.g., mammary tumors [273, 274]. Here, high numbers of animals are required to detect the increase of cancer incidence above the background cancer rates.

Therefore, genetically altered mouse models were developed in order to lower the number of mice and to mimic a specific cancer induction and promotion pathway, mostly for lung, gastrointestinal [275, 276] or liver cancer (hepatocellular carcinoma) [277, 278]. Using a genetically radio-sensitized model implies an assumption about the mechanisms of radiation-induced cancerogenesis—genetically engineered mice carry some, but not all mutations, needed to generate cancer. The rationale behind this approach is to consider somatic mutations in cancer genes such as *NOTCH1* and *TP53* that might be already present in astronauts when they depart for their first space missions as the number of mutations in the epithelium increases with age [279].

In risk models, development of leukemia (leukemogenesis) and induction of solid tumors are considered separately because of different latency periods after radiation exposure and dose–response relationships. Leukemogenesis is highly relevant for space missions because of its short latency in humans. The CBA mouse strain is susceptible to radiation-induced acute myeloid leukemia (AML) [280] which is explained by a deletion in chromosome 2 (PU.1) that can occur 1 month after irradiation. A point mutation in the second copy of the PU.1 gene causes a differentiation block in the myeloid cells which favor autocrine growth stimulation. In this model, the RBE of iron ions for induction of AML was 1, meaning that the risk of AML induction by high-LET iron ions and low-LET radiation is comparable. As only surviving

cells can be transformed into a cancer cell, a higher mutation and chromosomal aberration rate induced by HZE particles can be compensated by cell death from collateral damage after an HZE ion traversed a myeloid cell [277]. RBE for other cancer types can be much different as the effectiveness of HZE ions in inducing a specific cancer type depends on the mechanism responsible for the tumorigenesis in that particular cancer. For example, in the same mouse strain that was used for the AML studies, hepatocellular carcinoma (HCC) was induced by HZE particles with an RBE of up to 74 [278].

Concerning solid tumors, a special focus in the studies so far was to evaluate the stage of tumors that can be induced by HZE particles and on detailed studies on lung cancer, gastrointestinal cancer, and brain tumors (Box 10.7).

Box 10.7 Tumor Types Observed After HZE Particle Exposure of Outbred Mice Are Similar to Those Arising Spontaneously or After Gamma Irradiation

Pituitary adenoma, osteosarcoma, Harderian gland tumor, soft tissue sarcoma, thyroid adenoma, ovarian Granulosa cell tumor, mammary adenocarcinoma, histiocytic sarcoma, hemangiosarcoma, hepatocellular carcinoma (HCC), pulmonary adenocarcinoma, small cell lung cancer, myeloid leukemia, (thymic) lymphoma (T cell, B cell), brain tumors, e.g., gliomas [272].

The lung has the highest susceptibility to radiation-induced carcinoma incidence and mortality, based on analysis of human populations exposed to radiation (Life Span Study of atomic bomb survivors). A minimum of five genetic changes convert immortalized human lung epithelial cells to malignant tumors. For lung carcinogenesis, BALB/cByJ or C57/BL6 mice or the K-ras^{LA1} mouse model [281] were used. In C57/BL6 mice, lung tumors occurred in irradiated mice but not in controls and all were adenocarcinomas, with no significant differences between males and females and for dose fractionation (dividing a radiation dose into multiple fractions, see Chap. 4) versus single dose were found. Incidence of lung tumors was higher in high-LET-irradiated mice than in X-ray-irradiated mice, with an RBE above 6 for all investigated HZE particles (Fe, Si, and O ions) [282].

In the pathogenesis of gastrointestinal tumors, for instance, colorectal cancer and hepatocellular carcinoma (HCC), inflammation plays a crucial role. Animal experiments revealed that heavy ion radiation triggers a pro-inflammatory state which can be associated with late colonic tumors. Furthermore, premalignant polyps with mutations in the Adenomatous polyposis coli (APC) gene could be already present in middle-aged astronauts. In the small intestine, the formation of a few polyps and later adenomas and even adenocarcinomas can result from truncation of the APC gene at codon 1638 [283]. Therefore, a mouse model with a chain-terminating mutation by a mutation to a stop codon or a frameshift (see Chap. 4) in one allele of the APC gene was developed for colon cancer research (Apc$^{1638N/+}$). APC mutant mouse models show a good correlation with carcinogens implicated in human colorectal cancer. Delayed genomic instability in APC$^{1638N/+}$ mice paves the way to gastrointestinal tumorigenesis. In this model, no evidence for dose-rate effects with HZE particle exposure was found [275], indicating that the carcinogenic potential of HZE particles is independent of the dose rate.

Also, genetically altered mouse models for the formation of brain tumors are used in space radiation research as already experiments from the 1970s indicated that charged particles can induce glioblastomas: Monkeys (*Macaca mulatta*) irradiated with high-energy protons (55 MeV, penetration depth ~2.5 cm) surviving 2 years or longer developed glioblastomas [284]. Here, the focus is on the loss of tumor suppressors such as cyclin dependent kinase inhibitor 2A (Cdkn2a or Ink4-Arf), phosphatase and tensin homolog (Pten), and TP53 in astrocytes and on oncogene activation (e.g., epidermal growth factor receptor variant III, EGFRvIII) after irradiation. Iron and silicon ions were much more potent tumor inducers in "preinitiated" astrocytes than gamma rays [285].

The animal studies with single beam irradiations show that the efficiency of HZE particles to induce cancer is related to ion energy, LET with a peak RBE below 100 keV/μm, sex of the animals, and depends on the tumor type [275]. The RBE for cancer induction was recently determined to range from 5 to 16 [286], representing a snapshot that will be further updated as not all available data were included. Currently, based on the results of single beam irradiations, multiple beam experiments with up to 33 ion beams are performed at the NASA Space Radiation Laboratory (NSRL) using the GCR simulator in order to understand whether the effects of the different GCR components act in an additive or even in a synergistic manner in cancer induction.

10.6.2.5 Cataract

According to recent epidemiological evidence, radiation-induced cataract (see Chap. 2) occurs with a threshold absorbed dose of 0.5 Gy (0–1 Gy) of sparsely ionizing radiation, meaning that a cataract can arise after any ionizing radiation dose no matter how low if the remaining lifespan is long enough for its appearance. The 1 Sv GCR dose to be expected for a 1000-day Mars mission [83, 84] means that even the upper limit of the cataract-induction threshold dose confidence interval will be reached during a human Mars exploration mission. In astronauts, epidemiological data sug-

gest a higher risk for the development of cataracts in case of missions in LEO with high inclination [287].

Due to its germinative zone in the lens epithelium, the eye lens is a radiation-sensitive organ. These cells are actively proliferating during lifetime and finally differentiate into transparent lens fibers. In case cells are damaged, they cannot be eliminated from the lens which is covered by a capsule and not vascularized. Exposure of the eye lens to ionization radiation is thought to result in sub-capsular cortical lens opacification via various steps, starting with genetic damage of lens epithelial cells via changes in cell cycle control, apoptosis, differentiation, or other pathways controlling lens fiber cells' differentiation, and cellular disorganization.

Due to higher local dose and different patterns of cellular energy deposition from high-LET components of GCR, higher efficiency in the induction of lens-damaging effects is assumed than for low-LET radiation. Therefore, animal experiments were mostly performed to determine the RBE of HZE particles to induce lens opacification and to detect possible dose rate effects. In rats, the RBE reached 50–100 for HZE particles within LET above 80 keV/μm [288] and fractionation of exposure did not reduce the cataractogenic effect [289]. Neutrons as secondary particles occurring in spacecraft and on planetary or moon surfaces had also a high RBE for cataract-induction in rats [290].

To determine the role of genetic predispositions, mice that are heterozygous for Ataxia telangiectasia mutated protein (ATM) were exposed to HZE particles and cataract formation was followed. ATM plays a central role in the DNA damage response (DDR). Heterozygosity for the ATM gene predisposes carriers for early onset time and progression of cataracts even without exposure to ionizing radiation [291]. Also after gamma ray and 1 GeV/n iron ion exposure, cataracts appear earlier in ATM heterozygous animals compared to wild-type mice and the RBE for HZE particle induced cataract formation ranged from 4 to 200, whereby the highest values were found for the lowest dose (10 mGy) and RBE decreases with increasing dose [292, 293]. In conclusion, HZE particles present in GCR and neutrons as part of the secondary radiation field are highly cataractogenic and the mechanisms such as long-term changes in gene expression, complex DNA damage, and chromosomal aberrations in eye lens epithelial cells (LECs) are still under investigation.

10.6.2.6 Cardiovascular System

Exposure to space hazards, including microgravity and heavy ion exposure can cause harmful effects on the cardiovascular system during spaceflight. Upon entering microgravity, cephalad fluid shifts cause increased stroke volume and cardiac output. Furthermore, the cephalad fluid shift is also hypothesized to cause visual impairments due to increased cranial pressure [294]. During flight, mean arterial pressure is decreased, together with central venous pressure. Furthermore, decreased systemic vascular resistance, results from increased cardiac output, systemic arterial vasodilation, and decreased arterial pressure [295]. Other effects of microgravity exposure include hypovolemia, cardiac arrhythmia, cardiac atrophy, and orthostatic intolerance. Believed to be caused by fluid shifts and movement of interstitial water from the legs to the head, the fluid reduction and eventually hypovolemia results in a reduced number of red blood cells [296]. Moreover, cardiac atrophy occurs as a result of decreased metabolic demand and oxygen uptake during microgravity conditions. Together, cardiac deconditioning, i.e., hypovolemia, cardiac atrophy, and decreased cardiac output, causes a decreased exercise capacity and orthostatic intolerance post-flight [297].

While effects related to microgravity exposure during spaceflight are fairly well-known (albeit underexplored), impacts of the cardiovascular system from space radiation and heavy ion exposure during spaceflight are less known. Furthermore, studies from space analogs focusing on radiation effects have shown several effects on the cardiovascular system. Mice exposed to heavy ions show myocardial remodeling, resulting in hypertrophy and cardiac fibrosis [186]. Additionally, accelerated development of atherosclerosis has been found in mice after heavy ion exposure. Leading to a greater prevalence of myocardial infarction [298]. Both in vivo and in vitro models during space flight as well as using space analogs have been used to investigate underlying mechanisms of space-induced CVD. Important mechanisms include endothelial dysfunction, cellular apoptosis, cellular senescence, inflammation, and reactive oxygen species production [297].

10.6.2.7 Central Nervous System

Exposure to heavy ion, especially during long-term space mission, can also affect the central nervous system (CNS). The CNS is part of the nervous system and is composed of the brain and the spinal cord. It is responsible for perceiving any exterior information, transmitting, and subsequently processing it. Responsible for signal transmission are neurons, whereas glial cells (oligodendrocytes, microglia, or astrocytes) have diverse function such as the trophic support of neurons. As neurons are terminally differentiated and have a very restricted regeneration potential, damaged cells will usually not be replaced and thus damage might accumulate over months or years.

Acute CNS effects of ionizing radiation exposure are only observed after exposure to very high doses and can be expected in spaceflight only during very large Solar Particle Events (SPE) in case of insufficient shielding. Thus, for more than 20 years, possible effects of chronic low-dose exposure of the CNS to galactic cosmic rays (GCR) are discussed and a decrease in CNS performance of astronauts is suspected, which was also further evidenced in animal studies [299, 300]. Normally rodent animal experiments are performed at heavy ion accelerators simulating space radiation at doses below 1 Gy in a relatively short time, revealing impairment in

cognitive performance, reduction of dendrites, reduced neurogenesis, and increased neuroinflammation [301–303]. As these effects can be seen even months after irradiation, late effects are possible even after exposure to lower doses [304].

Whereby it has to be considered that in these heavy ion accelerator experiments, the dose can only be applied in a short time, and prolonged exposure over several weeks or months mimicking the real situation in spaceflight is not often possible. With the use of new, low dose rate neutron irradiation facilities, it is now possible to expose rodents to a chronic low-dose as expected during space flights [305]. Also, mice that were irradiated with this chronic neutron irradiation (for 6 months) resulted in diminished hippocampal neuron excitability, a region which is essential for memory and learning, and disrupted hippocampal and cortical long-term potentiation. In addition, mice showed severe impairments in memory and learning tasks as well as distress behaviors [305].

One limit of experiments at the accelerator is that only radiation exposure of a few single radiation types can be studied, while in space, radiation exposure consists of a complex radiation mixture. It is still unclear if humans' brains are affected to the same extent, but chronic low-dose radiation may cause problems for astronauts regarding decision-making processes or performance [306] (Box 10.8).

Box 10.8 Section Highlights

Since their discovery by Antonie van Leeuwenhoek in 1702, bdelloid rotifers and tardigrades have remained intriguing organisms. Their tolerance to desiccation at any stage of their life and their ability to survive a variety of stresses (e.g., low and high temperatures, absence of oxygen, vacuum, high level of ionizing radiation, etc.), makes them good candidates to study extreme resistance mechanisms in the context of space research. Tardigrades have a long history of space astrobiology experiments being among the first animals exposed to space vacuum and radiation. Recent experiments performed onboard of the ISS used bdelloid rotifers and tardigrades to study the adaptation to microgravity and cosmic radiation during spaceflight.

10.6.3 Tiny and Extremely Resistant: Why Bdelloid Rotifers and Tardigrades Are Animal Model Systems for Space Exploration?

10.6.3.1 Bdelloids and Tardigrades, Small Animals to Study Desiccation, Radiation Tolerance and Limit of Life

Bdelloid rotifers (Fig. 10.17) and tardigrades (Fig. 10.18) are among the smallest animals on Earth: most species are less than 1mm in size and contain ~1000 cells. Despite their small size, these animals have complete nervous, muscular, digestive, excretory, and reproductive systems. Mainly living in semi-terrestrial environments, such as lichens and mosses, most (but not all) bdelloid and tardigrade species are able to enter and survive complete desiccation (see Box 10.9 for definition) at any stage of their life cycle.

When water starts to evaporate, these animals begin to contract their muscles and their body to adopt a "tun" shape allowing an optimal desiccation resistance [307–310]. This proper contraction of the body, followed by a specific organization of internal structures is a key step in enabling a successful recovery of desiccated animals after rehydration [308, 309]. The desiccation resistance and recovery rate vary between species [311–314]. The survival rate depends on the length of the desiccation period, the relative humidity, temperature, and animal age. Tardigrades desiccated over 10–20 years, within dry mosses stored at room temperature, were successfully rehydrated confirming their desiccation resistance for periods [315] [316]. While being frozen, these animals were shown to survive over 30 years of desiccation [317]. Bdelloid rotifers have also been shown to survive long periods of desiccation, up to 9 years [318]. As for tardigrades, cold temperatures seem to extend the capacity of desiccated bdelloids to cope with the long duration of metabolic arrest. In a recent publication by Shmakova et al. bdelloid rotifer specimens were recovered from frozen permafrost soil 24,000 years old [319]. If no data are still available for tardigrades, studying old permafrost samples may reveal other records of small animals' life preservation. For example, some nematodes were described to successfully recover after melting from 30 to 40,000 years old samples [320].

Box 10.9 Desiccation or Drought Tolerance?

Desiccation tolerance must be differentiated from drought tolerance. Many organisms are able to tolerate drought as a reduction in water availability in the environment for longer or shorter times. However, a reduced number is able to survive a loss of 90% or more of their body water content. Complete desiccation is reached when the water content decreases below 10% of the dried mass, not enough to form a monolayer around macromolecules, preventing enzymatic reactions and therefore metabolism.

Mostly found in habitats where physical parameters can change unpredictably, tardigrades and bdelloid rotifers were described to be able to cope with a wide range of physical extremes besides desiccation and freezing, such as UV radia-

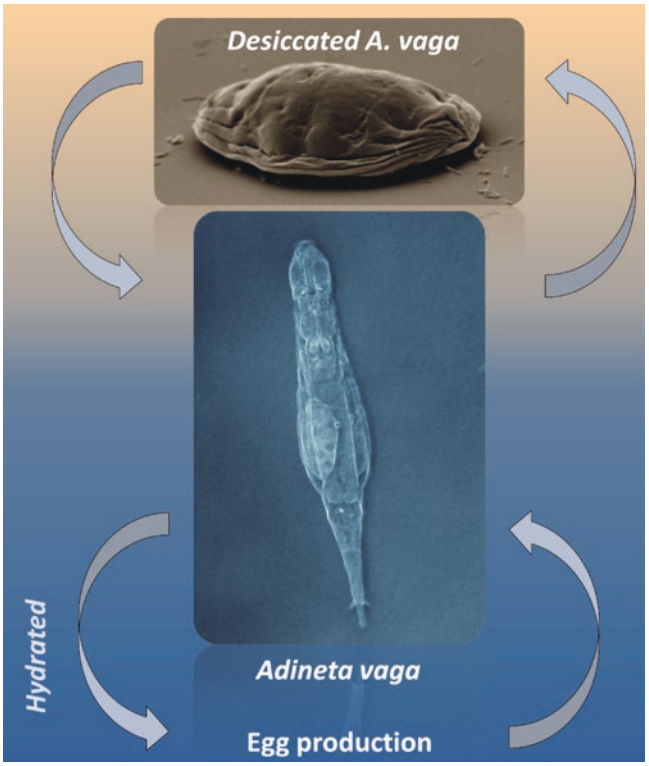

Fig. 10.17 Overview of the bdelloid rotifer *Adineta vaga* life cycle. Bdelloid rotifers live in limno-terrestrial habitats like mosses and lichens. Adapted to these environments, they can be desiccated at any stage of their life cycles including egg stage. When they are exposed to desiccation, adults adopt a "tun" shape allowing optimal desiccation resistance. *Adineta vaga* is about 200–250 µm long. (Credits B. Hespeels)

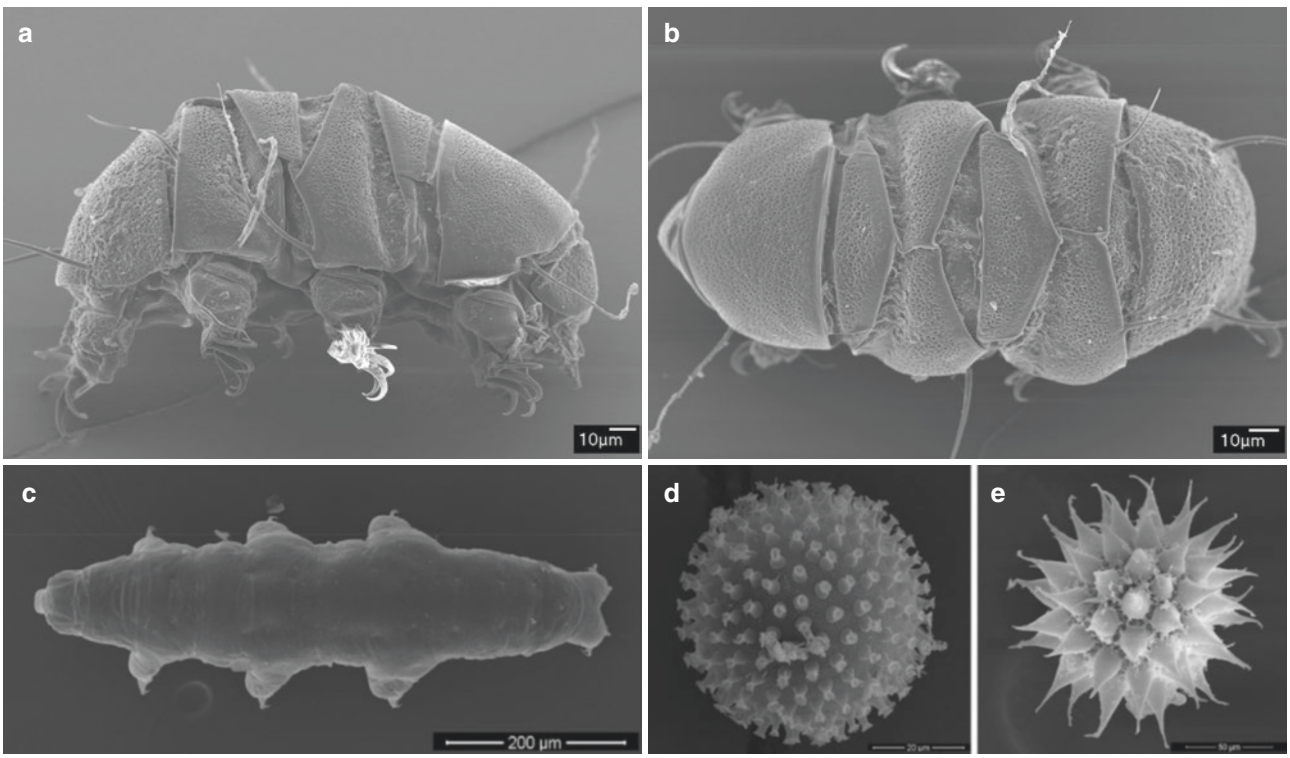

Fig. 10.18 Morphology of adult tardigrades and eggs. (**a**, **b**) Lateral and dorsal views of *Echiniscus testudo*. (**c**) Dorsal view of *Paramacrobiotus areolatus*. (**d**, **e**) Global morphology of eggs laid by *Macrobiotus kamilae* and *P. areolatus*. Pictures were captured using scanning electron microscopy. (Illustration kindly provided by Daniel Stec and reprinted with his permission)

tion, high temperatures (exceeding 100 °C for a few minutes), high pressure or deep space vacuum [317, 321–327].

Among others, bdelloid rotifers and tardigrades were described to be highly resistant to low- and high-LET [328] radiation. In 2008, it was demonstrated for the first time that two bdelloid rotifer species, *A. vaga* and *Philodina roseola*, were resistant to ionizing radiation while being hydrated, surviving up to 1200 Gy of gamma radiation with fecundity (i.e., the total number of daughters produced by irradiated animals) and fertility (i.e., the capacity to produce at least one daughter) showing a dose response [329]. Later, it was demonstrated that desiccated bdelloid rotifers survive doses >5000 Gy of X-ray and proton radiation. These levels of radiation exposure were contrasting the Lethal Dose 50 (LD50) (i.e., dose required to kill 50% of the irradiated population) of mammalian cells which range from 2 to 6 Gy after X-ray irradiation. Similarly, desiccation-resistant tardigrades were described to survive high dose of X-ray and gamma ray (LD50 ranging between 3000 and 6000 Gy) (reviewed in [322]). Unexpectedly, radio-resistance of hydrated and desiccated tardigrades appeared to be more tolerant to high-LET radiation. For example [330], LD50 of the eutardigrade *Richtersius coronifer* was approx. 10,000 Gy. A major difference in comparison with bdelloid rotifers was that, despite a high survival after irradiation, most tardigrades were unable to produce fertile eggs for doses >100 Gy [322]. As an example, the tardigrade *Hypsibius dujardini* treated with gamma radiation had an estimated LD50/48 h for survival of ~4200 Gy, and doses above 100 Gy dramatically impaired the production and hatching of laid eggs [331].

10.6.3.2 Small Animals and Space Research

As an alternative to other animal models, the use of rotifers and tardigrades was proposed for space research. Indeed, these animals may contribute to better understanding damage and consequences induced by exposure to radiation and/or microgravity. How these organisms may respond and adapt to these stresses pave the road to the discovery of new molecules or candidate genes. Ultimately research outputs may be used to improve health span and protect astronauts or individuals subjected to radiation during space flights or medical treatments.

The use of rotifers and tardigrades as space research models was proposed because of the following aspects. (1) Complexity: they are Metazoans (multicellular animals), containing tissues and organs, having a complete gut and a complex muscular structure, yet being very simple animals. Rotifers and tardigrades are however made up of about 1000 cells, while a human is made up of several millions of cells. This simplification allows to disentangle complex problems through easier approaches. (2) Miniaturization: rotifers and tardigrades are small; experiments performed with numerous individuals require small vessels. (3) Distribution: rotifers and tardigrades are readily found in nature and are easily cultivated under controlled conditions. (4) Life span: rotifers and tardigrades have short life cycles that can be studied in a reasonable time period. (5) Reproductive mode: all bdelloid rotifers and some tardigrade species reproduce parthenogenetically. This reproduction system offers two key advantages: a rapid expansion of the population, and a high degree of reliability, as the genome is fully transmitted to the offspring. Therefore, the use of clonal lines reduces the biological variability noise in biological experiments. (6) Extremotolerance: both bdelloid rotifers and tardigrades were described to be able to deal with a high number of DNA DSBs and various stressors encountered by astronauts during space flight. Small extremotolerant animals can provide new perspectives in the adaptation of life to the space environment and ultimately lead to enhancing radio-resistance. For both clades, radiation resistance and radiation-sensitive species can be used in comparative experiments. (7) Storage: as most tardigrades and bdelloids survive desiccation and freezing, they can be stored easily before and after scientific experiments with limited impact on their biology and the scientific output. (8) Desiccation resistance: the desiccated state of tardigrades and bdelloid rotifers correlates with increased resistance to stresses, including deep space vacuum and extreme temperatures. These multiple properties and advantages for space experiments make bdelloid rotifers and tardigrades good candidates to test the limits of life during space exposure. An overview of space experiments involving tardigrades and rotifers is presented in the next two sub-sections.

10.6.3.3 Tardigrades, Pioneer Animals of Astrobiology Field

In September 2007, tardigrades were exposed to LEO within the Biopan-6 experimental platform provided by the European Space Agency (ESA) ("Tardigrades in Space," TARDIS. FOTON-M3 mission). During 10 days at LEO (258–281 km above sea level) samples of desiccated adult eutardigrades of the species *Richtersius coronifer*, *Milnesium tardigradum*, *Echiniscus testudo,* and *Ramazzottius oberhaeuseri* were exposed to space vacuum, cosmic radiations, and two different UV-radiation spectral ranges [323]. It was demonstrated that tardigrades were able to survive space vacuum and cosmic radiation with a survival rate ranging between 70% and 80%. Any impact on the reproductive capacities of exposed animals was reported. However, samples exposed to full solar radiation experienced high mortality. A small fraction of survivors died a few days post-rehydration without the production of any viable offspring. By filtering UV and restricting the exposure of desiccated tardigrades only to UVA and UVB, a significant part of desiccated tardigrades was able to be reactivated and was

able to reproduce. Since the fertility of descendant generations of *M. tardigradum* was not impacted, it was suggested that survivors were able to repair a priori the damages induced by the spaceflight and did not transfer them to future generations [332].

In parallel to the TARDIS experiment (Fig. 10.19), two other experiments were launched onboard of the FOTON-M3: the (1) RoTaRad mission (Rotifers, Tardigrades, and Radiation) and (2) Tarse project (Tardigrade Resistance to Space Effects). RoTaRad experiment confirmed that desiccated tardigrades stored under controlled atmosphere were able to survive while being exposed to a combination of cosmic radiations and microgravity. However, the survival rates were reduced during this experiment likely due to the applied desiccation protocol [333]. With the Tarse project focusing on the eutardigrade *Macrobiotus richtersi* species, hydrated and desiccated individuals were exposed to the space environment for 12 days. In both states, microgravity and radiation had no effect on the survival rate, reproductive capacity, and DNA integrity of exposed animals. Despite the absence of visible morphological changes, it was nevertheless reported that the activity of key antioxidant proteins (including catalase and superoxide dismutase) was decreased during spaceflight. The amount of Heat Shock Proteins 70 and 90, known to be involved in stress resistances of tardigrades, did not differ after this short-term exposure to spaceflight.

A few years later, the TARDIKISS experiments (Tardigrades In Space) were launched with the last Space Shuttle mission (STS-134 2011) [334]. During this 16-days mission, the enzyme activity of key antioxidants was investigated in desiccated tardigrades from the two species *Paramacrobiotus richtersi* and *Ramazzottius oberhaeuseri* [334]. Supporting the idea that desiccated animals were weakly affected by microgravity and cosmic radiation, comparative data analysis between flight and ground samples showed no significant differences in the enzymatic activity of antioxidants.

In June 2021, a fifth experiment was launched onboard of the ISS to investigate the short-term and multigenerational survival of tardigrades. The aim of the Cell Science-04 experiment (CS-04) was to evaluate the transcriptomic response of hydrated tardigrades cultured on the ISS using a dedicated cell culture system (Bioculture System, developed at NASA Ames Research Center). For this experiment, the tardigrade *Hypsibius exemplaris* was used as model species. Scientists are currently evaluating the ability of these animals to survive onboard of ISS for short and long periods of time (up to four generations). In parallel, the transcriptomic responses of these animals are being investigated to follow the evolution of the expression profiles of tardigrades in a microgravity environment. A progressive adaptation of tardigrades onboard of ISS may lead to a better understanding of the molecular responses involved in gravity sensing and will help expand research to secure astronaut's health for future space missions. Among others, tardigrades were described to express several antioxidant proteins to face desiccation and radiation stresses [322, 335]. In particular, tardigrades were described to express specific proteins binding to DNA and protecting their genome from ROS induced by desiccation and ionizing radiation [336, 337].

10.6.3.4 Bdelloid Rotifers, a New Model Species for Space exploration

How microgravity and cosmic radiation may affect desiccated bdelloid rotifers was tested for the first time in 1997.

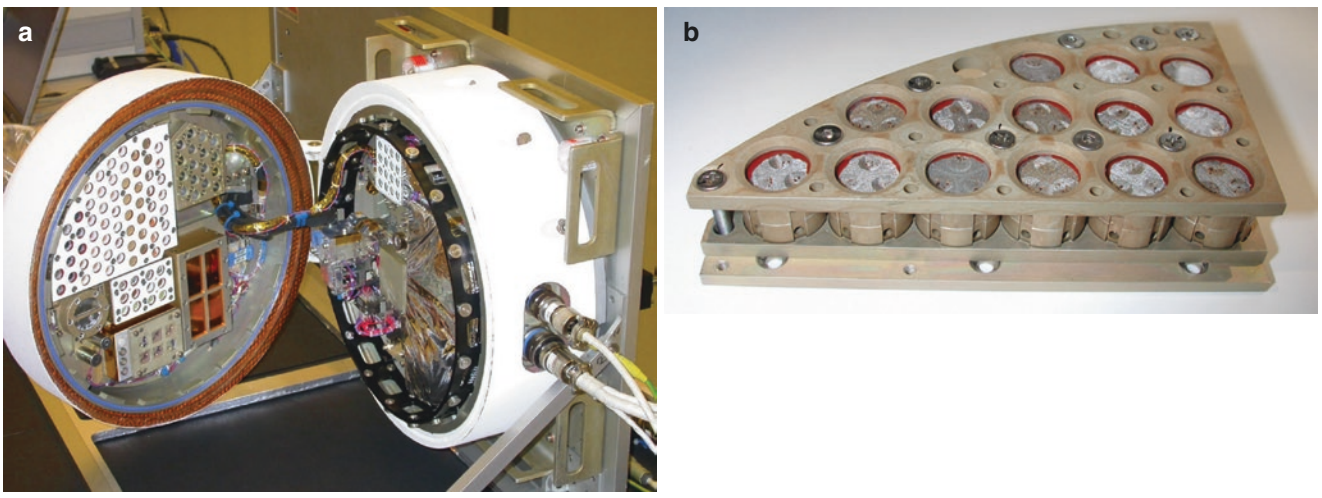

Fig. 10.19 View of TARDIS experiment. (**a**) View of the exobiology Biopan platform containing TARDIS experiment. For 12 days in September 2007, approximately 3000 water bears were launched in space during the Foton-M3 mission. Reprinted with permission from ESA. (**b**) Details of the sample holder containing the tardigrades *Richtersius coronifer. Tardigrades on the top level were exposed to the Sun and were optionally protected with filters.* (Image kindly provided by K. Ingemar Jönsson and reprinted with his permission)

For their first exposure to space, dry samples of *Macrotrachela quadricornifera* were transported onboard of the space shuttle STS-81 for a total of 10 days. The data revealed a similar survival rate and reproductive fitness for ground controls and flight samples [312]. Since desiccated rotifers appeared to be protected from the impact of microgravity and cosmic radiation, at least in this short-term exposure experiment, researchers started to investigate the consequences of space flight on hydrated bdelloids. In absence of gravity, it has been hypothesized that the distribution of cytoskeletal elements or yolk granules in the egg cytoplasm is impacted. This abnormal organization of the cytoskeleton could impact the rotifer reproduction. Therefore, researchers first investigate the capacity of bdelloid rotifers to complete their embryological development under microgravity was initially investigated. Pre-flight experiments were performed under hyper-gravity environment (up to 20 g) and under simulated microgravity (as low as 0.0001 g) using a 3D random positioning machine (3DRPM). Results showed that the rotifer development remained constant regardless of the treatment experienced, except for some minor modifications in early embryos experiencing 20 g with no subsequent impact on the development. This first investigation suggests that bdelloid rotifers continue embryological development despite changes in g-force. Unfortunately, no data from flight experiment development associated with embryological development of bdelloid rotifers exposed to space environment was released post-flight.

Twenty years later, the bdelloid rotifer *A. vaga* was sent onboard of the ISS for two independent experiments. In December 2019, two autonomous hardware, each containing five culture bags loaded with 10,000 individuals, were transported onboard of ISS. Hydrated animals were exposed to launch conditions and exposed to 12 days of microgravity. At the same time, a ground reference experiment was implemented on Earth to compare the biological responses of rotifers to space conditions on ISS. The aim of this first experiment (RoB1, Fig. 10.20) was to compare the transcriptomic responses of hydrated *A. vaga* samples exposed to space environment with the ground control samples. Preliminary results

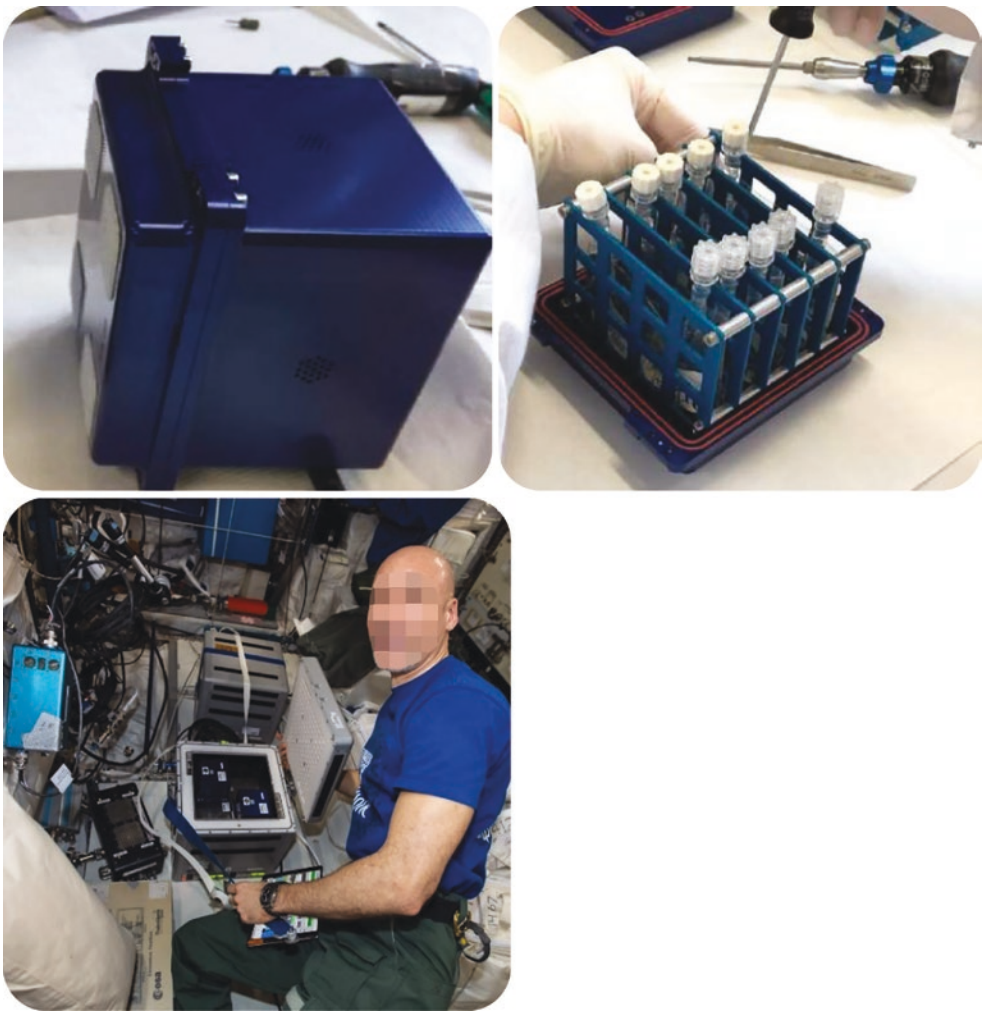

Fig. 10.20 View of Rob1 hardware used to culture hydrated *A. vaga* individuals onboard of ISS (December 2019). *Top left*: Rob1 hardware after its assembly at the launch site at Kennedy Space Center. Rob1 hardware is a passive hardware containing five culture bags containing hydrated specimens of *A. vaga*. Hardware enables gas exchanges between rotifer cultures and the outside through a permeable membrane. *Top right*: View of the culture bags assembled inside Rob1 hardware. Culture bags, loaded with 10,000 *A. vaga* individuals each, are made of Teflon and ensure an optimal gas exchange between the culture medium and the outside. Bags are waterproof and avoid any leakage of the medium (composed of mineral water and sterile lettuce juice) or rotifers. Reprinted with permission of Marc Guillaume. *Bottom left*: View of ESA astronaut Luca Parmitano loading two Rob1 hardware on KUBIK. KUBIK is a small incubator, temperature-controlled, with removable inserts designed for self-contained microgravity experiments. (Reprinted with permission of NASA)

Fig. 10.21 View of one Rob2 hardware used onboard of the ISS (left) and Astronauts checking the correct rehydration of *A. vaga* individuals. Sixteen pieces of hardware were sent to ISS, each containing 40,000 dry rotifers. Once onboard, rotifers were automatically rehydrated and cultivated 11 days before their fixation and download to Earth. (Reprinted with permission of Boris Hespeels and NASA)

confirmed the successful maintenance of hydrated bdelloid individuals on ISS, without additional food or oxygen supply and without astronaut intervention. All the replicates (ten) of the autonomous *A.vaga* cultures survived and reproduced on ISS with no visible impact on the morphology in space-exposed samples.

While it is well documented that astronauts experience DNA damage when exposed to cosmic radiation, accumulating DNA mutations and/or genomic rearrangements [163], the combined effect of cosmic radiation and microgravity on the living organism is still debated. It is suspected that microgravity reduces the efficiency of DNA repair and increases cancer risk [207, 215, 338]. Several studies using simulated microgravity highlighted a decrease in DNA repair efficiency. However, no effects of spaceflight on the cellular capacity to repair artificially induced DNA was observed (see Moreno-Villanueva et al. [209] for review). In order to obtain more insights, bdelloid rotifers have been used as a model system to evaluate their DNA repair efficiency of induced DNA breaks in space environment as compared to Earth samples. By the end of 2020, desiccated and irradiated *A. vaga* individuals were sent onboard of ISS. Before launch, desiccated animals were irradiated with 500 Gy of X-ray or proton radiation. Onboard, bdelloids were rehydrated and cultivated for different time periods to (1) follow the putative DNA repair process occurring post-rehydration and (2) investigate whether these irradiated rotifers still produce offspring under microgravity. In addition, half of the samples were exposed to simulated gravity using a centrifuge on ISS. Finally, a ground experiment was conducted in parallel at the launch site at Kennedy Space Center for comparison. Data generated by this second space experiment (entitled RoB2, see Fig. 10.21) will enable: first, to compare the DNA repair kinetic of rehydrated bdelloids post irradiation in 1G, μG, and simulated 1G; second, to compare the radiation responses of rehydrated rotifers after exposure to low LET or high LET; and third, to compare the DNA repair efficiency in space and on Earth by isolating eggs or juveniles from the exposed samples and use whole genome sequencing to compare the genomic structure of these animals pre- and post-exposure. This space experiment with bdelloid rotifers will contribute to our understanding of DNA repair process activity in space, in the presence or absence of microgravity. Moreover, studying the molecular processes involved in the DDR process of *A. vaga* will be of huge interest for future space travel.

In general, the ongoing rotifer space experiments will contribute to a better understanding of the mechanisms involved in the protection and repair of damages induced by radiation. They pave the road to the discovery of new molecules or candidate genes that could ultimately be used to improve health span and protect astronauts or individuals subjected to radiation during space flights or medical treatments. This research is also of fundamental importance for the understanding of extreme biology and the questions raised on the origin of life and its ability to spread through outer space. A third experiment, supported by ESA, is under preparation to evaluate whether rotifers can survive full space exposure, outside ISS, as was previously reported for tardigrades.

10.7 Plant Experimental Models and Biological Changes of Space Radiation

10.7.1 Plants vs. Animal Models

Long space exploration missions, settlement on orbital stations, or future planetary settlement (e.g., on Mars) will require further development of Life Support Systems (LSS). The LSS are able to regenerate a great amount of essential resources for survival and represent an ideal solution since it is not technically and economically feasible in long space missions to transport a large amount of consumables from the Earth [339–341]. Bioregenerative Life Support Systems (BLSS) are an artificial closed ecosystem characterized by the same structure as a terrestrial ecosystem: producers (plants), consumers (humans/animals), and decomposers (microorganisms).

Among biological components within BLSS, higher plants would have the same role on Earth as producers. Through photosynthesis, plants would utilize carbon dioxide produced by space crew and provide oxygen and fresh food. Moreover, they would use nutrients derived from human wastes and guarantee water purification by transpiration. Furthermore, plant cultivation in space also would provide psychological support against isolation [342, 343].

Each organism in Space is subjected to several factors which are potential constraints for biological life. Among the environmental factors (e.g., altered gravity, interaction between microgravity and fluid-dynamics, modified conditions of pressure, temperature, confinement, etc.) limiting plant growth in space, ionizing radiation influences severely the development of organisms at molecular, morpho-structural, and physiological levels [163, 182, 344]. Indeed, ionizing radiation is considered one of the main constraints for the long permanence of humans in Space.

All organisms in extraterrestrial environments are subject to higher levels of ionizing radiation than on Earth and, notwithstanding the large number of studies aimed at understanding the effect of ionizing radiation on animals, the knowledge on plant reaction is limited. Available information is limited to horticultural model crops which are candidate for fresh food production in BLSS. Moreover, most experiments are based on the irradiation of dry seeds and data from irradiation tests using other biological models (e.g., seedlings, adult plants, actively growing tissues) are scanty.

In Fig. 10.22, a comparison of the responses of plants and mammals to ionizing radiation exposure is shown. Generally, plants are more resistant than mammals. Ionizing radiation is known to have differential effects on plant growth, develop-

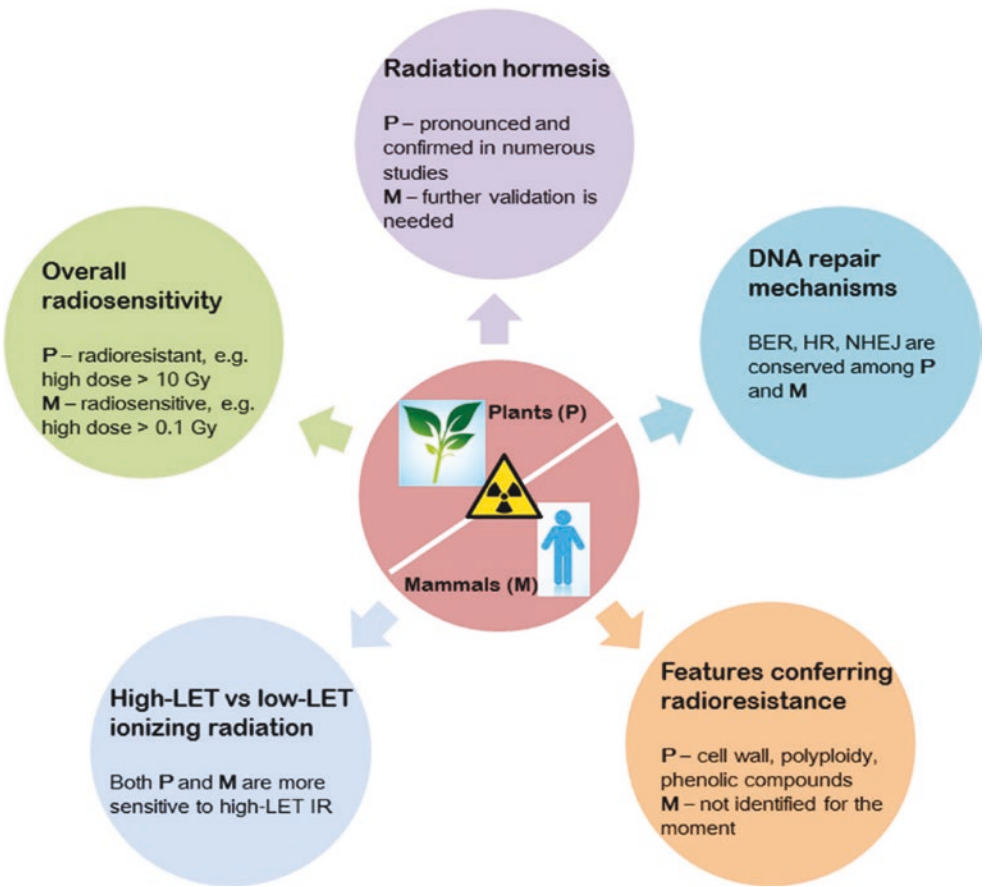

Fig. 10.22 A comparison among different responses of Plants (P) and Mammals (M) to ionizing radiation. (Reprinted with permission from Arena et al. [346])

ment, and reproduction, ranging from detrimental outcomes at high doses, harmful consequences at intermediate levels, and stimulatory effects at very low doses. This phenomenon is called "hormesis." Particularly, low doses of ionizing radiation have been reported to stimulate seed germination and root growth [345, 346].

However, ionizing radiation can also induce dwarf growth that is a desirable trait under conditions of limited volume availability in missions on orbital stations or during exploration traveling. The increased radioresistance of plants is still a debated issue since it can be associated with a genetic basis, but it can also reflect biochemical and biomolecular mechanisms of shelter from genotoxic damage.

The severity of the effects of ionizing radiation on plants is dependent upon several factors including radiation-related parameters (e.g., dose, LET) and organism-related traits (e.g., species, cultivar, physiological status, and structural properties, as well as plant genome organization including the polyploidy) [345, 347].

10.7.2 Biological Changes from Genetics to Organogenesis

In adult plants, in the case of organs at complete development, resistance to stressors can be often ascribed to integrated mechanisms of adaptation operating at morpho-structural and eco-physiological levels since the limits of major metabolic and physiological processes are dictated by the plant's structure [348, 349]. Growth, reproduction, and, ultimately, survival of plants in Space depend on photosynthesis which is strongly responsive to ionizing radiation acting on the various components of the photosynthetic apparatus, such as pigment–protein complexes responsible for light absorption, electron transport carriers, and enzymes of carbon reduction cycle [345]. Ionizing radiation leads to several detrimental effects in photosynthetic apparatus, such as loss of functionality of photosystem II (PSII) and generation of free radicals causing photosynthetic membranes' oxidation [350–352]. Changes in the total antioxidant pool and in the distribution of phenolic compounds in leaf tissues were observed in plants exposed to very high doses of X-rays, namely 50 and 100 Gy [353].

However, chronic exposure to low doses of ionizing radiation seems to enhance the activity of some antioxidant enzymes, providing plants with a radio-resistance [354, 355]. Moreover, the degree of plasticity of leaf cytological and anatomical traits in response to environmental changes can be responsible for enhancing or constraining processes such as light interception and gas exchanges, definitely affecting photosynthesis. Similarly, the correct functioning of the whole water transport system throughout the plant is responsible for water supply up to the leaves, necessary for efficient photosynthesis. The ability of xylem to transport water efficiently depends on the morphological features of its conduits and on the ultra-structural properties of conduit cell walls, whose main components can be differently affected by ionizing radiation.

Apart from a few findings mainly related to specific ultra-structural modifications occurring on irradiated seeds, the effect of cosmic radiation on organ/tissue organization, especially in relationship with eco-physiological traits, is still poorly explored. Moreover, most of the studies regard experiments with low-LET ionizing radiation [346, 355], and only a few data are available on the effects of chronic radiation exposure on plants in general, mainly deriving from nuclear accidents as Chernobyl in Ukraine (1986) and Fukushima in Japan (2011).

10.8 Eukaryotic Cell Experimental Models and Biological Changes of Space Radiation

10.8.1 Definition of Eukaryotes

Regarding the complexity of their cells, all living organisms can be classified into two groups-prokaryotes and eukaryotes. Compared to prokaryotes, eukaryotic cells are highly organized and contain a cell nucleus. Prokaryotes are bacteria and archaea, while protists, plants (see Sect. 10.5.8), animals (see Sect. 10.5.7), and fungi (see Sect. 10.5.9) are eukaryotes.

In the following the effect of space radiation on in vitro models (conducted in a cell culture dish) and ex vivo models (experiments outside a living body) will be described.

10.8.2 Definition of In Vitro Models

In vitro models used in science, are very important, as they provide insight into cells. With this, the function of primary cells and cell lines of various origin (vertebrates including human, insects, and mussels) can be studied.

10.8.3 Definition of Ex Vivo Models

Ex vivo models or tissue explants allow studying complex functions and interactions of different cells within an organ. For these experiments, the living tissues are directly removed from a living organism or can be generated by means of pluripotent stem cells and cultivated under controlled conditions.

10.8.4 3D Cell Culture Models

10.8.4.1 Definition 3D Cultures

In comparison to cells in monolayer cultures (2D), cells in 3D cultures react completely differently. The biggest disadvantages of 2D cultures are the unnatural contact with a plastic or glass surface, the flat morphology of the cells on the growth surface that restricts intercellular contacts and the lack of an extracellular matrix which surrounds cells in vivo. These conditions modify the metabolism and functioning of cells and often result in the loss of the specific differentiation of a cell. The structure, function, and composition of organs and tissues can thus be better studied in 3D cell culture systems. They enable cell–cell and cell–extracellular matrix interactions in a three-dimensional space. 3D cultures are a very helpful tool before performing whole-animal studies. They can further be used to study the understanding of how processes in tissues are affected by spaceflight conditions, including space radiation and microgravity, which otherwise cannot be investigated in animal or human subject studies.

There are many different models of 3D cell cultures, including organoids, *ex vivo* tissue, or slice cultures, which are explained in the following. Furthermore, it is possible to create these models with 3D bioprinting, which have then a structure which closely resembles the organization of tissue or organs. In fact, the European Space Agency (ESA) recently summarized the capability science requirements for 3D bioprinting on the ISS to support medical treatment on long-term space missions.

In all given examples two or more cell types can be co-cultured, closely simulating the situation in organs or tissues, e.g., investigation of cellular differentiation processes in tissues, nerve-muscle function, tissue regeneration and repair, vascular tissue function, brain tissue homeostasis and aging, immune system processes or cardiac muscle function.

10.8.4.2 Organoids

Human organoids, derived from stem cells or progenitor cells, are tiny self-organized organ-specific 3D cultures, recreating the physiological and cytoarchitecture of human organs. With this, the model reflects the in vivo situation much better than single cell cultures. For research purposes, it is feasible to create organoids that resemble the brain, kidney, lung, intestine, stomach, and liver.

Organoids will help to study the effect of space radiation on the overall response of organs, including cellular heterogeneity, cell-matrix interactions, cell-cell interactions, morphology, and functional changes [356, 357], which cannot be studied in in vitro systems. One major disadvantage compared to in vivo systems is the lack of microenvironment.

The effects of microgravity on human brain organoids were tested on the ISS during the Space Tango-human Brain investigation in 2019 (NASA). Of special interest was the effect on the brain cells including survival, migration, metabolism, and the formation of neuronal networks (Muotri, unpublished).

10.8.4.3 Spheroids

Spheroids are also 3D cell cultures, but in comparison to organoids, they form simple clusters into sphere-like formation, but they cannot self-assemble or regenerate. Whereby the cellular functions inside spheroids are closely correlated to the size, uniformity is especially important for reproducible results. To guarantee this, several methods for culturing are available such as hanging drops, scaffolds, liquid overlay technique, and hydrogels [358]. Nowadays spheroids are highly used to study the microenvironments of tumors or their response to radiotherapy.

Already in 2016, the SPHEROIDS project was launched on the ISS. Here, endothelial cells, which under simulated microgravity form small, rudimentary blood vessels, were exposed to real microgravity for 12 days on the ISS. The formation of spheroids under space conditions and under simulated microgravity on Earth were similar [359], underlining the important role of microgravity in spheroids formation.

Differences between the three types of cultures are summarized in Fig. 10.23.

10.8.4.4 Organotypic Slice Cultures

Organotypic slice cultures are tissue samples that are cut in thinly, about 300 µm, thick slice and are then cultivated on semipermeable insert. Most common are organotypic slice cultures that originate from different parts of the brain (e.g., hippocampus, cerebellum, or cortex) and can be kept in cultures for long term, while slices originating from liver tumors can only be kept in culture for a short time [360, 361]. Also,

	Monolayer	Spheroid	Organoid
Cell types	Single cells	Multiple cells types	Epithelial and mesenchymal cells
Derived from	Donor Patients, Animals	Cell line monoculture	Stem cells
Morphology	Non-natural, flatten	Simple cell clusters	More complex cell clusters
Represent	Replicate only tissues, but not organs	Single tissue of an organ	Multiple tissues of an organ or "Mini-organs"
Example	MEF, ESCs, iPSCs	Muscle spheroids, lung epithelial spheroids, Tumor spheroids	Organoids for brains, guts, lungs, hearts

Fig. 10.23 Difference between the different cultures

this 3D culture has the advantage that the composition and architecture of the extracellular matrix as well as the tissue are preserved. During analysis of the slices, it has to be considered that every slice, even from the same organ, has a partly different composition, cell counts, and viability, limiting the reproducibility of results produced by this method.

10.8.4.5 Organ Cultures

Organ cultures were developed from tissue and slice cultures. By using organ cultures, it is possible to study the functions of an organ in various conditions and states in an in vitro organ. Hereby, the entire organs or only a part of the organ are excised from the body and cultured. Also, with this method, the 3D structure of the tissue of choice is preserved.

For space exploration, the eye lens is of special interest, because it is amongst the most radiosensitive tissues in the human body. Ionizing radiation can cause a posterior subcapsular cataract [287, 362, 363]. Whole lenses and lens epithelial cells in culture enable the study of early mechanisms of space radiation-induced cataractogenesis and of the relative biological efficiency of different space radiation components to induce early changes. With regard to the human lens in anatomy and size, the porcine eye is very similar. Thus, it is used to study the radiation response in the whole organ. Translation to the human eye lens can be enabled by using human-transformed epithelial cells or lens epithelial cells from donor patients. As the viability of eye lenses in cultures is limited to a few weeks, studies on radiation-induced full-blown cataract formation usually require animal experiments over their lifespan (Sect. 10.5).

In addition to that, the microgravity environment on the ISS suits perfectly to 3D print tissue cultures and later maybe entire organs. Compared to conditions on Earth where scaffolds or matrices are needed to form organoids, in space cells can easily self-organize into their precise structure. On the one hand, the bioprinted tissue could be used in the future to treat injured astronauts [364] and on the other hand the technique can be transferred to Earth and then be applied to the field of regenerative medicine for organ transplantations [365]. In July 2019, the 3D BioFabrication Facility (BFF—see Fig. 10.24) has arrived onboard of the ISS, with this it is now possible to study 3D bioprinting of different human tissues in space. Also, here real microgravity has the benefit that printed structures will not collapse, enabling also the printing of soft human tissue (NASA) (Box 10.10).

Box 10.10 Highlights

- Several cell cultures system can be studied under space conditions
- The microgravity environment on the ISS suits perfectly to print 3D tissue cultures

Fig. 10.24 NASA's 3D BioFabrication Facility BFF. (Image JSC2019E037579, Credits NASA)

10.8.5 Omics Approaches in Space Life Sciences

Understanding the effects of the space environment on microorganisms has witnessed recently considerable progress (whereas the main factors are microgravity, radiation, and vacuum). However, explicit knowledge of molecular mechanisms responsible for survival and adaptation in space is still missing. Space environment affects a variety of physiological features of microorganisms. The above features include metabolism, motility and proliferation rate, division of cells, and also virulence and biofilm production (Fig. 10.25) [366]. Molecular-level understanding of the above effects in space-exposed microorganisms is still lacking. It is believed that omics-based approach, together with classical phenotyping and physiological measurements, will be a useful toolbox for understanding mechanisms of microbial survivability in the harsh conditions of outer space. "Omics" stands for genomics, transcriptomics, proteomics, metabolomics, and more.

Systems biology is an interdisciplinary approach in biomedical research aiming at understanding the biological system at the organism, tissue, and cell level. Systems biology incorporates the results of –omics techniques, genome-scale metabolic and regulatory biomathematical models to understand molecular interactions, evolution, functional and phenotypical diversity, and molecular adaptation. The omics-based approach integrates various pieces of biological information from genomes, mRNA, and proteins to metabolites [367].

The –omics-based approach has recently opened a window for a deep insight into molecular machinery implicated in the survivability of space-exposed microorganisms by revealing expression, metabolic functioning, and regulation of the genes and proteins encoded by the genomes of "space travelers." The diverse biological activities of microorgan-

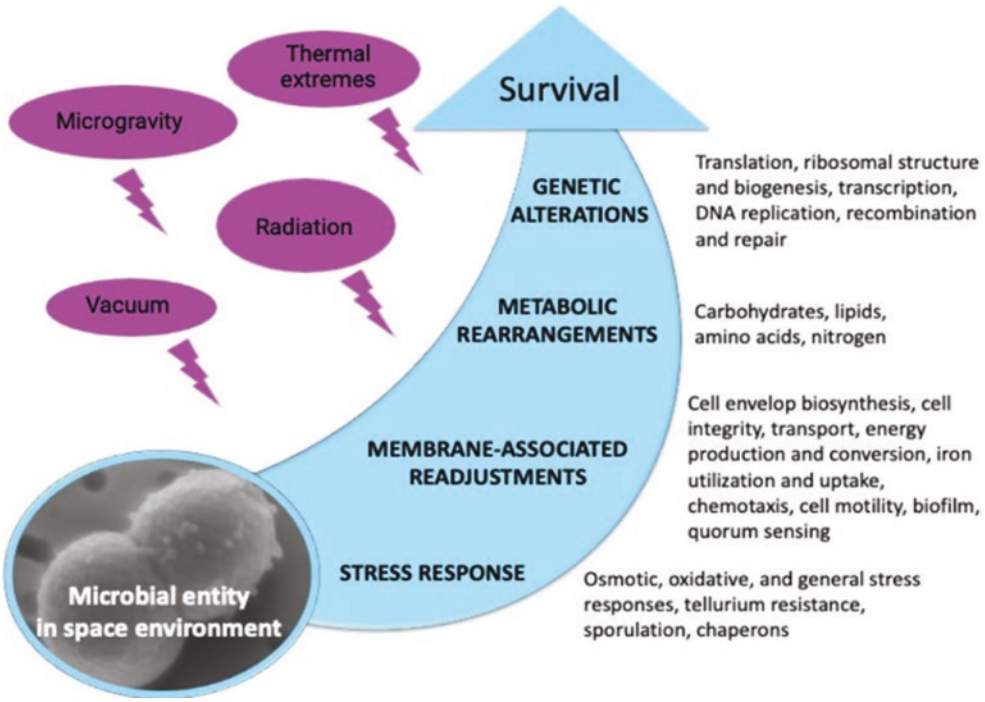

Fig. 10.25 Molecular response experienced by microorganisms in the outer space environment revealed with the help of global and integrative –omics approaches of systems biology that have been recently used to study microorganisms exposed to real and simulated space conditions. (Reprinted with permission from Milojevic et al. [366])

isms in space are affected by metabolic alterations caused in turn by genetic regulations (Fig. 10.26). It has been demonstrated by means of –omics-based approaches that exposed microbes switch to "energy saving mode." Research identified some global regulatory molecules that drive molecular response of a few space-exposed microorganisms [366–369]. Various kinds of stress responses (e.g., general, osmotic, and oxidative) experienced by microorganisms in conditions of real and simulated outer space have been deciphered via –omics-assisted analyses [366]. Various genes with altered expression after microbs' exposure to real and simulated outer space environment (Fig. 10.25) have been identified [366].

State-of-the-art –omics technologies have been successfully used to understand molecular mechanisms responsible for alterations of microbial virulence in space conditions (Fig. 10.27) [366].

Space exposure imposes stresses that affect microbial survival rates and may lead to certain discrepancies in –omics-assisted analysis of returned/exposed microorganisms. The composition of the cultivation medium influences the microbial space response [369], e.g., by providing specific antioxidants presented in rich medium, which may protect microbial cells against ionizing radiation. The majority of space experiments have been performed on satellites, where microorganisms are cultivated in environment protected from all factor but microgravity [366]. Direct exposure to real space environment outside the ISS followed by investigation with –omics techniques was performed on a few microbial species only [367, 370, 371]. Therefore, in order to broaden our knowledge of molecular mechanisms of microbial survivability in outer space, there is an urgent need for further experiments with direct exposure. Often, a multi-omics post-flight analysis has the problem of a limited number of microbiological samples exposed to the space environment. Therefore, the researchers should critically assess the design of outerspace experiments to provide a sufficient number of independent biological samples in order to enable statistically significant results in processing the –omics data. It is also extremely important to avoid artifacts: due to very high sensitivity of the –omics techniques of occasional occurrence of uncontrolled conditions, stress-related artifacts cannot be ruled out. In this context, it is highly desired to develop novel approaches for the efficient extraction of DNA, RNA, proteins, and metabolites simultaneously from the minimal amount of microbial cells [367, 372]. Furthermore, the absence of detailed reports regarding the environmental conditions during space exposure and corresponding ground control experiments is, unfortunately, a frequent reality that requires a critical reassessment of research planning. Providing a full record of controlled parameters (like temperature, humidity, and pressure profiles) during flight, simulated, and control experiments is highly desired to achieve a comprehensive and artifacts-free analysis of the effects of the space environment on the physiology and molecular machinery of microorganisms.

It has been proposed that in future space experiments, detailed metabolomic analysis of exposed microorganisms should be performed in addition to the proteotranscriptomic profiling. This novel approach has provided already plenty of

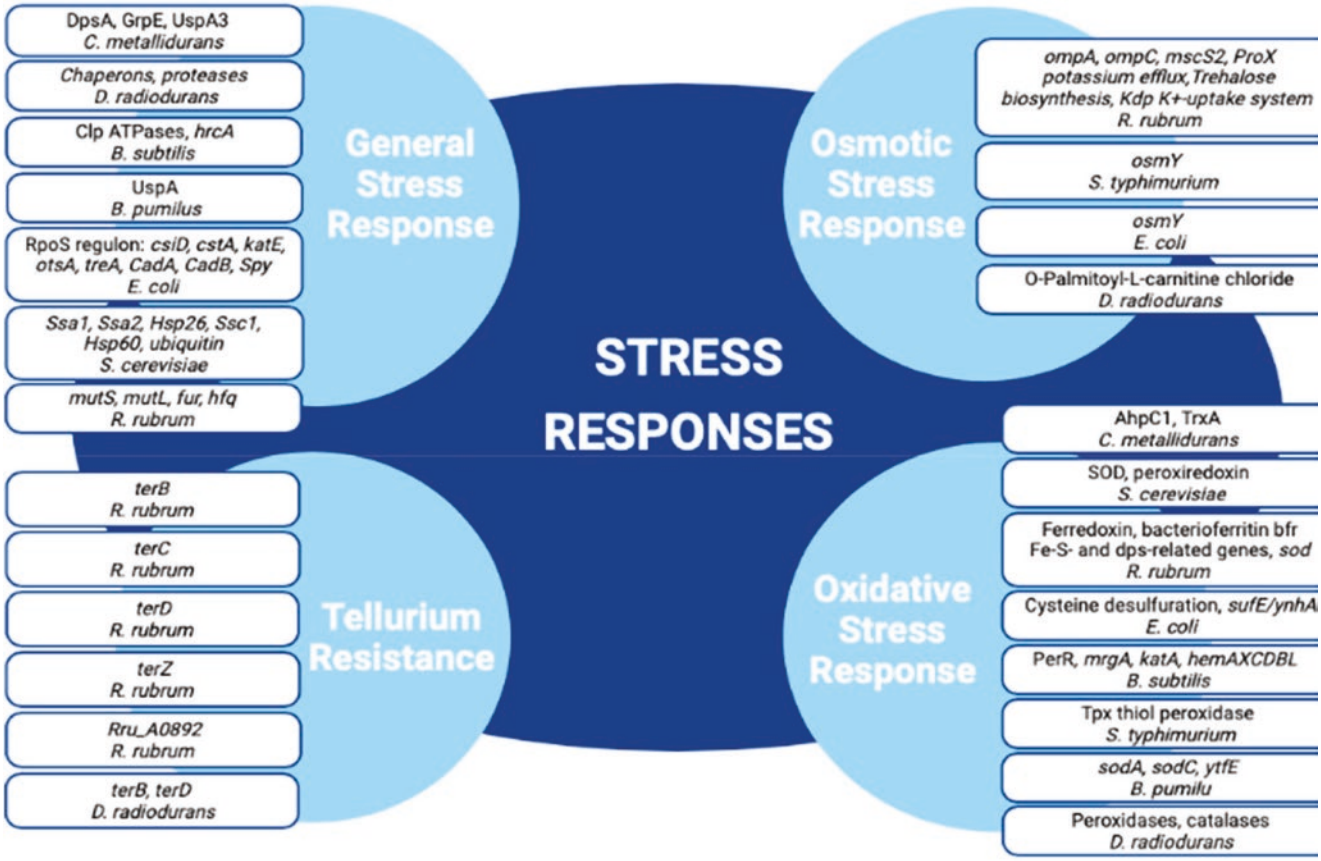

Fig. 10.26 Stress responses experienced by microorganisms in outer space real and simulated conditions, revealed with –omics-assisted investigations. Proteins and genes of stress responses with altered abundance and expression after exposure of microorganisms to the outer space real and simulated environment [366]

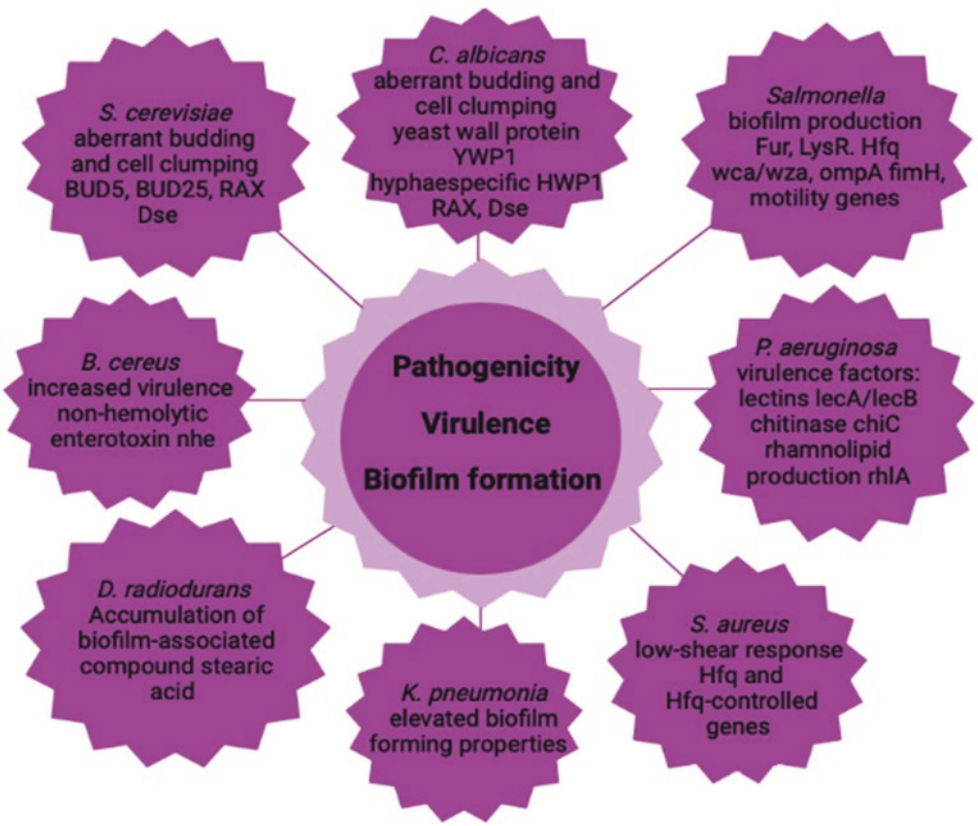

Fig. 10.27 Molecular alterations underlying microbial pathogenicity, virulence, and biofilm formation in the outer space environment, resolved with –omics-assisted investigations [366]

new findings on fine molecular networks regulating the space response [367]. Recent works (e.g., the NASA twins' study) used a multi-omics, systems biology analytical approach to analyze biomedical profiles of astronauts [120]. Results of performed targeted and untargeted metabolomics combined with proteomics effectively revealed the biomedical responses of a human body during a year-long spaceflight indicating mitochondrial stress as a consistent phenotype of spaceflight [120, 373]. Finally, the combination of molecular data with a genome-scale metabolic reconstruction of the respective species should be implemented, delivering the space-induced microbiome signatures [366].

10.9 Space Radiation Resistance

10.9.1 Health Risk Reduction from Space Radiation Exposure in Humans

Humans have all evolved in an environment containing a persistent low level of constant exposure to different endogenous and exogenous mutagenic agents, and consequently have developed many cellular mechanisms for either DNA protection or repair (see Chap. 2). However, when humans travel into space, these naturally evolved cellular mechanisms might not be enough as many major health threats from space radiation has been identified, e.g., central nervous system injury, cardiovascular diseases, immune dysfunction, cancer development, and premature aging. To reduce the risk of humans in space, there are some possible interventions which can limit the effects of space radiation. A dedicated review can be found elsewhere [374].

One way of reducing the health risk from space radiation exposure in humans is selecting more radioresistant humans during the selection campaigns of space agencies. The most used way is to perform in vitro adaptive response studies, in which cells collected from the candidates are used to measure their response to a fixed dose of ionizing radiation. While the results of these studies are not necessarily used during candidate selection, they hold great value in selecting the right people that will be more protected against space radiation. Another strategy would be to pharmacologically hamper the processes underlying the molecular (side) effects of space radiation exposure. Examples are the application of radioprotectors and geroprotectors, as well as supplementation with antioxidants or antioxidative capacity increasing compounds (see Chap. 11). While these pharmaceuticals hold great promise, many of them are still under investigation and not allowed to be used on humans.

An alternative method to elevate humans' natural radiation protection capacity is inducing a hibernating or hypostasis state. It is well-known that natural hibernators become more radioresistant during their inactive state. The reason for this has not yet been fully elucidated. It is probably due to several factors related to slower cell metabolism and increased tissue hypoxia.

In recent years, a technique has been developed that allows hibernation to be reproduced even in those animals that would not usually be able to hibernate, such as rats. This technique is nowadays known as synthetic hibernation or synthetic torpor [375]. Although this research has a big potential to limit radiation-associated risks in space, it is quite far from practical use yet. Another futuristic method is the use of deuterium, the stable isotope of hydrogen. As carbon-deuterium bonds need more energy to break than normal carbon-hydrogen bonds, the necessary energy to break the hydrogen bonds between DNA bases would be higher, making deuterated DNA less sensitive than normal DNA to DNA damage following ionizing radiation exposure. However, a lot of issues have to be solved before deuterium could be applied in humans: lack of evolutionary adaption to catabolize organic compounds containing deuterium, consequent slower rate of vital metabolic reactions, and their potential toxic effects. Nevertheless, it has been shown that deuterated food or water intake helps to increase life or health spans from numerous model organisms.

Gene therapy stands for the use of genetic modifying techniques in order to achieve a therapeutic effect. In the context of radiation and radiation protection, this has been studied for several radioresistance mechanisms making these techniques interesting for deep space missions, where radiation protection concerns arise [374]

One of the strategies for gene therapy in radioresistance is the overexpression of endogenous antioxidants, for example, magnesium superoxide dismutase (MnSOD) that acts as a scavenger for reactive oxygen species produced after the interaction of radiation with the cell [376].

Another angle in which gene therapy can be useful for improving radioresistance is by enhancing the DNA damage repair such as the overexpression of certain repair proteins that are normally active in repairing the damage in the DNA strands after radiation exposure [377].

A promising approach takes its inspiration from extremophiles and their impressive radioresistance capabilities, in concrete, the tardigrades, a microscopic animal that is capable of surviving in extreme conditions. A protein identified in these organisms, termed damaged suppressor (Dsup), has been made to be expressed in human cell lines, reducing the number of DNA strand breaks and preserving cellular proliferative abilities after high doses of radiation [337].

10.9.2 Mechanisms in Extremophiles

10.9.2.1 What is an Extremophile?

Extreme conditions in a natural environment are only extreme from a human point of view. Extremophiles can only live under these conditions and depend on them. Often organisms living under these conditions are called "extremophiles" or "polyextremophiles" since most of them are coping with different extremes in their natural environment [378].

10.9.2.2 Which Adaptations/Mechanisms Are Known?

Plenty of different (poly) extremophiles in natural and human-made extreme environments exist in natural and human-made harsh environments. Examples include anaerobes, (hyper-) thermophiles, psychrophiles, halophiles, acidophiles, xerophiles, and piezophiles. For all the named organismic groups, cellular adaptation mechanisms are known that protect the cells themselves or enable them to live under extreme conditions in their natural habitat. In addition to the intracellular protection mechanisms, general protection mechanisms like spore formation are well-known. For example, the spore of the Bacterium *Bacillus subtilis* is characterized by a thick layer of peptidoglycan, a low water content inside the cell, a DNA conformation changed from B to A, and the presence of α/β-type small acid-soluble spore proteins which accumulate within the spore. In general, spores are more tolerant to inactivating physical stresses, like radiation as vegetative cells [379, 380]. Spore formation is known to be an answer to changing conditions in the environment that is used by microorganisms and fungi; special forms like the anhydrobiotic state are also observed in other eukaryotic cells like tardigrades, nematodes, and rotifers [381]. Spore formation and the anhydrobiotic state, as well as intracellular adaptation mechanisms, are relevant for possible survival after exposure to ionizing (space) radiation [323, 382]. In addition to spore formation, biofilm growth by the production of extracellular polymeric substances (EPS) also leads to a higher ionizing radiation tolerance [383].

Besides the named cellular adaptation mechanisms, there are also different intracellular adaptation mechanisms possible to cope with extreme environmental stresses. As described before, ionizing radiation exposure does not only lead to direct effects and intracellular damage, such as DNA strand breaks, it also leads to indirect effects, like ROS production. Hyperthermophilic Archaea, like *Pyrococcus furiosus*, are partly tolerant to the indirect effects of ionizing radiation, due to mechanisms protecting the DNA from the influence of ROS [384]. In these Archaea, DNA binding proteins play a major role as they bind and protect the DNA thereby limiting the accessibility of the DNA to ROS. In addition, increased expression of different enzymes like superoxide dismutase and the glutathione peroxidase can also reduce the level of intracellular ROS.

For the Bacterium *Deinococcus radiodurans* as well as for the Archaeon *Halobacterium salinarum* special intracellular Mn/Fe ratios are described: they demonstrate an intracellular accumulation of high amounts of manganese along with low iron levels, which contribute to their high radiation tolerance [385, 386]. This special Mn/Fe ratio was not found in radiation-tolerant anaerobic microorganisms. It is proposed that the low levels of IR-generated ROS under anaerobic conditions combined with highly constitutively expressed detoxification systems in these anaerobes are key to their radiation resistance and circumvent the need for the accumulation of Mn-antioxidant complexes in the cell [387].

Furthermore, polyploidy or the presence of several DNA copies within one single cell has been discussed to contribute to tolerance to desiccation and therefore also to ionizing radiation [388].

Halophilic organisms have different strategies to cope with a high salt concentration in their natural habitat. One option is the intracellular accumulation of salt or other compatible solutes [389]. It is also known that compatible solutes can contribute to the tolerance to ionizing radiation in halophilic microorganisms [389]. Additionally, protective mechanisms such as membrane pigments, including carotenoids, melanin, scytonemin, and bacterioruberin were found to be important in ionizing radiation protection in different organisms through the scavenging of hydroxyl radicals [390, 391].

10.9.2.3 How Relevant Are These Adaptations/Mechanisms for Space Radiation?

In general, there is no direct adaptation of microorganisms to space conditions or space radiation known as all organisms evolved on Earth. Nevertheless, there have been and still are space experiments ongoing where the adaptability of different organisms is investigated during exposure to space conditions. In this context, we speak about the side effects of other tolerances or resistances which enable the organisms to endure space stressors. In general, organisms which are tolerant to desiccation developed mechanisms to repair the DNA which is damaged during the desiccation process. The same repair mechanisms can also be used to repair DNA damage caused by other stressors, such as ionizing radiation. One prominent example is the desiccation and radiation tolerance of the microorganism *Deinococcus radiodurans*. This organism uses the same cellular adaptation and repair strategies after exposure to drought and ionizing radiation exposure. However, not all desiccation-tolerant organisms are tolerant to (ionizing) radiation exposure [392]. The same is true for other repair machineries, where no direct correlation between hyper-/thermophilic organisms or the ability to produce compatible solutes and radiation tolerance could be identified [393, 394]. In addition, some microorganisms (e.g., *Ignicoccus hospitalis*) demonstrate a high survival rate after ionizing radiation exposure but possess a repair mechanism which is not known up to now [395].

10.10 Irradiation Experiments at Ground-Based Facilities for Simulation of the Space Environment

10.10.1 Low Dose Rate Irradiation Facilities

As mentioned at the beginning of this chapter, protons account for nearly 87% of the total flux of the galactic cosmic radiation (GCR), helium ions—for approximately 12%, and the remaining heavy ions, or high-Z elements (HZE),—for less than 1%. However, the relative distribution of the effective dose is quite different. Multiplying the abundance by Z^2 provides an estimate of the contribution to the dose. One should further consider the quality factor of the biological effectiveness of the corresponding radiation. As a result, HZE particles contribute approximately 89% of the total dose equivalent (mSv) in free space. Among the HZE particles in GCR, iron is the largest contributor (26%) to the effective dose [396].

10.10.2 Low Dose Rate Particle Irradiation Facilities

Low dose rate irradiation is usually provided in a laboratory either by X-ray machines or radioactive sources, and neither mimics GCR well. The X-rays are low-energy radiation and do not mimic the penetrating capability of GCR. Usual radioactive sources emit α-, β-, and γ-radiation. While α-particles are helium nuclei abundant in GCR, the energy of typical α-particles is 4–9 MeV as compared with above 1000 MeV in GCR. As a result, α-particles cannot penetrate the thinnest screen (even the skin) and cannot be used for GCR simulation.

γ-Radiation has a much stronger penetration capability, and γ-emitters are used [397]. However, the biological effects of γ-radiation and ions are different. As for the β-radiation, in the sense of GCR simulation it combines the drawbacks of α and γ: having low penetrating capability, its biological effects are similar to γ and far from high-energy ions.

A partial solution has been found by using a unique artificial isotope Californium-252, which exhibits exceptionally high neutron emission. ^{252}Cf is used, e.g., at the ESA test station and the new facility in Japan [398].

10.10.3 Low Energy Particle Irradiation Facilities

Although low-energy charged particles (up to about 20 MeV) do not reproduce the characteristics found in the GCR spectrum, low-energy facilities are widely available and are useful to help in the screening and the design of experiments that will be further carried out on higher energy accelerators (see next subsection).

Several accelerator types can be used to produce such low-energy beams, but electrostatic tandem accelerators are probably the most widely used. A schematic representation of such accelerator is given in Fig. 10.28. The first part consists of an ion source, which can produce any negative ion

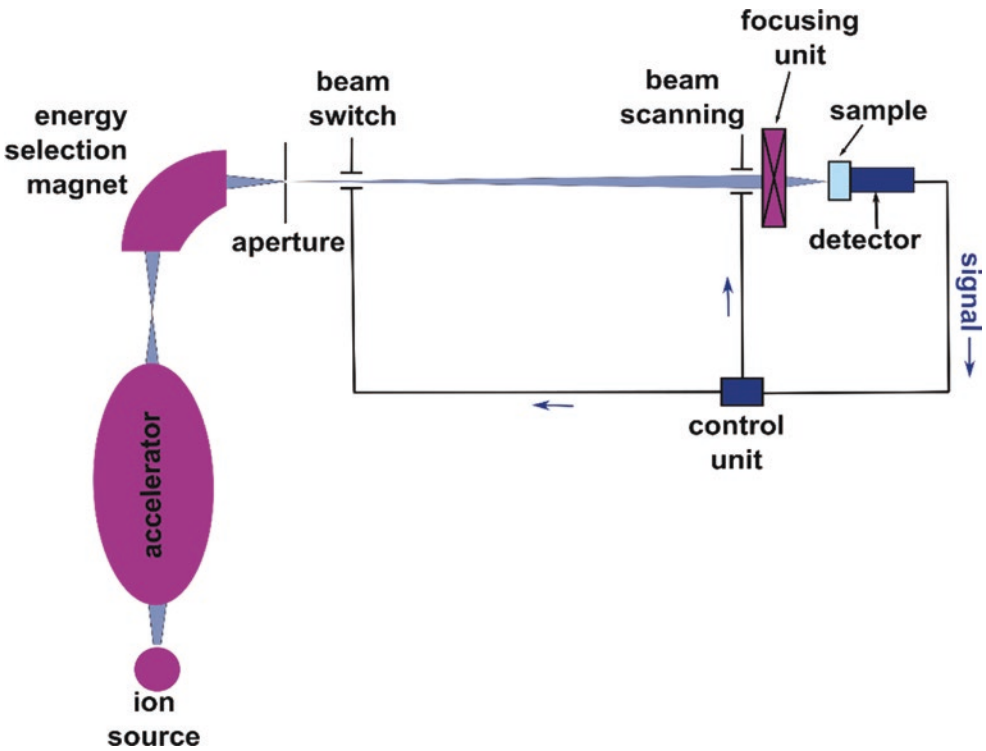

Fig. 10.28 Schematic view of the SNAKE (Superconducting nanoprobe for (kern) particle physics experiments) setup, including linear particle accelerator (orange), focusing unit (superconducting magnetic lens) and detection system with the particle detector and ultrafast high-voltage switch

(with one extra electron) from hydrogen to uranium. The produced negative ion beam is then extracted from the source and guided to the main tube. The acceleration is carried out in two stages hence the name "tandem accelerator." First, the negative ions are attracted to the positive high-voltage "terminal" located in the center of the tube. Then, negative ions can be stripped of part of their electrons (usually 2–3) in the stripper channel, turning to positive ions. These positive ions are repelled by the positive terminal voltage to the end of the tube, which is at ground potential. High-energy ions are focused by (usually superconducting) magnets and deflected into one of the beamlines, according to the particle energy, mass, and charge.

Regarding the beam size, two configurations are used: microbeam and broad beam.

The initial accelerated ion beam is always a microbeam with a diameter often below 5 μm. Microbeams are a useful tool in studying the bystander effect (described in detail in Chap. 2). Indeed, such a beam permits to irradiate selectively one or more cells inside a population. This offers the possibility to either target the cell nucleus, the conventional target in radiobiology, the cytoplasm, or organelles. It also provides the advantage of knowing precisely the dose delivered to the cells and the number of particle shoots being determined in advance. In the context of space radiation, where the flux of high-mass particles is very low and the occurrence of a single shoot-in through a cell is very high, the bystander effect is a topic of crucial importance. Indeed, it is observed through a variety of endpoints: reduction in cell survival, double strand break induction, micronuclei, mutations, and expression of apoptosis, inflammation, and cell cycle-related genes.

Broad beams can be produced either by using scattering foils, by scanning microbeam, or by defocusing them. Beam homogeneity is controlled by plastic scintillators or silicon-based detectors.

10.10.4 High-Energy Particle Irradiation Facilities

The importance of accelerator-based studies was acknowledged by NASA decades ago. After preliminary research at the existing accelerators, it was decided to build a dedicated beamline. In 2003, the NASA Space Radiation Laboratory (NSRL) was commissioned at the Brookhaven National Laboratory (BNL). The NSRL layout is presented in Fig. 10.29. The facility is capable of supplying particles from protons (p) to gold (Au). Available beam energies range from 50 to 2500 MeV for protons and 50 to 1500 MeV per nucleon for ions between helium (He-2) and iron (Fe-56; $Z = 26$).

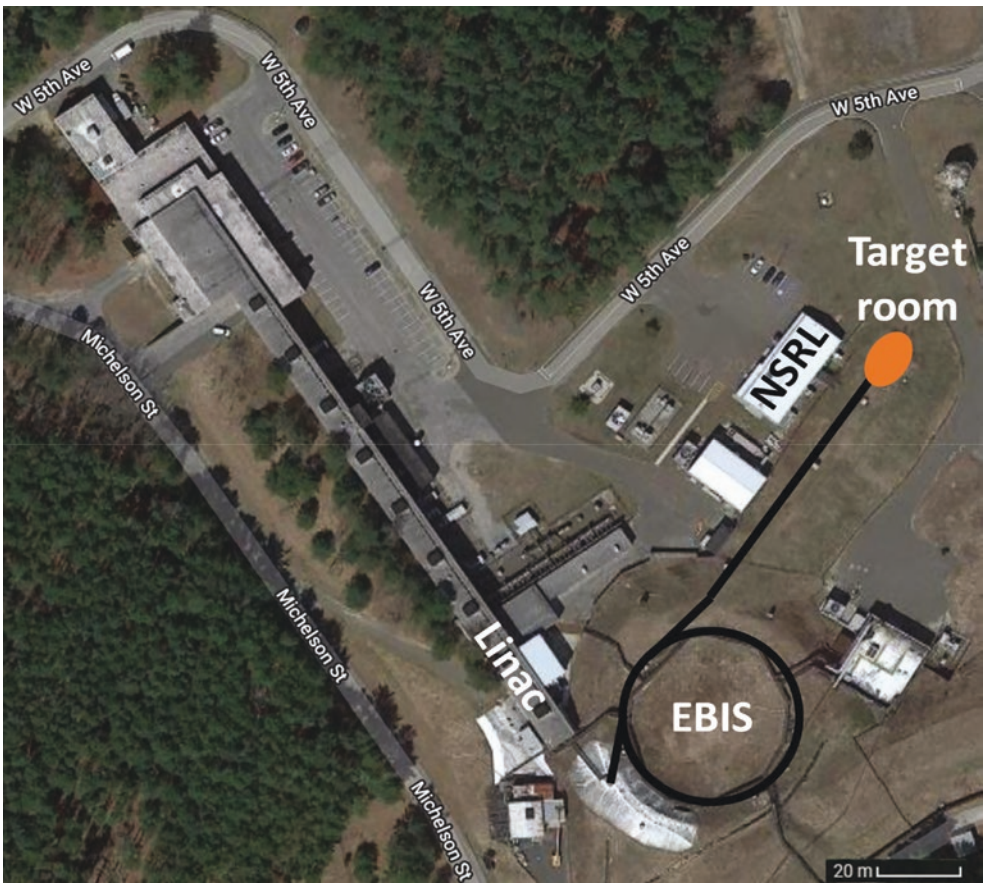

Fig. 10.29 Aerial view and general layout of the NASA Space Radiation Laboratory (NSRL) facility in Upton, NY, USA. *EBIS* electron beam ion source. (Satellite view courtesy Google Earth)

Heavier ions with atomic numbers up to $Z = 79$ (Au) are limited to approximately 350–500 MeV per nucleon (https://www.bnl.gov/nsrl/).

The choice of Fe-56 ions is justified by a sharp decline in abundance for ions heavier than iron [396] while the chosen energy is around the peak of the galactic cosmic radiation spectrum. Moreover, the linear energy transfer is about 140 keV/μm, around the peak of effectiveness for late radiation effects [399]. The three key areas developed together to ultimately provide the GCR simulator at NSRL are illustrated in Fig. 10.30. Several important results have been obtained at NSRL. We can mention, for example, the observation that, despite being high-LET particles, heavy ions are not more effective than γ-radiation in the induction of leukemia in mice [400]. Another example is the discovery of specific types of brain damage caused by heavy ions [401], types that had not been known from X-ray studies.

The basic idea of a high-energy accelerator is illustrated schematically in Fig. 10.31. Each accelerating section itself consists of a sequence of resonant cavities in which the RF (radio frequency) electromagnetic field is oscillating. Ions traverse RF cavities subsequently; the timing of the passage of each cavity is synchronized with the direction and phase of the electric field—therefore, each ion is accelerated from cavity to cavity. In case of a linear accelerator (LINAC), the accelerating sections are positioned adjacently along a straight line. In case of a synchrotron (like EBIS in Fig. 10.31), the accelerating sections are positioned along a circumference, while the charged particle beam is bent between the sections by a magnetic field.

The resonant frequency is usually either about 1 GHz (L-band of the RF spectrum) or about 3 GHz (S-band). The electromagnetic power for feeding the RF cavities is generated usually by a high-power klystron.

The accelerating cavities can be made either of normal-conducting metal ("warm" cavities usually made of copper) or of superconductor (usually, niobium). In the last case, cryogenic cooling to liquid-helium temperature is needed. Accelerating gradients are usually in the range of 10–30 MeV/m, e.g., the 3-km long SLAC accelerator commissioned back in the 1960s, accelerating electrons to the energy of 50 GeV, has an average accelerating gradient of about 17 MeV/m (with 3-GHz copper cavities).

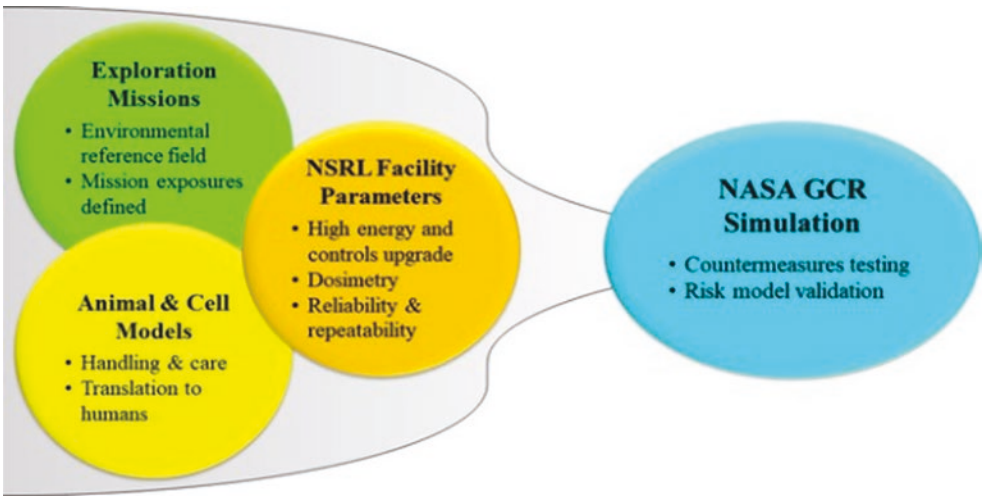

Fig. 10.30 Three key areas developed to provide the GCR simulator at NSRL. (Source: Simonsen et al. [396], reproduced with permission)

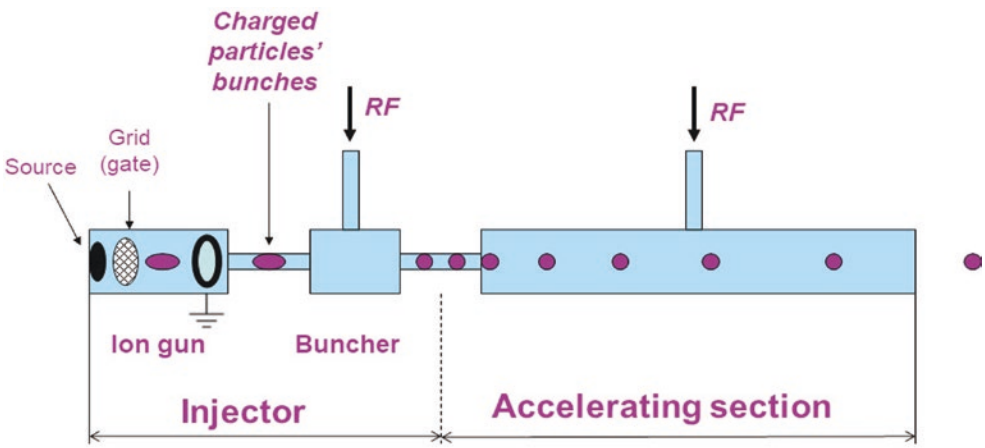

Fig. 10.31 General layout of a linear high-energy particle accelerator. *RF* radio frequency

Output of RF-driven particle accelerator necessarily consists of single bunches. Such bunches are called micropulse, and their duration is just a fraction of the oscillating field period. For example, for the S-band with period of about 300 ps = $(3\ \text{GHz})^{-1}$, the typical micropulse duration is below 20 ps. The train of micropulse is called "macropulse." While there is no theoretical limit for macropulse length, practically it is limited by the driving klystron pulse length: For S-band normal-conducting linacs the typical value is 5–20 μs, for L-band superconducting linacs—much longer (1 ms and more).

Particle beams are collimated and bent "magnetic lenses"—magnetic fields created by electromagnets or permanent magnets. These magnetic devices, governing the charged particle beam propagation, are called electron-optic (or ion-optic) devices. Such devices have some similarities to classical light optics in terms of mathematics, but in general comprise a separate field of knowledge. The reader interested in learning the field of particle beam optics is referred to the classical textbook of Reiser [402].

10.10.5 Space Environment Simulation Platforms

Although ionizing radiations were identified as the main showstopper to exploration mission, there are additional stresses in the space environment. While most of the factors below are not relevant to astronauts, they are important in studying extremophiles.

1. Low pressure: The pressure varies from 10^{-1} Pa near Earth atmosphere to 10^{-14} Pa in deep space. Due to the degassing, pressure around the ISS is higher than in deep space ranging from 10^{-7} Pa in the Ram direction (e.g., front of the ISS relative to flight direction) to 10^{-4} Pa in the Wake direction (e.g., rear of the ISS relative to flight direction) [403].
2. Cold temperature: The low-pressure environment previously described drastically increases the molecular mean free path in space resulting in low heat transfer. Consequently, the temperature in deep space ranges from 3 to 4 K (–270 to –260°C) [404].
3. Solar radiation: Highly energetic phenomena are occurring in the Sun leading to the emission of high-intensity electromagnetic radiations. By moving away from the Sun, the emitted solar radiations are spread out over a large surface area reducing the solar irradiance with increased Sun-object distance. ISS, located at one astronomical unit distance from the Sun, is exposed to an approximate 1400 W/m^2 heat flux. The associated electromagnetic spectrum extends from X-rays to radio waves with a higher proportion in the visible (47%), infrared (45%), and ultraviolet (7%) ranges [405].
4. Day and night cycles: As ISS orbits around the Earth and the latter around the Sun, the stress exposure has a cyclic temporal behavior with two main periods. The "day and night" cycle caused by the rotation around the Earth has a period of 91 min resulting in fluctuation in total irradiance and temperature of more than 1000 W/m^2 and 5–10 °C. The second cycle (period of approximately 1 month) is due to the position change of ISS orbital plane relative to the Sun. In this case, greater variations of temperature (up to 60 °C) with a maximal temperature of about 50 °C were reported [406].

To study the biological impact of the space environment, modules outside the ISS are an ideal environment to expose biological samples to LEO, where the conditions strongly differ from the ones encountered on Earth. However, the poor availability of these facilities stimulated the creation of exposure chambers on Earth capable of reproducing this LEO environment. The Laboratory for Analysis by Nuclear Reactions (LARN, University of Namur, Belgium, https://www.unamur.be/en/sci/physics/ur-en/larn-en) has developed an exposure module to simulate the aforementioned conditions on the ground for extended periods of time (several months). To this end, biological samples are placed into a vacuum chamber and exposed to various constraints. A cooling system located underneath the sample tray and an electromagnetic source reproducing the solar spectrum are controlled by a monitoring system capable to simulate the slow and fast cycles described above. In addition, a variety of neutral density filters and cut-off waveband filters enables to create multiple irradiance conditions within the same experiment, in order to investigate what part of the UV-visible spectrum is the most deleterious.

A similar facility also exists at DLR Cologne and has been recurrently used for pre-flight test programs and mission ground reference experiments for several astrobiological long-term space missions [405].

10.11 Exercises and Self-Assessment

Q1. Which types of radiation exist in space?
Q2. Are astronauts fully protected from radiation by spacecraft walls?
Q3. Can you describe the difference between the radiation environment on Earth (on ground) and the one at the surface of Mars?
Q4. What do we know now about specific health problems of astronauts?
Q5. What is the role of plants in Bioregenerative Life Support Systems (BLSS)?
Q6. What is the 3R Principle?

Q7. What kind of chronic effects on the CNS (central nervous system) were observed?
Q8. What is the difference between organoids and spheroids?
Q9. From which cells organoids can be cultured?
Q10. What is the main reason why bioprinting and other 3D cultures can be better cultured in Space?
Q11. What parameters should be considered if we would like to simulate conditions on Moon/Mars surface or in deep space (including stress unrelated to radiation)?
Q12. What is the interest to study the biological effects of low energy charged particles in the context of space radiation exposure?

10.12 Exercise Answers

SQ1. Galactic Cosmic Rays, Solar Energetic Particles, Trapped radiation, and the solar wind
SQ2. No, the high penetrating character of GCRs and the cascades of secondary particles generated by the passage of GRCs ions through the spacecraft walls create an intravehicular field which is of high concern for the health risk of astronauts
SQ3. On Earth we are protected by both the atmosphere and the magnetic field: GCRs hitting the top of the atmosphere create particle showers but only a few of such secondaries (and very few of direct GCR ions) reach the ground. SEP are mostly shielded by the atmosphere and are of concern only for extreme events and mostly for high latitude/high-altitude flights for eventual biological risks, or on ground for infrastructures. On Mars, the very thin atmosphere offers very little shielding, and the exposure to GRCs, their secondary particles, and SEP is a concern.
SQ4. Though there are many concerns, the present evidence does not provide a conclusive answer. Astronauts as a cohort are not less healthy than US Air Force pilots, e.g., and much healthier than the general public (due to selection). The LNT-estimated cancer death risk for prolonged missions is considerable, but applicability of LNT for low dose rates is questionable.
SQ5. Plants in LSS remove carbon dioxide and provide oxygen, help water purification, can recycle wastes of the astronauts, and provide fresh food for the crew.
SQ6. Reduction (first R) of animal numbers, Refining (second) the test methods to lower the harm to the animal to a minimum, and Replace (third) animal experiments with alternative methods, when possible
SQ7. Reduction of dendrites, reduced neurogenesis and increased neuroinflammation, diminished hippocampal neuron excitability
SQ8. Spheroids are also a 3D cell cultures, but in comparison to organoids, they form simple clusters into sphere-like formation, but they cannot self-assemble or regenerate.
SQ9. Pluripotent stem cells
SQ10. Microgravity
SQ11. The particular profile of radiation spectrum can vary according to the location of interest. The ISS environment benefits from some protection granted by the Earth magnetic field. This is not the case for deep space or Mars, where the full spectrum of galactic cosmic rays should be considered. Solar proton events should be included, can vary in magnitude and their extent also depends on the distance to the sun. Beside radiation, day and night cycle can impact temperature conditions, which lead to biological effects on some model organisms. Pressure value and the presence or not of atmosphere should also be considered.
SQ12. Although the vast majority of particles in the GCR spectrum have very high energy, low energy charged particles are still produced in shielding materials and arise from fragmentation of heavier energetic nuclei. These low-energy particles often traverse shielding and remain of concern.

References

1. Lear J. Kepler's dream. University of California Press; 1965.
2. Curie P. Oeuvres de Pierre Curie. Editions des Archives Contemporaines. 1984.
3. Todd P, Tobias CA, Silver IL. Current topics in space radiation biology. In: Tobias C, Todd P, editors. Space radiation biology and related topics. Academic Press; 1974. p. 1–18.
4. Millikan RA. Electrons (+ and -), protons, photons, neutrons, mesotrons and cosmic rays. University of Chicago Press; 1947.
5. Hess VF, Eugster JAG. Cosmic radiation and its biological effects. Fordham University Press; 1949.
6. Maalouf M, Durante M, Foray N. Biological effects of space radiation on human cells: history, advances and outcomes. J Radiat Res. 2011;52(2):126–46. https://doi.org/10.1269/jrr.10128.
7. Van Allen JA, Frank LA. Radiation around the earth to a radial distance of 107,400 km. Nature. 1959;183(4659):430–4. https://doi.org/10.1038/183430a0.
8. Van Allen JA, Frank LA. Radiation measurements to 658,300 km with Pioneer IV. Nature. 1959;184(4682):219–24. https://doi.org/10.1038/184219a0.
9. Neugebauer M, Snyder CW. Interplanetary solar wind measurements by Mariner II. In: Muller P, editor. Space research, vol. 4. North-Holland Publications; 1964. p. 89–113.
10. Bucker H. The Biostack experiments I and II aboard Apollo 16 and 17. Life Sci Space Res. 1974;12:43–50. https://www.ncbi.nlm.nih.gov/pubmed/11908528.

11. Rabbow E, Rettberg P, Parpart A, Panitz C, Schulte W, Molter F, Jaramillo E, Demets R, Weiß P, Willnecker R. EXPOSE-R2: the astrobiological ESA mission on board of the International Space Station. Front Microbiol. 2017;8(1533) https://doi.org/10.3389/fmicb.2017.01533.
12. Yamagishi A, Hashimoto H, Yano H, Imai E, Tabata M, Higashide M, Okudaira K. Four-year operation of Tanpopo: astrobiology exposure and micrometeoroid capture experiments on the JEM exposed facility of the International Space Station. Astrobiology. 2021;21(12):1461–72. https://doi.org/10.1089/ast.2020.2430.
13. Senatore G, Mastroleo F, Leys N, Mauriello G. Effect of microgravity & space radiation on microbes. Future Microbiol. 2018;13:831–47. https://doi.org/10.2217/fmb-2017-0251.
14. Beuther H, Klessen RS, Dullemond CP, Henning TK. Protostars and planets VI. University of Arizona Press; 2014. https://books.google.be/books?id=tQswBQAAQBAJ.
15. Chancellor J, Nowadly C, Williams J, Aunon-Chancellor S, Chesal M, Looper J, Newhauser W. Everything you wanted to know about space radiation but were afraid to ask. J Environ Sci Health C. 2021;39(2):113–28. https://doi.org/10.1080/26896583.2021.1897273.
16. Reitz G. Characteristic of the radiation field in low Earth orbit and in deep space. Z Med Phys. 2008;18(4):233–43. https://doi.org/10.1016/j.zemedi.2008.06.015.
17. Hellweg CE, Baumstark-Khan C. Getting ready for the manned mission to Mars: the astronauts' risk from space radiation. Naturwissenschaften. 2007;94(7):517–26. https://doi.org/10.1007/s00114-006-0204-0.
18. Heber B, Fichtner H, Scherer K. Solar and heliospheric modulation of galactic cosmic rays. Space Sci Rev. 2006;125(1–4):81–93. https://doi.org/10.1007/s11214-006-9048-3.
19. Mewaldt RA, Davis AJ, Lave KA, Leske RA, Stone EC, Wiedenbeck ME, Binns WR, Christian ER, Cummings AC, de Nolfo GA, Israel MH, Labrador AW, von Rosenvinge TT. Record-setting cosmic-ray intensities in 2009 and 2010. Astrophys J Lett. 2010;723(1):L1–6. https://doi.org/10.1088/2041-8205/723/1/L1.
20. Badhwar GD, O'Neill PM. Galactic cosmic radiation model and its applications. Adv Space Res. 1996;17(2):7–17. https://doi.org/10.1016/0273-1177(95)00507-b.
21. Townsend LW, Badhwar GD, Braby LA, Blakely EA, Cucinotta FA, Curtis DB, Fry RJM, Land CE, Smart DF. Report No. 153—Information needed to make radiation protection recommendations for space missions beyond low-earth orbit (report no. 153). 2006.
22. Cane HV. Coronal mass ejections and forbush decreases. Space Sci Rev. 2000;93(1–2):55–77. https://doi.org/10.1023/A:1026532125747.
23. Beatty J, Ahn HS, Allison PS, Choi MJ, Conklin N, Stephane C, Michael AD, Ganel O, Jaminion S, Kim KC, Lee MH, Lutz L, Pier Simone M, Minnick S, Mognet SI, Kyung-wook M, Nutter SL, Park H, Park IH, et al. The Cosmic Ray Energetics and Mass (CREAM) experiment timing charge detector. Proc SPIE. 2003;4858:248.
24. Yi-ran Z, Si-ming LIU. The origin of cosmic rays from supernova remnants. Chin Astron Astrophys. 2020;44(1):1–31. https://doi.org/10.1016/j.chinastron.2020.04.001.
25. Mishev A. Short- and medium-term induced ionization in the earth atmosphere by galactic and solar cosmic rays. Int J Atmos Sci. 2013;2013:1–9. https://doi.org/10.1155/2013/184508.
26. Usoskin IG, Desorgher L, Velinov P, Storini M, Fluckiger E, Butikofer R, Kovaltsov GA. Ionization of the earth's atmosphere by solar and galactic cosmic rays. Acta Geophys. 2009;57(1):88–101. https://doi.org/10.2478/s11600-008-0019-9.
27. Huff J. Evidence report: risk of acute radiation syndromes due to solar particle events. 2016.
28. Meier MM, Matthia D. A space weather index for the radiation field at aviation altitudes. J Space Weather Space Climate. 2014;4:A13. https://doi.org/10.1051/swsc/2014010.
29. Malandraki OE, Crosby NB. Solar energetic particles and space weather: science and applications. In: Malandraki OE, Crosby NB, editors. Solar particle radiation storms forecasting and analysis. Springer International Publishing; 2018. p. 1–26. https://doi.org/10.1007/978-3-319-60051-2_1.
30. Schwenn R. Solar wind sources and their variations over the solar cycle. Space Sci Rev. 2006;124(1–4):51–76. https://doi.org/10.1007/s11214-006-9099-5.
31. Wu H, Huff J, Casey R, Kim M, Cucinotta F. Risk of acute radiation syndromes due to solar particle events, human health and performance risks of space exploration missions, NASA SP-2009-3405. 2009. p. 171–90.
32. Meyer-Vernet N. Basics of the solar wind. Cambridge University Press; 2007. https://doi.org/10.1017/cbo9780511535765.
33. Hellweg CE, Matthiä D, Berger T, Baumstark-Khan C. Radiation in space: the physics. In: Radiation in space: relevance and risk for human missions. Springer International Publishing; 2020. p. 7–43. https://doi.org/10.1007/978-3-030-46744-9_2.
34. Reitz G, Beaujean R, Benton E, Burmeister S, Dachev T, Deme S, Luszik-Bhadra M, Olko P. Space radiation measurements on-board ISS—the DOSMAP experiment. Radiat Prot Dosimetry. 2005;116(1–4 Pt 2):374–9. https://doi.org/10.1093/rpd/nci262.
35. Ersmark T, Carlson P, Daly E, Fuglesang C, Gudowska I, Lund-Jensen B, Nierninen P, Pearce M, Santin G. Geant4 Monte Carlo Simulations of the belt proton radiation environment on board the International Space Station/Columbus. IEEE Trans Nucl Sci. 2007;54(4):1444–53. https://doi.org/10.1109/Tns.2007.896344.
36. Ersmark T, Carlson P, Daly E, Fuglesang C, Gudowska I, Lund-Jensen B, Nieminen P, Pearce M, Santin G. Geant4 Monte Carlo simulations of the galactic cosmic ray radiation environment on-board the International Space Station/Columbus. IEEE Trans Nucl Sci. 2007;54(5):1854–62. https://doi.org/10.1109/Tns.2007.906276.
37. Dietze G, Bartlett DT, Cool DA, Cucinotta FA, Jia X, McAulay IR, Pelliccioni M, Petrov V, Reitz G, Sato T. ICRP Publication 123. Assessment of radiation exposure of astronauts in space. Ann ICRP. 2013;42(4):1–339. https://doi.org/10.1016/j.icrp.2013.05.004.
38. Watts JW, Parnell TA, Heckman HH. Approximate angular distribution and spectra for geomagnetically trapped protons in low-Earth orbit. AIP Conf Proc. 1989;186(1):75–85. https://doi.org/10.1063/1.38168.
39. Dobynde MI, Shprits YY. Radiation environment created with GCRs inside a spacecraft. Life Sci Space Res (Amst). 2020;24:116–21. https://doi.org/10.1016/j.lssr.2019.09.001.
40. Dyer CS, Truscott PR, Evans H, Sims AJ, Hammond N, Comber C. Secondary radiation environments in heavy space vehicles and instruments. Adv Space Res. 1996;17(2):53–8. https://doi.org/10.1016/0273-1177(95)00512-d.
41. Hassler DM, Zeitlin C, Wimmer-Schweingruber RF, Bottcher S, Martin C, Andrews J, Bohm E, Brinza DE, Bullock MA, Burmeister S, Ehresmann B, Epperly M, Grinspoon D, Kohler J, Kortmann O, Neal K, Peterson J, Posner A, Rafkin S, et al. The Radiation Assessment Detector (RAD) investigation. Space Sci Rev. 2012;170(1–4):503–58. https://doi.org/10.1007/s11214-012-9913-1.
42. Guo JN, Zeitlin C, Wimmer-Schweingruber RF, Hassler DM, Posner A, Heber B, Kohler J, Rafkin S, Ehresmann B, Appel JK, Bohm E, Bottcher S, Burmeister S, Brinza DE, Lohf H, Martin C, Reitz G. Variations of dose rate observed by MSL/RAD in transit to Mars. Astron Astrophys. 2015;577:A58. https://doi.org/10.1051/0004-6361/201525680.

43. Iosim S, MacKay M, Westover C, Mason CE. Translating current biomedical therapies for long duration, deep space missions. Prec Clin Med. 2019;2(4):259–69. https://doi.org/10.1093/pcmedi/pbz022.
44. Zhang S, Wimmer-Schweingruber RF, Yu J, Wang C, Fu Q, Zou Y, Sun Y, Wang C, Hou D, Bottcher SI, Burmeister S, Seimetz L, Schuster B, Knierim V, Shen G, Yuan B, Lohf H, Guo J, Xu Z, et al. First measurements of the radiation dose on the lunar surface. Sci Adv. 2020;6(39):eaaz1334. https://doi.org/10.1126/sciadv.aaz1334.
45. Naito M, Hasebe N, Shikishima M, Amano Y, Haruyama J, Matias-Lopes JA, Kim KJ, Kodaira S. Radiation dose and its protection in the Moon from galactic cosmic rays and solar energetic particles: at the lunar surface and in a lava tube. J Radiol Prot. 2020;40(4):947–61. https://doi.org/10.1088/1361-6498/abb120.
46. Da Pieve F, Gronoff G, Guo J, Mertens CJ, Neary L, Gu B, Koval NE, Kohanoff J, Vandaele AC, Cleri F. Radiation environment and doses on Mars at Oxia Planum and Mawrth Vallis: support for exploration at sites with high biosignature preservation potential. J Geophys Res Planets. 2021;126(1):e2020JE006488. https://doi.org/10.1029/2020je006488.
47. Guo JN, Zeitlin C, Wimmer-Schweingruber RF, McDole T, Kuhl P, Appel JC, Matthia D, Krauss J, Kohler J. A generalized approach to model the spectra and radiation dose rate of solar particle events on the surface of Mars. Astron J. 2018;155(1):49. https://doi.org/10.3847/1538-3881/aaa085.
48. Saganti PB, Cucinotta FA, Wilson JW, Schimmerling W. Visualization of particle flux in the human body on the surface of Mars. J Radiat Res. 2002;43(Suppl):S119–24. https://doi.org/10.1269/jrr.43.s119.
49. Röstel L, Guo J, Banjac S, Wimmer-Schweingruber RF, Heber B. Subsurface radiation environment of mars and its implication for shielding protection of future habitats. J Geophys Res Planets. 2020;125(3):e2019JE006246. https://doi.org/10.1029/2019je006246.
50. Cucinotta FA, To K, Cacao E. Predictions of space radiation fatality risk for exploration missions. Life Sci Space Res (Amst). 2017;13:1–11. https://doi.org/10.1016/j.lssr.2017.01.005.
51. Cucinotta F, Kim MY, Chappell L. Space radiation cancer risk projections and uncertainties. NASA TP, 2011-216155. 2011.
52. Guo J, Zeitlin C, Wimmer-Schweingruber RF, Rafkin S, Hassler DM, Posner A, Heber B, Köhler J, Ehresmann B, Appel JK, Böhm E, Böttcher S, Burmeister S, Brinza DE, Lohf H, Martin C, Kahanpää H, Reitz G. Modeling the variations of dose rate measured by rad during the firstmslmartian year: 2012–2014. Astrophys J. 2015;810(1):24. https://doi.org/10.1088/0004-637x/810/1/24.
53. McKenna-Lawlor S, Goncalves P, Keating A, Morgado B, Heynderickx D, Nieminen P, Santin G, Truscott P, Lei F, Foing B, Balaz J. Characterization of the particle radiation environment at three potential landing sites on Mars using ESA's MEREM models. Icarus. 2012;218(1):723–34. https://doi.org/10.1016/j.icarus.2011.04.004.
54. Dartnell LR, Desorgher L, Ward JM, Coates AJ. Martian sub-surface ionising radiation: biosignatures and geology. Biogeosciences. 2007;4(4):545–58. https://doi.org/10.5194/bg-4-545-2007.
55. Pavlov AA, Vasilyev G, Ostryakov VM, Pavlov AK, Mahaffy P. Degradation of the organic molecules in the shallow subsurface of Mars due to irradiation by cosmic rays. Geophys Res Lett. 2012;39(13):L13202. https://doi.org/10.1029/2012gl052166.
56. Wilson JW, Badavi FF, Cucinotta FA, Shinn JL, Badhwar GD, Silberberg R, Tsao CH, Townsend LW, Tripathi RK. HZETRN: description of a free-space ion and nucleon transport and shielding computer program. 1995.
57. Wilson JW, Cucinotta FA, Shinn JL, Simonsen LC, Badavi FF. Overview of HZETRN and BRNTRN space radiation shielding codes. Proc SPIE. 1996; https://doi.org/10.1117/12.254055.
58. Walsh L, Schneider U, Fogtman A, Kausch C, McKenna-Lawlor S, Narici L, Ngo-Anh J, Reitz G, Sabatier L, Santin G, Sihver L, Straube U, Weber U, Durante M. Research plans in Europe for radiation health hazard assessment in exploratory space missions. Life Sci Space Res (Amst). 2019;21:73–82. https://doi.org/10.1016/j.lssr.2019.04.002.
59. Cleri F. Monte-Carlo methods for the study of the diffusion of charged particles through matter. World Scientific Publishing Co; 1990. http://inis.iaea.org/search/search.aspx?orig_q=RN:23017642.
60. Allison J, Amako K, Apostolakis J, Araujo H, Dubois PA, Asai M, Barrand G, Capra R, Chauvie S, Chytracek R, Cirrone GAP, Cooperman G, Cosmo G, Cuttone G, Daquino GG, Donszelmann M, Dressel M, Folger G, Foppiano F, et al. Geant4 developments and applications. IEEE Trans Nucl Sci. 2006;53(1):270–8. https://doi.org/10.1109/Tns.2006.869826.
61. Battistoni G. The FLUKA code, galactic cosmic ray and solar energetic particle events: from fundamental physics to space radiation and commercial aircraft doses. In: 2008 IEEE nuclear science symposium conference record, 19–25 Oct 2008.
62. Sato T, Niita K, Matsuda N, Hashimoto S, Iwamoto Y, Noda S, Ogawa T, Iwase H, Nakashima H, Fukahori T, Okumura K, Kai T, Chiba S, Furuta T, Sihver L. Particle and heavy ion transport code system, PHITS, version 2.52. J Nucl Sci Technol. 2013;50(9):913–23. https://doi.org/10.1080/00223131.2013.814553.
63. Mrigakshi AI, Matthia D, Berger T, Reitz G, Wimmer-Schweingruber RF. Assessment of galactic cosmic ray models. J Geophys Res Space Phys. 2012;117(A8):A08109. https://doi.org/10.1029/2012ja017611.
64. Tylka AJ, Adams JH, Boberg PR, Brownstein B, Dietrich WF, Flueckiger EO, Petersen EL, Shea MA, Smart DF, Smith EC. CREME96: a revision of the cosmic ray effects on microelectronics code. IEEE Trans Nucl Sci. 1997;44(6):2150–60. https://doi.org/10.1109/23.659030.
65. Nymmik RA, Panasyuk MI, Pervaja TI, Suslov AA. A model of galactic cosmic-ray fluxes. Nuclear Tracks Radiat Meas. 1992;20(3):427–9. https://doi.org/10.1016/1359-0189(92)90028-T.
66. O'Neill PM. Badhwar–O'Neill 2010 galactic cosmic ray flux model—revised. IEEE Trans Nucl Sci. 2010;57(6):3148–53. https://doi.org/10.1109/tns.2010.2083688.
67. Usoskin IG, Alanko-Huotari K, Kovaltsov GA, Mursula K. Heliospheric modulation of cosmic rays: monthly reconstruction for 1951-2004. J Geophys Res Space Phys. 2005;110(A12):A12108. https://doi.org/10.1029/2005ja011250.
68. Matthia D, Berger T, Mrigakshi AI, Reitz G. A ready-to-use galactic cosmic ray model. Adv Space Res. 2013;51(3):329–38. https://doi.org/10.1016/j.asr.2012.09.022.
69. Mertens CJ, Slaba TC. Characterization of solar energetic particle radiation dose to astronaut crew on deep-space exploration missions. Space Weather Int J Res Appl. 2019;17(12):1650-1658. https://doi.org/10.1029/2019sw002363.
70. Banjac S, Heber B, Herbst K, Berger L, Burmeister S. On-the-fly calculation of absorbed and equivalent atmospheric radiation dose in a water phantom with the atmospheric radiation interaction simulator (AtRIS). J Geophys Res Space Phys. 2019;124(12):9774–90. https://doi.org/10.1029/2019ja026622.
71. Picone JM, Hedin AE, Drob DP, Aikin AC. NRLMSISE-00 empirical model of the atmosphere: statistical comparisons and scientific issues. J Geophys Res Space Phys. 2002;107(A12):1468. https://doi.org/10.1029/2002ja009430.
72. Köhli M, Weimar J, Schrön M, Baatz R, Schmidt U. Soil moisture and air humidity dependence of the above-ground cosmic-ray neutron intensity [Original Research]. Front Water. 2021;2(66) https://doi.org/10.3389/frwa.2020.544847.
73. Matthia D, Ehresmann B, Lohf H, Kohler J, Zeitlin C, Appel J, Sato T, Slaba T, Martin C, Berger T, Boehm E, Boettcher S,

Brinza DE, Burmeister S, Guo J, Hassler DM, Posner A, Rafkin SCR, Reitz G, et al. The Martian surface radiation environment—a comparison of models and MSL/RAD measurements. J Space Weather Space Climate. 2016;6:A13. https://doi.org/10.1051/swsc/2016008.
74. Ehresmann B. The Martian radiation environment—early mars and future measurements with the radiation assessment detector. 2012. https://macau.uni-kiel.de/receive/diss_mods_00008315.
75. Vuolo M, Baiocco G, Barbieri S, Bocchini L, Giraudo M, Gheysens T, Lobascio C, Ottolenghi A. Exploring innovative radiation shielding approaches in space: a material and design study for a wearable radiation protection spacesuit. Life Sci Space Res (Amst). 2017;15:69–78. https://doi.org/10.1016/j.lssr.2017.08.003.
76. Gronoff G, Norman RB, Mertens CJ. Computation of cosmic ray ionization and dose at Mars. I: a comparison of HZETRN and Planetocosmics for proton and alpha particles. Adv Space Res. 2015;55(7):1799–805. https://doi.org/10.1016/j.asr.2015.01.028.
77. Vetter RJ, Baker ES, Borak TB, Bartlett DT, Langhorst SM, McKeever S, Preston R, Miller J, Wilson J, Meinhold CB, Rosenstein M, O'Brien CL, Tenforde T. Operational radiation safety program for astronauts in low-earth orbit: a basic framework. NCRP Report, i–ix+1. 2002.
78. ICRP. The 2007 Recommendations of the International Commission on Radiological Protection. Ann ICRP. ICRP publication 103. 2007. 0146-6453 (Print).
79. Cucinotta FA. A new approach to reduce uncertainties in space radiation cancer risk predictions. PLoS One. 2015;10(3):e0120717. https://doi.org/10.1371/journal.pone.0120717.
80. White RJ, Averner M. Humans in space. Nature. 2001;409(6823):1115–8. https://doi.org/10.1038/35059243.
81. Berger T, Bilski P, Hajek M, Puchalska M, Reitz G. The MATROSHKA experiment: results and comparison from extravehicular activity (MTR-1) and intravehicular activity (MTR-2A/2B) exposure. Radiat Res. 2013;180(6):622–37. https://doi.org/10.1667/RR13148.1.
82. Puchalska M, Bilski P, Berger T, Hajek M, Horwacik T, Korner C, Olko P, Shurshakov V, Reitz G. NUNDO: a numerical model of a human torso phantom and its application to effective dose equivalent calculations for astronauts at the ISS. Radiat Environ Biophys. 2014;53(4):719–27. https://doi.org/10.1007/s00411-014-0560-7.
83. Hassler DM, Zeitlin C, Wimmer-Schweingruber RF, Ehresmann B, Rafkin S, Eigenbrode JL, Brinza DE, Weigle G, Bottcher S, Bohm E, Burmeister S, Guo J, Kohler J, Martin C, Reitz G, Cucinotta FA, Kim MH, Grinspoon D, Bullock MA, et al. Mars' surface radiation environment measured with the Mars Science Laboratory's Curiosity rover. Science. 2014;343(6169):1244797. https://doi.org/10.1126/science.1244797.
84. Zeitlin C, Hassler DM, Cucinotta FA, Ehresmann B, Wimmer-Schweingruber RF, Brinza DE, Kang S, Weigle G, Bottcher S, Bohm E, Burmeister S, Guo J, Kohler J, Martin C, Posner A, Rafkin S, Reitz G. Measurements of energetic particle radiation in transit to Mars on the Mars Science Laboratory. Science. 2013;340(6136):1080–4. https://doi.org/10.1126/science.1235989.
85. Charles M. UNSCEAR report 2000: sources and effects of ionizing radiation. United Nations Scientific Committee on the Effects of Atomic Radiation. J Radiol Prot. 2001;21(1):83–6. https://doi.org/10.1088/0952-4746/21/1/609.
86. Drouet M, Herodin F. Radiation victim management and the haematologist in the future: time to revisit therapeutic guidelines? Int J Radiat Biol. 2010;86(8):636–48. https://doi.org/10.3109/09553001003789604.
87. Hamm PB, Billica RD, Johnson GS, Wear ML, Pool SL. Risk of cancer mortality among the Longitudinal Study of Astronaut Health (LSAH) participants. Aviat Space Environ Med. 1998;69(2):142–4. https://www.ncbi.nlm.nih.gov/pubmed/9491253.
88. Elgart SR, Little MP, Chappell LJ, Milder CM, Shavers MR, Huff JL, Patel ZS. Radiation exposure and mortality from cardiovascular disease and cancer in early NASA astronauts. Sci Rep. 2018;8(1):8480. https://doi.org/10.1038/s41598-018-25467-9.
89. Cucinotta FA, Nikjoo H, Goodhead DT. The effects of delta rays on the number of particle-track traversals per cell in laboratory and space exposures. Radiat Res. 1998;150(1):115–9. https://www.ncbi.nlm.nih.gov/pubmed/9650608.
90. Burns FJ, Jin Y, Garte SJ, Hosselet S. Estimation of risk based on multiple events in radiation carcinogenesis of rat skin. Adv Space Res. 1994;14(10):507–19. https://doi.org/10.1016/0273-1177(94)90506-1.
91. Dicello JF, Christian A, Cucinotta FA, Gridley DS, Kathirithamby R, Mann J, Markham AR, Moyers MF, Novak GR, Piantadosi S, Ricart-Arbona R, Simonson DM, Strandberg JD, Vazquez M, Williams JR, Zhang Y, Zhou H, Huso D. In vivo mammary tumourigenesis in the Sprague-Dawley rat and microdosimetric correlates. Phys Med Biol. 2004;49(16):3817–30. https://doi.org/10.1088/0031-9155/49/16/024.
92. Cucinotta FA, Wu H, Shavers MR, George K. Radiation dosimetry and biophysical models of space radiation effects. Gravit Space Biol Bull. 2003;16(2):11–8. https://www.ncbi.nlm.nih.gov/pubmed/12959127.
93. Durante M. Biomarkers of space radiation risk. Radiat Res. 2005;164(4 Pt 2):467–73. https://doi.org/10.1667/rr3359.1.
94. Edwards AA. The use of chromosomal aberrations in human lymphocytes for biological dosimetry. Radiat Res. 1997;148(5 Suppl):S39–44. https://www.ncbi.nlm.nih.gov/pubmed/9355855.
95. Testard I, Ricoul M, Hoffschir F, Flury-Herard A, Dutrillaux B, Fedorenko B, Gerasimenko V, Sabatier L. Radiation-induced chromosome damage in astronauts' lymphocytes. Int J Radiat Biol. 1996;70(4):403–11. https://doi.org/10.1080/095530096144879.
96. Gooch PC, Berry CA. Chromosome analyses of Gemini astronauts. Aerosp Med. 1969;40(6):610–4. https://www.ncbi.nlm.nih.gov/pubmed/5785487.
97. Druzhinin SV. Cytogenetic effect in lymphocytes in astronauts after 2 lengthy flights on board MIR orbital station. Aviakosm Ekolog Med. 1999;33(4):3–5. https://www.ncbi.nlm.nih.gov/pubmed/10530376 (Tsitogeneticheskie effekty v limfotsitakh krovi kosmonavtov posle dvukh prodolzhitel'nykh poletov na orbital'nom komplekse "Mir").
98. Fedorenko B, Druzhinin S, Yudaeva L, Petrov V, Akatov Y, Snigiryova G, Novitskaya N, Shevchenko V, Rubanovich A. Cytogenetic studies of blood lymphocytes from cosmonauts after long-term space flights on Mir station. Adv Space Res. 2001;27(2):355–9. https://doi.org/10.1016/s0273-1177(01)00011-4.
99. Fedorenko BS, Shevchenko VA, Snigireva GP, Druzhinin SV, Repina LA, Novitskaia NN, Akatov I, A. Cytogenetic studies of blood lymphocytes of cosmonauts after long-term, space flights. Radiat Biol Radioecol. 2000;40(5):596–602. https://www.ncbi.nlm.nih.gov/pubmed/11252235 (Tsitogeneticheskie issledovaniia limfotsitov krovi kosmonavtov posle dlitel'nykh poletov).
100. Fedorenko BS, Snigireva GP, Bogomazova AN, Novitskaia NN, Shevchenko VA. Cytogenetic effects on blood lymphocytes of cosmonauts after low doses of space radiation. Aviakosm Ekolog Med. 2008;42(3):13–8. https://www.ncbi.nlm.nih.gov/pubmed/19055005.
101. George K, Durante M, Wu H, Willingham V, Badhwar G, Cucinotta FA. Chromosome aberrations in the blood lymphocytes of astronauts after space flight. Radiat Res. 2001;156(6):731–8. https://doi.org/10.1667/0033-7587(2001)156[0731:caitbl]2.0.co;2.
102. George K, Wu H, Willingham V, Cucinotta FA. The effect of space radiation on the induction of chromosome damage. Phys

Med. 2001;17(Suppl 1):222–5. https://www.ncbi.nlm.nih.gov/pubmed/11776981.
103. Greco O, Durante M, Gialanella G, Grossi G, Pugliese M, Scampoli P, Snigiryova G, Obe G. Biological dosimetry in Russian and Italian astronauts. Adv Space Res. 2003;31(6):1495–503. https://doi.org/10.1016/s0273-1177(03)00087-5.
104. Obe G, Johannes I, Johannes C, Hallman K, Reitz G, Facius R. Chromosomal aberrations in blood lymphocytes of astronauts after long-term space flights. Int J Radiat Biol. 1997;72(6):727–34. https://doi.org/10.1080/095530097142889.
105. George K, Willingham V, Cucinotta FA. Stability of chromosome aberrations in the blood lymphocytes of astronauts measured after space flight by FISH chromosome painting. Radiat Res. 2005;164(4 Pt 2):474–80. https://doi.org/10.1667/rr3323.1.
106. Feiveson A, George K, Shavers M, Moreno-Villanueva M, Zhang Y, Babiak-Vazquez A, Crucian B, Semones E, Wu H. Predicting chromosome damage in astronauts participating in international space station missions. Sci Rep. 2021;11(1):5293. https://doi.org/10.1038/s41598-021-84242-5.
107. George K, Durante M, Willingham V, Cucinotta FA. Chromosome aberrations of clonal origin are present in astronauts' blood lymphocytes. Cytogenet Genome Res. 2004;104(1-4):245–51. https://doi.org/10.1159/000077498.
108. Testard I, Sabatier L. Biological dosimetry for astronauts: a real challenge. Mutat Res. 1999;430(2):315–26. https://doi.org/10.1016/s0027-5107(99)00144-x.
109. Durante M, Snigiryova G, Akaeva E, Bogomazova A, Druzhinin S, Fedorenko B, Greco O, Novitskaya N, Rubanovich A, Shevchenko V, Von Recklinghausen U, Obe G. Chromosome aberration dosimetry in cosmonauts after single or multiple space flights. Cytogenet Genome Res. 2003;103(1–2):40–6. https://doi.org/10.1159/000076288.
110. George K, Rhone J, Beitman A, Cucinotta FA. Cytogenetic damage in the blood lymphocytes of astronauts: effects of repeat long-duration space missions. Mutat Res. 2013;756(1–2):165–9. https://doi.org/10.1016/j.mrgentox.2013.04.007.
111. Obe G, Facius R, Reitz G, Johannes I, Johannes C. Manned missions to Mars and chromosome damage. Int J Radiat Biol. 1999;75(4):429–33. https://doi.org/10.1080/095530099140348.
112. Yang TC, George K, Johnson AS, Durante M, Fedorenko BS. Biodosimetry results from space flight Mir-18. Radiat Res. 1997;148(5 Suppl):S17–23. https://www.ncbi.nlm.nih.gov/pubmed/9355852.
113. Hortsmann M, Durante M, Johannes C, Obe G. Chromosomal intrachanges induced by swift iron ions. Adv Space Res. 2005;35(2):276–9. https://doi.org/10.1016/j.asr.2004.12.031.
114. Johannes C, Horstmann M, Durante M, Chudoba I, Obe G. Chromosome intrachanges and interchanges detected by multicolor banding in lymphocytes: searching for clastogen signatures in the human genome. Radiat Res. 2004;161(5):540–8. https://doi.org/10.1667/rr3157.
115. Horstmann M, Durante M, Johannes C, Pieper R, Obe G. Space radiation does not induce a significant increase of intrachromosomal exchanges in astronauts' lymphocytes. Radiat Environ Biophys. 2005;44(3):219–24. https://doi.org/10.1007/s00411-005-0017-0.
116. Luxton JJ, McKenna MJ, Taylor LE, George KA, Zwart SR, Crucian BE, Drel VR, Garrett-Bakelman FE, Mackay MJ, Butler D, Foox J, Grigorev K, Bezdan D, Meydan C, Smith SM, Sharma K, Mason CE, Bailey SM. Temporal telomere and DNA damage responses in the space radiation environment. Cell Rep. 2020;33(10):108435. https://doi.org/10.1016/j.celrep.2020.108435.
117. Anderson RM, Marsden SJ, Wright EG, Kadhim MA, Goodhead DT, Griffin CS. Complex chromosome aberrations in peripheral blood lymphocytes as a potential biomarker of exposure to high-LET alpha-particles. Int J Radiat Biol. 2000;76(1):31–42. https://doi.org/10.1080/095530000138989.
118. Ray FA, Robinson E, McKenna M, Hada M, George K, Cucinotta F, Goodwin EH, Bedford JS, Bailey SM, Cornforth MN. Directional genomic hybridization: inversions as a potential biodosimeter for retrospective radiation exposure. Radiat Environ Biophys. 2014;53(2):255–63. https://doi.org/10.1007/s00411-014-0513-1.
119. Cornforth MN, Durante M. Radiation quality and intra-chromosomal aberrations: size matters. Mutat Res Genet Toxicol Environ Mutagen. 2018;836(Pt A):28–35. https://doi.org/10.1016/j.mrgentox.2018.05.002.
120. Garrett-Bakelman FE, Darshi M, Green SJ, Gur RC, Lin L, Macias BR, McKenna MJ, Meydan C, Mishra T, Nasrini J, Piening BD, Rizzardi LF, Sharma K, Siamwala JH, Taylor L, Vitaterna MH, Afkarian M, Afshinnekoo E, Ahadi S, et al. The NASA Twins Study: a multidimensional analysis of a year-long human spaceflight. Science. 2019;364(6436) https://doi.org/10.1126/science.aau8650.
121. Luxton JJ, Bailey SM. Twins, telomeres, and aging-in space! Plast Reconstr Surg. 2021;147(1S-2):7S–14S. https://doi.org/10.1097/PRS.0000000000007616.
122. Fazio GG, Jelley JV, Charman WN. Generation of Cherenkov light flashes by cosmic radiation within the eyes of the Apollo astronauts. Nature. 1970;228(5268):260–4. https://doi.org/10.1038/228260a0.
123. Pinsky LS, Osborne WZ, Bailey JV, Benson RE, Thompson LF. Light flashes observed by astronauts on Apollo 11 through Apollo 17. Science. 1974;183(4128):957–9. https://doi.org/10.1126/science.183.4128.957.
124. Bidoli V, Casolino M, De Pascale MP, Furano G, Morselli A, Narici L, Picozza P, Reali E, Sparvoli R, Galper AM, Ozerov Yu V, Popov AV, Vavilov NR, Alexandrov AP, Avdeev SV, Baturin Y, Budarin Y, Padalko G, Shabelnikov VG, et al. Study of cosmic rays and light flashes on board Space Station MIR: the SilEye experiment. Adv Space Res. 2000;25(10):2075–9. https://doi.org/10.1016/s0273-1177(99)01017-0.
125. Pinsky LS, Osborne WZ, Hoffman RA, Bailey JV. Light flashes observed by astronauts on skylab 4. Science. 1975;188(4191):928–30. https://doi.org/10.1126/science.188.4191.928.
126. Budinger TF, Tobias CA, Huesman RH, Upham FT, Wieskamp TF, Hoffman RA. Apollo-Soyuz light-flash observations. Life Sci Space Res. 1977;15:141–6. https://www.ncbi.nlm.nih.gov/pubmed/11958208.
127. Avdeev S, Bidoli V, Casolino M, De Grandis E, Furano G, Morselli A, Narici L, De Pascale MP, Picozza P, Reali E, Sparvoli R, Boezio M, Carlson P, Bonvicini W, Vacchi A, Zampa N, Castellini G, Fuglesang C, Galper A, et al. Eye light flashes on the Mir space station. Acta Astronaut. 2002;50(8):511–25. https://doi.org/10.1016/s0094-5765(01)00190-4.
128. Narici L. Heavy ions light flashes and brain functions: recent observations at accelerators and in spaceflight. N J Phys. 2008;10(7):075010. https://doi.org/10.1088/1367-2630/10/7/075010.
129. Narici L, Belli F, Bidoli V, Casolino M, De Pascale MP, Di Fino L, Furano G, Modena I, Morselli A, Picozza P, Reali E, Rinaldi A, Ruggieri D, Sparvoli R, Zaconte V, Sannita WG, Carozzo S, Licoccia S, Romagnoli P, et al. The ALTEA/ALTEINO projects: studying functional effects of microgravity and cosmic radiation. Adv Space Res. 2004;33(8):1352–7. https://doi.org/10.1016/j.asr.2003.09.052.
130. Casolino M, Bidoli V, Morselli A, Narici L, De Pascale MP, Picozza P, Reali E, Sparvoli R, Mazzenga G, Ricci M, Spillantini P, Boezio M, Bonvicini V, Vacchi A, Zampa N, Castellini G, Sannita WG, Carlson P, Galper A, et al. Space travel: dual origins of light flashes seen in space. Nature. 2003;422(6933):680. https://doi.org/10.1038/422680a.

131. Bidoli V, Casolino M, De Pascale MP, Furano G, Minori M, Morselli A, Narici L, Picozza P, Reali E, Sparvoli R, Fuglesang C, Sannita W, Carlson P, Castellini G, Galper A, Korotkov M, Popov A, Navilov N, Avdeev S, et al. The Sileye-3/Alteino experiment for the study of light flashes, radiation environment and astronaut brain activity on board the International Space Station. J Radiat Res. 2002;43(Suppl):S47–52. https://doi.org/10.1269/jrr.43.s47.
132. Schardt D, Kavatsyuk O, Kramer M, Durante M. Light flashes in cancer patients treated with heavy ions. Brain Stimul. 2013;6(3):416–7. https://doi.org/10.1016/j.brs.2012.08.003.
133. Fuglesang C, Narici L, Picozza P, Sannita WG. Phosphenes in low earth orbit: survey responses from 59 astronauts. Aviat Space Environ Med. 2006;77(4):449–52. https://www.ncbi.nlm.nih.gov/pubmed/16676658.
134. Curtis SB. Single-track effects and new directions in GCR risk assessment. Adv Space Res. 1994;14(10):885–94. https://doi.org/10.1016/0273-1177(94)90554-1.
135. Chase HB, Post JS. Damage and repair in mammalian tissues exposed to cosmic ray heavy nuclei. J Aviat Med. 1956;27(6):533–40. https://www.ncbi.nlm.nih.gov/pubmed/13376499.
136. Bucker H, Horneck G, Allkofer OC, Bartholoma KP, Beaujean R, Cuer P, Enge W, Facius R, Francois H, Graul EH, Henig G, Heinrich W, Kaiser R, Kuhn H, Massue JP, Planel H, Portal G, Reinholz E, Ruther W, et al. The Biostack experiment on Apollo 16. Life Sci Space Res. 1973;11:295–305. https://www.ncbi.nlm.nih.gov/pubmed/12001958.
137. Bucker H, Facius R, Hildebrand D, Horneck G. Results of the Bacillus subtilis unit of the Biostack II experiment: physical characteristics and biological effects of individual cosmic HZE particles. Life Sci Space Res. 1975;13:161–6. https://www.ncbi.nlm.nih.gov/pubmed/11913421.
138. Horneck G, Facius R, Enge W, Beaujean R, Bartholoma KP. Microbial studies in the Biostack experiment of the Apollo 16 mission: germination and outgrowth of single Bacillus subtilis spores hit by cosmic HZE particles. Life Sci Space Res. 1974;12:75–83. https://doi.org/10.1016/b978-0-08-021783-3.50014-3.
139. Ruther W, Graul EH, Heinrich W, Allkofer OC, Kaiser R, Cuer P. Preliminary results on the action of cosmic heavy ions on the development of eggs of Artemia salina. Life Sci Space Res. 1974;12:69–74. https://doi.org/10.1016/b978-0-08-021783-3.50013-1.
140. Graul EH, Ruther W, Heinrich W, Allkofer OC, Kaiser R, Pfohl R, Schopper E, Henig G, Schott JU, Bucker H. Radiobiological results of the Biostack experiment on board Apollo 16 and 17. Life Sci Space Res. 1975;13:153–9. https://www.ncbi.nlm.nih.gov/pubmed/11913420.
141. Bucker H. Biologic effect of cosmic particle radiation, results of the Biostack experiments in the Apollo program. Strahlenschutz Forsch Prax. 1976;16:31–50. https://www.ncbi.nlm.nih.gov/pubmed/1036850 (Die biologische Wirkung der kosmischen Teilchenstrahlung, Ergebnisse der Biostack-Experimente im Apollo-Programm)
142. Heinrich W. Predicted LET-spectra of HZE-particles for the Free Flyer Biostack Experiment on the long duration exposure facility mission. Life Sci Space Res. 1980;18:143–52. https://doi.org/10.1016/b978-0-08-024436-5.50019-6.
143. Bucker H, Baltschukat K, Beaujean R, Bonting SL, Delpoux M, Enge W, Facius R, Francois H, Graul EH, Heinrich W, Horneck G, Kranz AR, Pfohl R, Planel G, Portal G, Reitz G, Ruther W, Schafer M, Schopper E, Schott JU. Advanced Biostack: experiment 1 ES 027 on Spacelab-1. Adv Space Res. 1984;4(10):83–90. https://doi.org/10.1016/0273-1177(84)90228-x.
144. Bucker H, Facius R, Horneck G, Reitz G, Graul EH, Berger H, Hoffken H, Ruther W, Heinrich W, Beaujean R, Enge W. Embryogenesis and organogenesis of Carausius morosus under spaceflight conditions. Adv Space Res. 1986;6(12):115–24. https://doi.org/10.1016/0273-1177(86)90074-8.
145. Bucker H, Horneck G, Facius R, Reitz G, Schafer M, Schott JU, Beaujean R, Enge W, Schopper E, Heinrich H, Beer J, Wiegel B, Pfohl R, Francois H, Portal G, Bonting SL, Graul EH, Ruther W, Kranz AR, et al. Life sciences: radiobiological advanced Biostack experiment. Science. 1984;225(4658):222–4. https://doi.org/10.1126/science.225.4658.222.
146. Horneck G, Eschweiler U, Reitz G, Wehner J, Willimek R, Strauch K. Biological responses to space: results of the experiment "Exobiological Unit" of ERA on EURECA I. Adv Space Res. 1995;16(8):105–18. https://doi.org/10.1016/0273-1177(95)00279-N.
147. Horneck G. HZE particle effects in space. Acta Astronaut. 1994;32(11):749–55. https://doi.org/10.1016/0094-5765(94)90170-8.
148. Reitz G, Bucker H, Facius R, Horneck G, Graul EH, Berger H, Ruther W, Heinrich W, Beaujean R, Enge W, Alpatov AM, Ushakov IA, Zachvatkin YA, Mesland DA. Influence of cosmic radiation and/or microgravity on development of Carausius morosus. Adv Space Res. 1989;9(10):161–73. https://doi.org/10.1016/0273-1177(89)90435-3.
149. Barendsen GW, Walter HM, Fowler JF, Bewley DK. Effects of different ionizing radiations on human cells in tissue culture. III. Experiments with cyclotron-accelerated alpha-particles and deuterons. Radiat Res. 1963;18:106–19. https://www.ncbi.nlm.nih.gov/pubmed/13966644.
150. Bolus NE. Basic review of radiation biology and terminology. J Nucl Med Technol. 2017;45(4):259. https://doi.org/10.2967/jnmt.117.195230.
151. Friedrich T, Scholz U, Elsasser T, Durante M, Scholz M. Systematic analysis of RBE and related quantities using a database of cell survival experiments with ion beam irradiation. J Radiat Res. 2013;54(3):494–514. https://doi.org/10.1093/jrr/rrs114.
152. Hendry JH, Potten CS, Merritt A. Apoptosis induced by high- and low-LET radiations. Radiat Environ Biophys. 1995;34(1):59–62. https://doi.org/10.1007/BF01210548.
153. Aoki M, Furusawa Y, Yamada T. LET dependency of heavy-ion induced apoptosis in V79 cells. J Radiat Res. 2000;41(2):163–75. https://doi.org/10.1269/jrr.41.163.
154. Harada K, Obiya Y, Nakano T, Kawashima M, Miki T, Kobayashi Y, Watanabe H, Okaichi K, Ohnishi T, Mukai C, Nagaoka S. Cancer risk in space due to radiation assessed by determining cell lethality and mutation frequencies of prokaryotes and a plasmid during the Second International Microgravity Laboratory (IML-2) Space Shuttle experiment. Oncol Rep. 1997;4(4):691–5. https://doi.org/10.3892/or.4.4.691.
155. Takahashi A, Ohnishi K, Yokota A, Kumagai T, Nakano T, Ohnishi T. Mutation frequency of plasmid DNA and Escherichia coli following long-term space flight on Mir. J Radiat Res. 2002;43(Suppl):S137–40. https://doi.org/10.1269/jrr.43.s137.
156. Takahashi A, Ohnishi K, Takahashi S, Masukawa M, Sekikawa K, Amano T, Nakano T, Nagaoka S, Ohnishi T. The effects of microgravity on induced mutation in Escherichia coli and Saccharomyces cerevisiae. Adv Space Res. 2001;28(4):555–61. https://doi.org/10.1016/s0273-1177(01)00391-x.
157. Harada K, Nagaoka S, Mohri M, Ohnishi T, Sugahara T. Lethality of high linear energy transfer cosmic radiation to Escherichia coli DNA repair-deficient mutants during the 'SL-J/FMPT' space experiment. FEMS Microbiol Lett. 1998;164(1):39–45. https://doi.org/10.1111/j.1574-6968.1998.tb13065.x.
158. Ohnishi T, Takahashi A, Okaichi K, Ohnishi K, Matsumoto H, Takahashi S, Yamanaka H, Nakano T, Nagaoka S. Cell growth and morphology of Dictyostelium discoideum in space environment. Biol Sci Space. 1997;11(1):29–34. https://doi.org/10.2187/bss.11.29.

159. Takahashi A, Ohnishi K, Fukui M, Nakano T, Yamaguchi K, Nagaoka S, Ohnishi T. Mutation frequency of Dictyostelium discoideum spores exposed to the space environment. Biol Sci Space. 1997;11(2):81–6. https://doi.org/10.2187/bss.11.81.
160. Takahashi A, Ohnishi K, Takahashi S, Masukawa M, Sekikawa K, Amano T, Nakano T, Nagaoka S, Ohnishi T. Differentiation of Dictyostelium discoideum vegetative cells into spores during Earth orbit in space. Adv Space Res. 2001;28(4):549–53. https://doi.org/10.1016/s0273-1177(01)00388-x.
161. Obe G, Pfeiffer P, Savage JR, Johannes C, Goedecke W, Jeppesen P, Natarajan AT, Martinez-Lopez W, Folle GA, Drets ME. Chromosomal aberrations: formation, identification and distribution. Mutat Res. 2002;504(1–2):17–36. https://doi.org/10.1016/s0027-5107(02)00076-3.
162. Cornforth MN. Perspectives on the formation of radiation-induced exchange aberrations. DNA Repair (Amst). 2006;5(9–10):1182–91. https://doi.org/10.1016/j.dnarep.2006.05.008.
163. Durante M, Cucinotta FA. Heavy ion carcinogenesis and human space exploration. Nat Rev Cancer. 2008;8(6):465–72. https://doi.org/10.1038/nrc2391.
164. Sridharan DM, Asaithamby A, Blattnig SR, Costes SV, Doetsch PW, Dynan WS, Hahnfeldt P, Hlatky L, Kidane Y, Kronenberg A, Naidu MD, Peterson LE, Plante I, Ponomarev AL, Saha J, Snijders AM, Srinivasan K, Tang J, Werner E, Pluth JM. Evaluating biomarkers to model cancer risk post cosmic ray exposure. Life Sci Space Res (Amst). 2016;9:19–47. https://doi.org/10.1016/j.lssr.2016.05.004.
165. Kawata T, Ito H, George K, Wu H, Cucinotta FA. Chromosome aberrations induced by high-LET radiations. Biol Sci Space. 2004;18(4):216–23. https://doi.org/10.2187/bss.18.216.
166. Cornforth MN, Bedford JS, Bailey SM. Destabilizing effects of ionizing radiation on chromosomes: sizing up the damage. Cytogenet Genome Res. 2021;161(6–7):328–51. https://doi.org/10.1159/000516523.
167. Cornforth MN, Bailey SM, Goodwin EH. Dose responses for chromosome aberrations produced in noncycling primary human fibroblasts by alpha particles, and by gamma rays delivered at sublimiting low dose rates. Radiat Res. 2002;158(1):43–53. https://doi.org/10.1667/0033-7587(2002)158[0043:drfcap]2.0.co;2.
168. George K, Durante M, Willingham V, Wu H, Yang TC, Cucinotta FA. Biological effectiveness of accelerated particles for the induction of chromosome damage measured in metaphase and interphase human lymphocytes. Radiat Res. 2003;160(4):425–35. https://doi.org/10.1667/rr3064.
169. Goodwin EH, Cornforth MN. RBE: mechanisms inferred from cytogenetics. Adv Space Res. 1994;14(10):249–55. https://doi.org/10.1016/0273-1177(94)90474-x.
170. Loucas BD, Cornforth MN. The LET dependence of unrepaired chromosome damage in human cells: a break too far? Radiat Res. 2013;179(4):393–405. https://doi.org/10.1667/RR3159.2.
171. Loucas BD, Durante M, Bailey SM, Cornforth MN. Chromosome damage in human cells by gamma rays, alpha particles and heavy ions: track interactions in basic dose-response relationships. Radiat Res. 2013;179(1):9–20. https://doi.org/10.1667/RR3089.1.
172. Jackson SP, Bartek J. The DNA-damage response in human biology and disease. Nature. 2009;461(7267):1071–8. https://doi.org/10.1038/nature08467.
173. Pariset E, Penninckx S, Kerbaul CD, Guiet E, Macha AL, Cekanaviciute E, Snijders AM, Mao J-H, Paris F, Costes SV. 53BP1 Repair kinetics for prediction of *in vivo* radiation susceptibility in 15 mouse strains. Radiat Res. 2020;194(5):485–99. https://doi.org/10.1667/RADE-20-00122.1.
174. Asaithamby A, Hu B, Chen DJ. Unrepaired clustered DNA lesions induce chromosome breakage in human cells. Proc Natl Acad Sci U S A. 2011;108(20):8293–8. https://doi.org/10.1073/pnas.1016045108.
175. Eccles LJ, Lomax ME, O'Neill P. Hierarchy of lesion processing governs the repair, double-strand break formation and mutability of three-lesion clustered DNA damage. Nucleic Acids Res. 2010;38(4):1123–34. https://doi.org/10.1093/nar/gkp1070.
176. Hirayama R, Ito A, Tomita M, Tsukada T, Yatagai F, Noguchi M, Matsumoto Y, Kase Y, Ando K, Okayasu R, Furusawa Y. Contributions of direct and indirect actions in cell killing by high-LET radiations. Radiat Res. 2009;171(2):212–8. https://doi.org/10.1667/RR1490.1.
177. Ohnishi T, Ohnishi K, Takahashi A, Taniguchi Y, Sato M, Nakano T, Nagaoka S. Detection of DNA damage induced by space radiation in Mir and space shuttle. J Radiat Res. 2002;43(Suppl):S133–6. https://doi.org/10.1269/jrr.43.s133.
178. Ohnishi T, Takahashi A, Ohnishi K, Matsumoto H. DNA damage formation and p53 accumulation in mammalian cells exposed to the space environment. Biol Sci Space. 1999;13(2):82–7. https://doi.org/10.2187/bss.13.82.
179. Ohnishi T, Takahashi A, Wang X, Ohnishi K, Ohira Y, Nagaoka S. Accumulation of a tumor suppressor p53 protein in rat muscle during a space flight. Mutat Res. 1999;430(2):271–4. https://doi.org/10.1016/s0027-5107(99)00138-4.
180. Ohnishi T, Takahashi A, Nagamatsu A, Omori K, Suzuki H, Shimazu T, Ishioka N. Detection of space radiation-induced double strand breaks as a track in cell nucleus. Biochem Biophys Res Commun. 2009;390(3):485–8. https://doi.org/10.1016/j.bbrc.2009.09.114.
181. Lu T, Zhang Y, Kidane Y, Feiveson A, Stodieck L, Karouia F, Ramesh G, Rohde L, Wu H. Cellular responses and gene expression profile changes due to bleomycin-induced DNA damage in human fibroblasts in space. PLoS One. 2017;12(3):e0170358. https://doi.org/10.1371/journal.pone.0170358.
182. Cucinotta FA, Durante M. Cancer risk from exposure to galactic cosmic rays: implications for space exploration by human beings. Lancet Oncol. 2006;7(5):431–5. https://doi.org/10.1016/S1470-2045(06)70695-7.
183. Schollnberger H, Stewart RD, Mitchel RE, Hofmann W. An examination of radiation hormesis mechanisms using a multistage carcinogenesis model. Nonlinearity Biol Toxicol Med. 2004;2(4):317–52. https://doi.org/10.1080/15401420490900263.
184. Stenerlow B, Hoglund E, Carlsson J, Blomquist E. Rejoining of DNA fragments produced by radiations of different linear energy transfer. Int J Radiat Biol. 2000;76(4):549–57. https://doi.org/10.1080/095530000138565.
185. Ward JF. DNA damage as the cause of ionizing radiation-induced gene activation. Radiat Res. 1994;138(1 Suppl):S85–8. https://www.ncbi.nlm.nih.gov/pubmed/8146335.
186. Yan X, Sasi SP, Gee H, Lee J, Yang Y, Mehrzad R, Onufrak J, Song J, Enderling H, Agarwal A, Rahimi L, Morgan J, Wilson PF, Carrozza J, Walsh K, Kishore R, Goukassian DA. Cardiovascular risks associated with low dose ionizing particle radiation. PLoS One. 2014;9(10):e110269. https://doi.org/10.1371/journal.pone.0110269.
187. Rogakou EP, Boon C, Redon C, Bonner WM. Megabase chromatin domains involved in DNA double-strand breaks in vivo. J Cell Biol. 1999;146(5):905–16. https://doi.org/10.1083/jcb.146.5.905.
188. Rogakou EP, Pilch DR, Orr AH, Ivanova VS, Bonner WM. DNA double-stranded breaks induce histone H2AX phosphorylation on serine 139. J Biol Chem. 1998;273(10):5858–68. https://doi.org/10.1074/jbc.273.10.5858.
189. Penninckx S, Pariset E, Cekanaviciute E, Costes SV. Quantification of radiation-induced DNA double strand break repair foci to evaluate and predict biological responses to ionizing radiation. NAR Cancer. 2021;3(4):zcab046. https://doi.org/10.1093/narcan/zcab046.

190. Oizumi T, Ohno R, Yamabe S, Funayama T, Nakamura AJ. Repair kinetics of DNA double strand breaks induced by simulated space radiation. Life (Basel). 2020;10(12) https://doi.org/10.3390/life10120341.
191. Asaithamby A, Uematsu N, Chatterjee A, Story MD, Burma S, Chen DJ. Repair of HZE-particle-induced DNA double-strand breaks in normal human fibroblasts. Radiat Res. 2008;169(4):437–46. https://doi.org/10.1667/RR1165.1.
192. Costes SV, Boissiere A, Ravani S, Romano R, Parvin B, Barcellos-Hoff MH. Imaging features that discriminate between foci induced by high- and low-LET radiation in human fibroblasts. Radiat Res. 2006;165(5):505–15. https://doi.org/10.1667/RR3538.1.
193. Mukherjee B, Camacho CV, Tomimatsu N, Miller J, Burma S. Modulation of the DNA-damage response to HZE particles by shielding. DNA Repair (Amst). 2008;7(10):1717–30. https://doi.org/10.1016/j.dnarep.2008.06.016.
194. Baumstark-Khan C, Heilmann J, Rink H. Induction and repair of DNA strand breaks in bovine lens epithelial cells after high LET irradiation. Adv Space Res. 2003;31(6):1583–91. https://doi.org/10.1016/s0273-1177(03)00095-4.
195. Li Z, Jella KK, Jaafar L, Li S, Park S, Story MD, Wang H, Wang Y, Dynan WS. Exposure to galactic cosmic radiation compromises DNA repair and increases the potential for oncogenic chromosomal rearrangement in bronchial epithelial cells. Sci Rep. 2018;8(1):11038. https://doi.org/10.1038/s41598-018-29350-5.
196. Averbeck NB, Ringel O, Herrlitz M, Jakob B, Durante M, Taucher-Scholz G. DNA end resection is needed for the repair of complex lesions in G1-phase human cells. Cell Cycle. 2014;13(16):2509–16. https://doi.org/10.4161/15384101.2015.941743.
197. Yajima H, Fujisawa H, Nakajima NI, Hirakawa H, Jeggo PA, Okayasu R, Fujimori A. The complexity of DNA double strand breaks is a critical factor enhancing end-resection. DNA Repair (Amst). 2013;12(11):936–46. https://doi.org/10.1016/j.dnarep.2013.08.009.
198. Shikazono N, O'Neill P. Biological consequences of potential repair intermediates of clustered base damage site in Escherichia coli. Mutat Res. 2009;669(1–2):162–8. https://doi.org/10.1016/j.mrfmmm.2009.06.004.
199. Harada K, Sugahara T, Ohnishi T, Ozaki Y, Obiya Y, Miki S, Miki T, Imamura M, Kobayashi Y, Watanabe H, Akashi M, Furusawa Y, Mizuma N, Yamanaka H, Ohashi E, Yamaoka C, Yajima M, Fukui M, Nakano T, et al. Inhibition in a microgravity environment of the recovery of Escherichia coli cells damaged by heavy ion beams during the NASDA ISS phase I program of NASA Shuttle/Mir mission no. 6. Int J Mol Med. 1998;1(5):817–22. https://doi.org/10.3892/ijmm.1.5.817.
200. Horneck G, Rettberg P, Kozubek S, Baumstark-Khan C, Rink H, Schafer M, Schmitz C. The influence of microgravity on repair of radiation-induced DNA damage in bacteria and human fibroblasts. Radiat Res. 1997;147(3):376–84. https://www.ncbi.nlm.nih.gov/pubmed/9052686.
201. Lu T, Zhang Y, Wong M, Feiveson A, Gaza R, Stoffle N, Wang H, Wilson B, Rohde L, Stodieck L, Karouia F, Wu H. Detection of DNA damage by space radiation in human fibroblasts flown on the International Space Station. Life Sci Space Res (Amst). 2017;12:24–31. https://doi.org/10.1016/j.lssr.2016.12.004.
202. Ohnishi T, Takahashi A, Ohnishi K, Nakano T, Nagaoka S. Enzymic chemical reaction under microgravity environment in space. J Gravit Physiol. 2000;7(2):P69–70. https://www.ncbi.nlm.nih.gov/pubmed/12697569.
203. Horneck G. Radiobiological experiments in space—a review. Nuclear Tracks Radiat Meas. 1992;20(1):185–205. https://doi.org/10.1016/1359-0189(92)90099-H.
204. Takahashi A, Ohnishi K, Takahashi S, Masukawa M, Sekikawa K, Amano T, Nakano T, Nagaoka S, Ohnishi T. The effects of microgravity on ligase activity in the repair of DNA double-strand breaks. Int J Radiat Biol. 2000;76(6):783–8. https://doi.org/10.1080/09553000050028931.
205. Kiefer J, Pross HD. Space radiation effects and microgravity. Mutat Res. 1999;430(2):299–305. https://doi.org/10.1016/s0027-5107(99)00142-6.
206. Pross HD, Kost M, Kiefer J. Repair of radiation induced genetic damage under microgravity. Adv Space Res. 1994;14(10):125–30. https://doi.org/10.1007/978-1-4615-2918-7_12.
207. Horneck G, Rettberg P, Baumstark-Khan C, Rink H, Kozubek S, Schafer M, Schmitz C. DNA repair in microgravity: studies on bacteria and mammalian cells in the experiments REPAIR and KINETICS. J Biotechnol. 1996;47(2–3):99–112. https://doi.org/10.1016/0168-1656(96)01382-x.
208. Ohnishi T, Takahashi A, Ohnishi K, Takahashi S, Masukawa M, Sekikawa K, Amano T, Nakano T, Nagaoka S. Alkylating agent (MNU)-induced mutation in space environment. Adv Space Res. 2001;28(4):563–8. https://doi.org/10.1016/s0273-1177(01)00392-1.
209. Moreno-Villanueva M, Wong M, Lu T, Zhang Y, Wu H. Interplay of space radiation and microgravity in DNA damage and DNA damage response. NPJ Microgravity. 2017;3:14. https://doi.org/10.1038/s41526-017-0019-7.
210. Ohnishi T. Life science experiments performed in space in the ISS/Kibo facility and future research plans. J Radiat Res. 2016;57 Suppl 1:i41–6. https://doi.org/10.1093/jrr/rrw020.
211. Takahashi A, Suzuki H, Omori K, Seki M, Hashizume T, Shimazu T, Ishioka N, Ohnishi T. Expression of p53-regulated proteins in human cultured lymphoblastoid TSCE5 and WTK1 cell lines during spaceflight. J Radiat Res. 2012;53(2):168–75. https://doi.org/10.1269/jrr.11140.
212. Herranz R, Anken R, Boonstra J, Braun M, Christianen PC, de Geest M, Hauslage J, Hilbig R, Hill RJ, Lebert M, Medina FJ, Vagt N, Ullrich O, van Loon JJ, Hemmersbach R. Ground-based facilities for simulation of microgravity: organism-specific recommendations for their use, and recommended terminology. Astrobiology. 2013;13(1):1–17. https://doi.org/10.1089/ast.2012.0876.
213. Hauslage J, Cevik V, Hemmersbach R. Pyrocystis noctiluca represents an excellent bioassay for shear forces induced in ground-based microgravity simulators (clinostat and random positioning machine). NPJ Microgravity. 2017;3:12. https://doi.org/10.1038/s41526-017-0016-x.
214. Horneck G, Klaus DM, Mancinelli RL. Space microbiology. Microbiol Mol Biol Rev. 2010;74(1):121–56. https://doi.org/10.1128/MMBR.00016-09.
215. Gao Y, Li S, Xu D, Wang J, Sun Y. Changes in apoptotic microRNA and mRNA expression profiling in Caenorhabditis elegans during the Shenzhou-8 mission. J Radiat Res. 2015;56(6):872–82. https://doi.org/10.1093/jrr/rrv050.
216. Paul AM, Overbey EG, da Silveira WA, Szewczyk N, Nishiyama NC, Pecaut MJ, Anand S, Galazka JM, Mao XW. Immunological and hematological outcomes following protracted low dose/low dose rate ionizing radiation and simulated microgravity. Sci Rep. 2021;11(1):11452. https://doi.org/10.1038/s41598-021-90439-5.
217. Rabbow E, Stojicic N, Walrafen D, Baumstark-Khan C, Rettberg P, Schulze-Varnholt D, Franz M, Reitz G. The SOS-LUX-TOXICITY-test on the International Space Station. Res Microbiol. 2006;157(1):30–6. https://doi.org/10.1016/j.resmic.2005.08.005.
218. Stojicic N, Walrafen D, Baumstark-Khan C, Rabbow E, Rettberg P, Weisshaar MP, Horneck G. Genotoxicity testing on the international space station: preparatory work on the SOS-LUX test as part of the space experiment TRIPLE-LUX. Space Life Sci Aircraft Space Radiat Environ. 2005;36(9):1710–7. https://doi.org/10.1016/j.asr.2005.03.052.
219. Padgen MR, Liddell LC, Bhardwaj SR, Gentry D, Marina D, Parra M, Boone T, Tan M, Ellingson L, Rademacher A, Benton

J, Schooley A, Mousavi A, Friedericks C, Hanel RP, Ricco AJ, Bhattacharya S, Maria SRS. BioSentinel: a biofluidic nanosatellite monitoring microbial growth and activity in deep space. Astrobiology. 2021; https://doi.org/10.1089/ast.2020.2305.
220. Santa Maria SR, Marina DB, Massaro Tieze S, Liddell LC, Bhattacharya S. BioSentinel: long-term saccharomyces cerevisiae preservation for a deep space biosensor mission. Astrobiology. 2020; https://doi.org/10.1089/ast.2019.2073.
221. Cox R, Thacker J, Goodhead DT, Munson RJ. Mutation and inactivation of mammalian cells by various ionising radiations. Nature. 1977;267(5610):425–7. https://doi.org/10.1038/267425a0.
222. Goodhead DT, Thacker J, Cox R. Weiss Lecture. Effects of radiations of different qualities on cells: molecular mechanisms of damage and repair. Int J Radiat Biol. 1993;63(5):543–56. https://doi.org/10.1080/09553009314450721.
223. Shmakova NL, Krasavin EA, Govorun RD, Fadeeva TA, Koshlan IV. The lethal and mutagenic actions of radiations with different LETs on mammalian cells. Radiat Biol Radioecol. 1997;37(2):213–9. https://www.ncbi.nlm.nih.gov/pubmed/9181964 (Letal'noe i mutagennoe deistvie izluchenii s raznoi LPE na kletki mlekopitaiushchikh).
224. Hei TK, Hall EJ, Waldren CA. Mutation induction and relative biological effectiveness of neutrons in mammalian cells. Experimental observations. Radiat Res. 1988;115(2):281–91. https://www.ncbi.nlm.nih.gov/pubmed/3165536.
225. Suzuki M, Tsuruoka C, Kanai T, Kato T, Yatagai F, Watanabe M. Qualitative and quantitative difference in mutation induction between carbon- and neon-ion beams in normal human cells. Biol Sci Space. 2003;17(4):302–6. https://doi.org/10.2187/bss.17.302.
226. Zhou H, Randers-Pehrson G, Waldren CA, Vannais D, Hall EJ, Hei TK. Induction of a bystander mutagenic effect of alpha particles in mammalian cells. Proc Natl Acad Sci U S A. 2000;97(5):2099–104. https://doi.org/10.1073/pnas.030420797.
227. Yatagai F, Honma M, Takahashi A, Omori K, Suzuki H, Shimazu T, Seki M, Hashizume T, Ukai A, Sugasawa K, Abe T, Dohmae N, Enomoto S, Ohnishi T, Gordon A, Ishioka N. Frozen human cells can record radiation damage accumulated during space flight: mutation induction and radioadaptation. Radiat Environ Biophys. 2011;50(1):125–34. https://doi.org/10.1007/s00411-010-0348-3.
228. Fukuda T, Fukuda K, Takahashi A, Ohnishi T, Nakano T, Sato M, Gunge N. Analysis of deletion mutations of the rpsL gene in the yeast Saccharomyces cerevisiae detected after long-term flight on the Russian space station Mir. Mutat Res. 2000;470(2):125–32. https://doi.org/10.1016/s1383-5742(00)00054-5.
229. Yang TC, Craise LM, Mei MT, Tobias CA. Neoplastic cell transformation by heavy charged particles. Radiat Res Suppl. 1985;8:S177–87. https://www.ncbi.nlm.nih.gov/pubmed/3867082.
230. Hei TK, Komatsu K, Hall EJ, Zaider M. Oncogenic transformation by charged particles of defined LET. Carcinogenesis. 1988;9(5):747–50. https://doi.org/10.1093/carcin/9.5.747.
231. Suzuki M, Watanabe M, Suzuki K, Nakano K, Kaneko I. Neoplastic cell transformation by heavy ions. Radiat Res. 1989;120(3):468–76. https://www.ncbi.nlm.nih.gov/pubmed/2594968.
232. Han Z, Suzuki H, Suzuki F, Suzuki M, Furusawa Y, Kato T Jr, Ikenaga M. Neoplastic transformation of hamster embyro cells by heavy ions. Adv Space Res. 1998;22(12):1725–32. https://doi.org/10.1016/s0273-1177(99)00038-1.
233. Ding L-H, Park S, Xie Y, Girard L, Minna JD, Story MD. Elucidation of changes in molecular signalling leading to increased cellular transformation in oncogenically progressed human bronchial epithelial cells exposed to radiations of increasing LET. Mutagenesis. 2015;30(5):685–94. https://doi.org/10.1093/mutage/gev028.
234. Collyn-d'Hooghe M, Hemon D, Gilet R, Curtis SB, Valleron AJ, Malaise EP. Comparative effects of 60Co gamma-rays and neon and helium ions on cycle duration and division probability of EMT 6 cells. A time-lapse cinematography study. Int J Radiat Biol Relat Stud Phys Chem Med. 1981;39(3):297–306. https://doi.org/10.1080/09553008114550381.
235. Blakely E, Chang P, Lommel L, Bjornstad K, Dixon M, Tobias C, Kumar K, Blakely WF. Cell-cycle radiation response: role of intracellular factors. Adv Space Res. 1989;9(10):177–86. https://doi.org/10.1016/0273-1177(89)90436-5.
236. Scholz M, Kraft-Weyrather W, Ritter S, Kraft G. Cell cycle delays induced by heavy ion irradiation of synchronous mammalian cells. Int J Radiat Biol. 1994;66(1):59–75. https://doi.org/10.1080/09553009414550951.
237. Fournier C, Taucher-Scholz G. Radiation induced cell cycle arrest: an overview of specific effects following high-LET exposure. Radiother Oncol. 2004;73(Suppl 2):S119–22. https://doi.org/10.1016/s0167-8140(04)80031-8.
238. Xue L, Furusawa Y, Yu D. ATR signaling cooperates with ATM in the mechanism of low dose hypersensitivity induced by carbon ion beam. DNA Repair (Amst). 2015;34:1–8. https://doi.org/10.1016/j.dnarep.2015.07.001.
239. Jakob B, Scholz M, Taucher-Scholz G. Characterization of CDKN1A (p21) binding to sites of heavy-ion-induced damage: colocalization with proteins involved in DNA repair. Int J Radiat Biol. 2002;78(2):75–88. https://doi.org/10.1080/09553000110090007.
240. Stewart J, Ko YH, Kennedy AR. Protective effects of L-selenomethionine on space radiation induced changes in gene expression. Radiat Environ Biophys. 2007;46(2):161–5. https://doi.org/10.1007/s00411-006-0089-5.
241. Hellweg CE, Spitta LF, Henschenmacher B, Diegeler S, Baumstark-Khan C. Transcription factors in the cellular response to charged particle exposure. Front Oncol. 2016;6:61. https://doi.org/10.3389/fonc.2016.00061.
242. Coleman MA, Sasi SP, Onufrak J, Natarajan M, Manickam K, Schwab J, Muralidharan S, Peterson LE, Alekseyev YO, Yan X, Goukassian DA. Low-dose radiation affects cardiac physiology: gene networks and molecular signaling in cardiomyocytes. Am J Physiol Heart Circ Physiol. 2015;309(11):H1947–63. https://doi.org/10.1152/ajpheart.00050.2015.
243. Hellweg CE, Baumstark-Khan C, Schmitz C, Lau P, Meier MM, Testard I, Berger T, Reitz G. Activation of the nuclear factor kappaB pathway by heavy ion beams of different linear energy transfer. Int J Radiat Biol. 2011;87(9):954–63. https://doi.org/10.3109/09553002.2011.584942.
244. Chishti AA, Baumstark-Khan C, Koch K, Kolanus W, Feles S, Konda B, Azhar A, Spitta LF, Henschenmacher B, Diegeler S, Schmitz C, Hellweg CE. Linear energy transfer modulates radiation-induced NF-kappa B activation and expression of its downstream target genes. Radiat Res. 2018;189(4):354–70. https://doi.org/10.1667/RR14905.1.
245. Ducray C, Sabatier L. Role of chromosome instability in long term effect of manned-space missions. Adv Space Res. 1998;22(4):597–602. https://doi.org/10.1016/s0273-1177(98)00082-9.
246. Aubert G, Lansdorp PM. Telomeres and aging. Physiol Rev. 2008;88(2):557–79. https://doi.org/10.1152/physrev.00026.2007.
247. Thompson CAH, Wong JMY. Non-canonical functions of telomerase reverse transcriptase: emerging roles and biological relevance. Curr Top Med Chem. 2020;20(6):498–507. https://doi.org/10.2174/1568026620666200131125110.
248. Kennedy EM, Powell DR, Li Z, Bell JSK, Barwick BG, Feng H, McCrary MR, Dwivedi B, Kowalski J, Dynan WS, Conneely KN, Vertino PM. Galactic cosmic radiation induces persistent epigenome alterations relevant to human lung cancer. Sci Rep. 2018;8(1):6709. https://doi.org/10.1038/s41598-018-24755-8.
249. Miousse IR, Chalbot MC, Aykin-Burns N, Wang X, Basnakian A, Kavouras IG, Koturbash I. Epigenetic alterations induced by

ambient particulate matter in mouse macrophages. Environ Mol Mutagen. 2014;55(5):428–35. https://doi.org/10.1002/em.21855.
250. Acharya MM, Baddour AA, Kawashita T, Allen BD, Syage AR, Nguyen TH, Yoon N, Giedzinski E, Yu L, Parihar VK, Baulch JE. Epigenetic determinants of space radiation-induced cognitive dysfunction. Sci Rep. 2017;7:42885. https://doi.org/10.1038/srep42885.
251. Kostomitsopoulos NG, Durasevic SF. The ethical justification for the use of animals in biomedical research. Arch Biol Sci. 2010;62(3):783–9. https://doi.org/10.2298/Abs1003783k.
252. Russell WMS, Burch RL. The principles of humane experimental technique. Med J Aust. 1960;1(13):500. https://doi.org/10.5694/j.1326-5377.1960.tb73127.x.
253. Dubbs C. Space dogs: pioneers of space travel. Writer's Showcase. 2003. https://books.google.de/books?id=J_pCZVl-KzEC.
254. Burge S, Matin R, Wallis D. Structure and function of the skin. In: Oxford handbook of medical dermatology. Oxford University Press; 2016. p. 1–15. https://doi.org/10.1093/med/9780198747925.003.0001.
255. Hu S, Kim MH, McClellan GE, Cucinotta FA. Modeling the acute health effects of astronauts from exposure to large solar particle events. Health Phys. 2009;96(4):465–76. https://doi.org/10.1097/01.HP.0000339020.92837.61.
256. Hopewell JW. The skin: its structure and response to ionizing radiation. Int J Radiat Biol. 1990;57(4):751–73. https://doi.org/10.1080/09553009014550911.
257. Sanzari JK, Diffenderfer ES, Hagan S, Billings PC, Gridley DS, Seykora JT, Kennedy AR, Cengel KA. Dermatopathology effects of simulated solar particle event radiation exposure in the porcine model. Life Sci Space Res (Amst). 2015;6:21–8. https://doi.org/10.1016/j.lssr.2015.06.003.
258. Wilson JM, Sanzari JK, Diffenderfer ES, Yee SS, Seykora JT, Maks C, Ware JH, Litt HI, Reetz JA, McDonough J, Weissman D, Kennedy AR, Cengel KA. Acute biological effects of simulating the whole-body radiation dose distribution from a solar particle event using a porcine model. Radiat Res. 2011;176(5):649–59. https://doi.org/10.1667/rr2541.1.
259. Mao XW, Mekonnen T, Kennedy AR, Gridley DS. Differential expression of oxidative stress and extracellular matrix remodeling genes in low- or high-dose-rate photon-irradiated skin. Radiat Res. 2011;176(2):187–97. https://doi.org/10.1667/rr2493.1.
260. Marshall JS, Warrington R, Watson W, Kim HL. An introduction to immunology and immunopathology. Allergy Asthma Clin Immunol. 2018;14(Suppl 2):49. https://doi.org/10.1186/s13223-018-0278-1.
261. Crucian BE, Chouker A, Simpson RJ, Mehta S, Marshall G, Smith SM, Zwart SR, Heer M, Ponomarev S, Whitmire A, Frippiat JP, Douglas GL, Lorenzi H, Buchheim JI, Makedonas G, Ginsburg GS, Ott CM, Pierson DL, Krieger SS, et al. Immune system dysregulation during spaceflight: potential countermeasures for deep space exploration missions. Front Immunol. 2018;9:1437. https://doi.org/10.3389/fimmu.2018.01437.
262. Crucian B, Stowe RP, Mehta S, Quiriarte H, Pierson D, Sams C. Alterations in adaptive immunity persist during long-duration spaceflight [Original Paper]. NPJ Microgravity. 2015;1(1):15013. https://doi.org/10.1038/npjmgrav.2015.13.
263. Mehta SK, Crucian BE, Stowe RP, Simpson RJ, Ott CM, Sams CF, Pierson DL. Reactivation of latent viruses is associated with increased plasma cytokines in astronauts. Cytokine. 2013;61(1):205–9. https://doi.org/10.1016/j.cyto.2012.09.019.
264. Lewis ML, Cubano LA, Zhao B, Dinh HK, Pabalan JG, Piepmeier EH, Bowman PD. cDNA microarray reveals altered cytoskeletal gene expression in space-flown leukemic T lymphocytes (Jurkat). FASEB J. 2001;15(10):1783–5. https://doi.org/10.1096/fj.00-0820fje.
265. Fernandez-Gonzalo R, Baatout S, Moreels M. Impact of particle irradiation on the immune system: from the clinic to mars. Front Immunol. 2017;8:177. https://doi.org/10.3389/fimmu.2017.00177.
266. Pecaut MJ, Dutta-Roy R, Smith AL, Jones TA, Nelson GA, Gridley DS. Acute effects of iron-particle radiation on immunity. Part I: population distributions. Radiat Res. 2006;165(1):68–77. https://doi.org/10.1667/rr3493.1.
267. Sanzari JK, Wan XS, Muehlmatt A, Lin L, Kennedy AR. Comparison of changes over time in leukocyte counts in Yucatan minipigs irradiated with simulated solar particle event-like radiation. Life Sci Space Res (Amst). 2015;4:11–6. https://doi.org/10.1016/j.lssr.2014.12.002.
268. Alpen EL, Powers-Risius P, Curtis SB, DeGuzman R. Tumorigenic potential of high-Z, high-LET charged-particle radiations. Radiat Res. 1993;136(3):382–91. https://www.ncbi.nlm.nih.gov/pubmed/8278580.
269. Alpen EL, Powers-Risius P, Curtis SB, DeGuzman R, Fry RJ. Fluence-based relative biological effectiveness for charged particle carcinogenesis in mouse Harderian gland. Adv Space Res. 1994;14(10):573–81. https://doi.org/10.1016/0273-1177(94)90512-6.
270. Chang PY, Cucinotta FA, Bjornstad KA, Bakke J, Rosen CJ, Du N, Fairchild DG, Cacao E, Blakely EA. Harderian gland tumorigenesis: low-dose and LET response. Radiat Res. 2016;185(5):449–60. https://doi.org/10.1667/RR14335.1.
271. Huang EG, Wang RY, Xie L, Chang P, Yao G, Zhang B, Ham DW, Lin Y, Blakely EA, Sachs RK. Simulating galactic cosmic ray effects: synergy modeling of murine tumor prevalence after exposure to two one-ion beams in rapid sequence. Life Sci Space Res (Amst). 2020;25:107–18. https://doi.org/10.1016/j.lssr.2020.01.001.
272. Edmondson EF, Gatti DM, Ray FA, Garcia EL, Fallgren CM, Kamstock DA, Weil MM. Genomic mapping in outbred mice reveals overlap in genetic susceptibility for HZE ion- and gamma-ray-induced tumors. Sci Adv. 2020;6(16):eaax5940. https://doi.org/10.1126/sciadv.aax5940.
273. Imaoka T, Nishimura M, Daino K, Kokubo T, Doi K, Iizuka D, Nishimura Y, Okutani T, Takabatake M, Kakinuma S, Shimada Y. Influence of age on the relative biological effectiveness of carbon ion radiation for induction of rat mammary carcinoma. Int J Radiat Oncol Biol Phys. 2013;85(4):1134–40. https://doi.org/10.1016/j.ijrobp.2012.08.035.
274. Imaoka T, Nishimura M, Kakinuma S, Hatano Y, Ohmachi Y, Yoshinaga S, Kawano A, Maekawa A, Shimada Y. High relative biologic effectiveness of carbon ion radiation on induction of rat mammary carcinoma and its lack of H-ras and Tp53 mutations. Int J Radiat Oncol Biol Phys. 2007;69(1):194–203. https://doi.org/10.1016/j.ijrobp.2007.05.026.
275. Suman S, Kumar S, Moon BH, Fornace AJ Jr, Datta K. Low and high dose rate heavy ion radiation-induced intestinal and colonic tumorigenesis in APC(1638N/+) mice. Life Sci Space Res (Amst). 2017;13:45–50. https://doi.org/10.1016/j.lssr.2017.04.003.
276. Suman S, Kumar S, Moon BH, Strawn SJ, Thakor H, Fan Z, Shay JW, Fornace AJ Jr, Datta K. Relative biological effectiveness of energetic heavy ions for intestinal tumorigenesis shows male preponderance and radiation type and energy dependence in APC(1638N/+) mice. Int J Radiat Oncol Biol Phys. 2016;95(1):131–8. https://doi.org/10.1016/j.ijrobp.2015.10.057.
277. Weil MM, Bedford JS, Bielefeldt-Ohmann H, Ray FA, Genik PC, Ehrhart EJ, Fallgren CM, Hailu F, Battaglia CL, Charles B, Callan MA, Ullrich RL. Incidence of acute myeloid leukemia and hepatocellular carcinoma in mice irradiated with 1 GeV/nucleon (56) Fe ions. Radiat Res. 2009;172(2):213–9. https://doi.org/10.1667/RR1648.1.

278. Weil MM, Ray FA, Genik PC, Yu Y, McCarthy M, Fallgren CM, Ullrich RL. Effects of 28Si ions, 56Fe ions, and protons on the induction of murine acute myeloid leukemia and hepatocellular carcinoma. PLoS One. 2014;9(7):e104819. https://doi.org/10.1371/journal.pone.0104819.
279. Martincorena I, Fowler JC, Wabik A, Lawson ARJ, Abascal F, Hall MWJ, Cagan A, Murai K, Mahbubani K, Stratton MR, Fitzgerald RC, Handford PA, Campbell PJ, Saeb-Parsy K, Jones PH. Somatic mutant clones colonize the human esophagus with age. Science. 2018;362(6417):911–7. https://doi.org/10.1126/science.aau3879.
280. Major IR, Mole RH. Myeloid leukaemia in x-ray irradiated CBA mice. Nature. 1978;272(5652):455–6. https://doi.org/10.1038/272455a0.
281. Delgado O, Batten KG, Richardson JA, Xie XJ, Gazdar AF, Kaisani AA, Girard L, Behrens C, Suraokar M, Fasciani G, Wright WE, Story MD, Wistuba II, Minna JD, Shay JW. Radiation-enhanced lung cancer progression in a transgenic mouse model of lung cancer is predictive of outcomes in human lung and breast cancer. Clin Cancer Res. 2014;20(6):1610–22. https://doi.org/10.1158/1078-0432.CCR-13-2589.
282. Wang X, Farris Iii AB, Wang P, Zhang X, Wang H, Wang Y. Relative effectiveness at 1 gy after acute and fractionated exposures of heavy ions with different linear energy transfer for lung tumorigenesis. Radiat Res. 2015;183(2):233–9. https://doi.org/10.1667/RR13884.1.
283. Smits R, Kartheuser A, Jagmohan-Changur S, Leblanc V, Breukel C, de Vries A, van Kranen H, van Krieken JH, Williamson S, Edelmann W, Kucherlapati R, Khan PM, Fodde R. Loss of Apc and the entire chromosome 18 but absence of mutations at the Ras and Tp53 genes in intestinal tumors from Apc1638N, a mouse model for Apc-driven carcinogenesis. Carcinogenesis. 1997;18(2):321–7. https://doi.org/10.1093/carcin/18.2.321.
284. Haymaker W, Rubinstein LJ, Miquel J. Brain tumors in irradiated monkeys. Acta Neuropathol. 1972;20(4):267–77. https://doi.org/10.1007/BF00691745.
285. Camacho CV, Todorova PK, Hardebeck MC, Tomimatsu N, Gil del Alcazar CR, Ilcheva M, Mukherjee B, McEllin B, Vemireddy V, Hatanpaa K, Story MD, Habib AA, Murty VV, Bachoo R, Burma S. DNA double-strand breaks cooperate with loss of Ink4 and Arf tumor suppressors to generate glioblastomas with frequent Met amplification. Oncogene. 2015;34(8):1064–72. https://doi.org/10.1038/onc.2014.29.
286. Chappell LJ, Elgart SR, Milder CM, Semones EJ. Assessing nonlinearity in Harderian gland tumor induction using three combined HZE-irradiated mouse datasets. Radiat Res. 2020;194(1):38–51. https://doi.org/10.1667/RR15539.1.
287. Cucinotta FA, Manuel FK, Jones J, Iszard G, Murrey J, Djojonegro B, Wear M. Space radiation and cataracts in astronauts. Radiat Res. 2001;156(5 Pt 1):460–6. https://doi.org/10.1667/0033-7587(2001)156[0460:sracia]2.0.co;2.
288. Brenner DJ, Medvedovsky C, Huang Y, Worgul BV. Accelerated heavy particles and the lens. VIII. Comparisons between the effects of acute low doses of iron ions (190 keV/microns) and argon ions (88 keV/microns). Radiat Res. 1993;133(2):198–203. https://www.ncbi.nlm.nih.gov/pubmed/8438061.
289. Worgul BV. Cataract analysis and the assessment of radiation risk in space. Adv Space Res. 1986;6(11):285–93. https://doi.org/10.1016/0273-1177(86)90304-2.
290. Worgul BV, Medvedovsky C, Huang YP, Marino SA, RandersPehrson G, Brenner DJ. Quantitative assessment of the cataractogenic potential of very low doses of neutrons. Radiat Res. 1996;145(3):343–9. https://doi.org/10.2307/3578991.
291. Kleiman NJ, David J, Elliston CD, Hopkins KM, Smilenov LB, Brenner DJ, Worgul BV, Hall EJ, Lieberman HB. Mrad9 and atm haploinsufficiency enhance spontaneous and X-ray-induced cataractogenesis in mice. Radiat Res. 2007;168(5):567–73. https://doi.org/10.1667/rr1122.1.
292. Hall EJ, Brenner DJ, Worgul B, Smilenov L. Genetic susceptibility to radiation. Adv Space Res. 2005;35(2):249–53. https://doi.org/10.1016/j.asr.2004.12.032.
293. Hall EJ, Worgul BV, Smilenov L, Elliston CD, Brenner DJ. The relative biological effectiveness of densely ionizing heavy-ion radiation for inducing ocular cataracts in wild type versus mice heterozygous for the ATM gene. Radiat Environ Biophys. 2006;45(2):99–104. https://doi.org/10.1007/s00411-006-0052-5.
294. Martin DS, Lee SMC, Matz TP, Westby CM, Scott JM, Stenger MB, Platts SH. Internal jugular pressure increases during parabolic flight. Physiol Rep. 2016;4(24):e13068. https://doi.org/10.14814/phy2.13068.
295. Prisk GK, Guy HJ, Elliott AR, Deutschman RA, West JB. Pulmonary diffusing capacity, capillary blood volume, and cardiac output during sustained microgravity. J Appl Physiol. 1993;75(1):15–26. https://doi.org/10.1152/jappl.1993.75.1.15.
296. Gunga H-C, Ahlefeld VW, Appell Coriolano H-J, Werner A, Hoffmann U. Cardiovascular system, red blood cells, and oxygen transport in microgravity. 1st ed. 2016. http://lib.ugent.be/catalog/ebk01:3710000000751183.
297. Baran R, Marchal S, Garcia Campos S, Rehnberg E, Tabury K, Baselet B, Wehland M, Grimm D, Baatout S. The cardiovascular system in space: focus on in vivo and in vitro studies. Biomedicines. 2022;10(1):59. https://www.mdpi.com/2227-9059/10/1/59.
298. Yu T, Parks BW, Yu S, Srivastava R, Gupta K, Wu X, Khaled S, Chang PY, Kabarowski JH, Kucik DF. Iron-ion radiation accelerates atherosclerosis in apolipoprotein E-deficient mice. Radiat Res. 2011;175(6):766–773, 768. https://doi.org/10.1667/RR2482.1.
299. Chancellor JC, Scott GB, Sutton JP. Space radiation: the number one risk to astronaut health beyond low earth orbit. Life (Basel). 2014;4(3):491–510. https://doi.org/10.3390/life4030491.
300. Jandial R, Hoshide R, Waters JD, Limoli CL. Space-brain: the negative effects of space exposure on the central nervous system. Surg Neurol Int. 2018;9:9. https://doi.org/10.4103/sni.sni_250_17.
301. Lledo PM, Alonso M, Grubb MS. Adult neurogenesis and functional plasticity in neuronal circuits. Nat Rev Neurosci. 2006;7(3):179–93. https://doi.org/10.1038/nrn1867.
302. Rola R, Fishman K, Baure J, Rosi S, Lamborn KR, Obenaus A, Nelson GA, Fike JR. Hippocampal neurogenesis and neuroinflammation after cranial irradiation with (56)Fe particles. Radiat Res. 2008;169(6):626–32. https://doi.org/10.1667/RR1263.1.
303. Ulrich-Lai YM, Herman JP. Neural regulation of endocrine and autonomic stress responses. Nat Rev Neurosci. 2009;10(6):397–409. https://doi.org/10.1038/nrn2647.
304. Nelson GA. Space radiation: central nervous system risks. In: Young LR, Sutton JP, editors. Handbook of bioastronautics. Switzerland AG: Springer Nature; 2021. p. 313–27. https://doi.org/10.1007/978-3-319-12191-8_84.
305. Acharya MM, Baulch JE, Klein PM, Baddour AAD, Apodaca LA, Kramar EA, Alikhani L, Garcia C Jr, Angulo MC, Batra RS, Fallgren CM, Borak TB, Stark CEL, Wood MA, Britten RA, Soltesz I, Limoli CL. New concerns for neurocognitive function during deep space exposures to chronic, low dose-rate, neutron radiation. eNeuro. 2019;6(4) https://doi.org/10.1523/ENEURO.0094-19.2019. (In the article "New concerns for neurocognitive function during deep space exposures to chronic, low dose-rate, neutron radiation," by Munjal M. Acharya, Janet E. Baulch, Peter M. Klein, Al Anoud D. Baddour, Lauren A. Apodaca, Eniko A. Kramár, Leila Alikhani, Camillo Garcia Jr., Maria C. Angulo, Raja S. Batra, Christine M. Fallgren, Thomas B. Borak, Craig E. L. Stark, Marcello A. Wood, Richard A. Britten, Ivan Soltesz, and Charles L. Limoli, which was published online on August 5, 2019, a formula appeared incorrectly

due to a production error. Within the formula on page 4, ("x 00") should be corrected to ("x 100")).
306. Cherry JD, Liu B, Frost JL, Lemere CA, Williams JP, Olschowka JA, O'Banion MK. Galactic cosmic radiation leads to cognitive impairment and increased abeta plaque accumulation in a mouse model of Alzheimer's disease. PLoS One. 2012;7(12):e53275. https://doi.org/10.1371/journal.pone.0053275.
307. Guidetti R, Altiero T, Rebecchi L. On dormancy strategies in tardigrades. J Insect Physiol. 2011;57(5):567–76. https://doi.org/10.1016/j.jinsphys.2011.03.003.
308. Hygum TL, Clausen LKB, Halberg KA, Jørgensen A, Møbjerg N. Tun formation is not a prerequisite for desiccation tolerance in the marine tidal tardigrade Echiniscoides sigismundi. Zool J Linnean Soc. 2016;178(4):907–11. https://doi.org/10.1111/zoj.12444.
309. Marotta R, Leasi F, Uggetti A, Ricci C, Melone G. Dry and survive: morphological changes during anhydrobiosis in a bdelloid rotifer. J Struct Biol. 2010;171(1):11–7. https://doi.org/10.1016/j.jsb.2010.04.003.
310. Wright JC, Westh P, Ramløv H. Cryptobiosis in tardigrada. Biol Rev. 1992;67(1):1–29. https://doi.org/10.1111/j.1469-185X.1992.tb01657.x.
311. Rebecchi L, Altiero T, Guidetti R. Anhydrobiosis: the extreme limit of desiccation tolerance. Invertebr Surv J. 2007;4(2):65–81. <Go to ISI>://WOS:000456193200001.
312. Ricci C. Anhydrobiotic capabilities of bdelloid rotifers. Hydrobiologia. 1998;387:321–6. https://doi.org/10.1023/A:1017086425934.
313. Wright JC. Desiccation tolerance and water-retentive mechanisms in tardigrades. J Exp Biol. 1989;142(1):267–92. https://doi.org/10.1242/jeb.142.1.267.
314. Wright JC. The significance of four xeric parameters in the ecology of terrestrial Tardigrada. J Zool. 1991;224(1):59–77. https://doi.org/10.1111/j.1469-7998.1991.tb04788.x.
315. Jørgensen A, Møbjerg N, Kristensen R. A molecular study of the tardigrade Echiniscus testudo (Echiniscidae) reveals low DNA sequence diversity over a large geographical area. J Limnol. 2007;66 https://doi.org/10.4081/jlimnol.2007.s1.77.
316. Roszkowska M, Kmita H, Kaczmarek Ł. Long-term anhydrobiosis in two taxa of moss dwelling Eutardigrada (Tardigrada) desiccated for 12 and 15 years, respectively. Eur Zool J. 2020;87(1):642–7. https://doi.org/10.1080/24750263.2020.1829110.
317. Tsujimoto M, Imura S, Kanda H. Recovery and reproduction of an Antarctic tardigrade retrieved from a moss sample frozen for over 30 years. Cryobiology. 2016;72(1):78–81. https://doi.org/10.1016/j.cryobiol.2015.12.003.
318. Guidetti R, Jönsson KI. Long-term anhydrobiotic survival in semi-terrestrial micrometazoans. J Zool. 2002;257(2):181–7. https://doi.org/10.1017/S095283690200078X.
319. Shmakova L, Malavin S, Iakovenko N, Vishnivetskaya T, Shain D, Plewka M, Rivkina E. A living bdelloid rotifer from 24,000-year-old Arctic permafrost. Curr Biol. 2021;31(11):R712–3. https://doi.org/10.1016/j.cub.2021.04.077.
320. Shatilovich AV, Tchesunov AV, Neretina TV, Grabarnik IP, Gubin SV, Vishnivetskaya TA, Onstott TC, Rivkina EM. Viable nematodes from late pleistocene permafrost of the Kolyma river lowland. Doklady Biol Sci. 2018;480(1):100–2. https://doi.org/10.1134/S0012496618030079.
321. Guidetti R, Rizzo AM, Altiero T, Rebecchi L. What can we learn from the toughest animals of the Earth? Water bears (tardigrades) as multicellular model organisms in order to perform scientific preparations for lunar exploration. Planet Space Sci. 2012;74(1):97–102. https://doi.org/10.1016/j.pss.2012.05.021.
322. Jönsson KI. Radiation tolerance in tardigrades: current knowledge and potential applications in medicine. Cancers (Basel). 2019;11(9) https://doi.org/10.3390/cancers11091333.
323. Jönsson KI, Rabbow E, Schill RO, Harms-Ringdahl M, Rettberg P. Tardigrades survive exposure to space in low Earth orbit. Curr Biol. 2008;18(17):R729–31. https://doi.org/10.1016/j.cub.2008.06.048.
324. Krisko A, Leroy M, Radman M, Meselson M. Extreme antioxidant protection against ionizing radiation in bdelloid rotifers. Proc Natl Acad Sci. 2012;109(7):2354. https://doi.org/10.1073/pnas.1119762109.
325. Møbjerg N, Halberg KA, Jørgensen A, Persson D, Bjørn M, Ramløv H, Kristensen RM. Survival in extreme environments—on the current knowledge of adaptations in tardigrades. Acta Physiol. 2011;202(3):409–20. https://doi.org/10.1111/j.1748-1716.2011.02252.x
326. Neves RC, Hvidepil LKB, Sørensen-Hygum TL, Stuart RM, Møbjerg N. Thermotolerance experiments on active and desiccated states of Ramazzottius varieornatus emphasize that tardigrades are sensitive to high temperatures. Sci Rep. 2020;10(1):94. https://doi.org/10.1038/s41598-019-56965-z.
327. Seki K, Toyoshima M. Preserving tardigrades under pressure. Nature. 1998;395(6705):853–4. https://doi.org/10.1038/27576.
328. Murshed H. Chapter 3—Radiation biology. In: Murshed H, editor. Fundamentals of radiation oncology. 3rd ed. Academic Press; 2019. p. 57–87. https://doi.org/10.1016/B978-0-12-814128-1.00003-9.
329. Gladyshev E, Meselson M. Extreme resistance of bdelloid rotifers to ionizing radiation. Proc Natl Acad Sci. 2008;105(13):5139. https://doi.org/10.1073/pnas.0800966105.
330. Nilsson EJ, Jönsson KI, Pallon J. Tolerance to proton irradiation in the eutardigrade Richtersius coronifer—a nuclear microprobe study. Int J Radiat Biol. 2010;86(5):420–7. https://doi.org/10.3109/09553000903568001.
331. Beltrán-Pardo E, Jönsson KI, Harms-Ringdahl M, Haghdoost S, Wojcik A. Tolerance to gamma radiation in the tardigrade hypsibius dujardini from embryo to adult correlate inversely with cellular proliferation. PLoS One. 2015;10(7):e0133658. https://doi.org/10.1371/journal.pone.0133658.
332. Jönsson KI, Schill RO, Rabbow E, Rettberg P, Harms-Ringdahl M. The fate of the TARDIS offspring: no intergenerational effects of space exposure. Zool J Linnean Soc. 2016;178(4):924–30. https://doi.org/10.1111/zoj.12499.
333. Persson D, Halberg KA, Jørgensen A, Ricci C, Møbjerg N, Kristensen RM. Extreme stress tolerance in tardigrades: surviving space conditions in low earth orbit. J Zool Syst Evol Res. 2011;49(S1):90–7. https://doi.org/10.1111/j.1439-0469.2010.00605.x.
334. Rizzo AM, Altiero T, Corsetto PA, Montorfano G, Guidetti R, Rebecchi L. Space flight effects on antioxidant molecules in dry tardigrades: the TARDIKISS experiment. BioMed Res Int. 2015;2015:167642. https://doi.org/10.1155/2015/167642.
335. Rizzo AM, Negroni M, Altiero T, Montorfano G, Corsetto P, Berselli P, Berra B, Guidetti R, Rebecchi L. Antioxidant defences in hydrated and desiccated states of the tardigrade Paramacrobiotus richtersi. Comp Biochem Physiol B Biochem Mol Biol. 2010;156(2):115–21. https://doi.org/10.1016/j.cbpb.2010.02.009.
336. Chavez C, Cruz-Becerra G, Fei J, Kassavetis GA, Kadonaga JT. The tardigrade damage suppressor protein binds to nucleosomes and protects DNA from hydroxyl radicals. Elife. 2019;8 https://doi.org/10.7554/eLife.47682.
337. Hashimoto T, Horikawa DD, Saito Y, Kuwahara H, Kozuka-Hata H, Shin IT, Minakuchi Y, Ohishi K, Motoyama A, Aizu T, Enomoto A, Kondo K, Tanaka S, Hara Y, Koshikawa S, Sagara H, Miura T, Yokobori SI, Miyagawa K, et al. Extremotolerant tardigrade genome and improved radiotolerance of human cultured cells by tardigrade-unique protein. Nat Commun. 2016;7(1):12808. https://doi.org/10.1038/ncomms12808.
338. Mognato M, Girardi C, Fabris S, Celotti L. DNA repair in modeled microgravity: double strand break rejoining activity in human

lymphocytes irradiated with gamma-rays. Mutat Res. 2009;663(1–2):32–9. https://doi.org/10.1016/j.mrfmmm.2009.01.002.
339. De Micco V, Aronne G, Colla G, Fortezza R, De Pascale S. Agro-biology for bioregenerative life support systems in long-term space missions: general constraints and the Italian efforts. J Plant Interact. 2009;4(4):241–52. https://doi.org/10.1080/17429140903161348.
340. Paradiso R, De Micco V, Buonomo R, Aronne G, Barbieri G, De Pascale S. Soilless cultivation of soybean for Bioregenerative Life-Support Systems: a literature review and the experience of the MELiSSA Project—food characterisation phase I. Plant Biol (Stuttg). 2014;16(Suppl 1):69–78. https://doi.org/10.1111/plb.12056.
341. Wheeler RM, Mackowiak CL, Stutte GW, Sager JC, Yorio NC, Ruffe LM, Fortson RE, Dreschel TW, Knott WM, Corey KA. NASA's Biomass Production Chamber: a testbed for bioregenerative life support studies. Adv Space Res. 1996;18(4–5):215–24. https://doi.org/10.1016/0273-1177(95)00880-n.
342. Bates S, Gushin V, Bingham G, Vinokhodova A, Marquit J, Sychev V. Plants as countermeasures: a review of the literature and application to habitation systems for humans living in isolated or extreme environments. Habitation. 2009;12(1):33–40. https://doi.org/10.3727/154296610x12686999887201.
343. Williams D. Isolation and integrated testing: an introduction to the lunar-mars life support test project. Isolation—NASA experiments in closed-environment living, 104. 2002.
344. De Micco V, Arena C, Aronne G. Anatomical alterations of Phaseolus vulgaris L. mature leaves irradiated with X-rays. Plant Biol (Stuttg). 2014;16(Suppl 1):187–93. https://doi.org/10.1111/plb.12125.
345. De Micco V, Arena C, Pignalosa D, Durante M. Effects of sparsely and densely ionizing radiation on plants. Radiat Environ Biophys. 2011;50(1):1–19. https://doi.org/10.1007/s00411-010-0343-8.
346. Arena C, De Micco V, Macaeva E, Quintens R. Space radiation effects on plant and mammalian cells. Acta Astronaut. 2014;104(1):419–31. https://doi.org/10.1016/j.actaastro.2014.05.005.
347. Wang W, Gorsuch JW, Hughes JS. Plants for environmental studies. CRC Press; 2020. https://books.google.be/books?id=zc79DwAAQBAJ.
348. Brodribb TJ. Xylem hydraulic physiology: the functional backbone of terrestrial plant productivity. Plant Sci. 2009;177(4):245–51. https://doi.org/10.1016/j.plantsci.2009.06.001.
349. Chiara A. Leaf morpho-anatomical traits in Vigna radiata L. affect plant photosynthetic acclimation to changing vapor pressure deficit. Environ Exp Bot. 2021;186(9):104453–102021, 104186. https://doi.org/10.1016/j.envexpbot.2021.104453. (Opyt izucheniia mneniia naseleniia o kachestve lechebno-profilakticheskogo obsluzhivaniia)
350. Cheng TS, Chandlee JM. The structural, biochemical, and genetic characterization of a new radiation-induced, variegated leaf mutant of soybean [Glycine max (L.) Merr]. Proc Natl Sci Counc Rep China B. 1999;23(1):27–37. https://www.ncbi.nlm.nih.gov/pubmed/9949722.
351. Mei M, Qiu Y, Sun Y, Huang R, Yao J, Zhang Q, Hong M, Ye J. Morphological and molecular changes of maize plants after seeds been flown on recoverablf satellite. Adv Space Res. 1998;22(12):1691–7. https://doi.org/10.1016/s0273-1177(99)00034-4.
352. Rea G, Esposito D, Damasso M, Serafini A, Margonelli A, Faraloni C, Torzillo G, Zanini A, Bertalan I, Johanningmeier U, Giardi MT. Ionizing radiation impacts photochemical quantum yield and oxygen evolution activity of Photosystem II in photosynthetic microorganisms. Int J Radiat Biol. 2008;84(11):867–77. https://doi.org/10.1080/09553000802460149.
353. Arena C, De Micco V, Aronne G, Pugliese M, De Santo AV, De Maio A. Response of Phaseolus vulgaris L. plants to low-let ionizing radiation: growth and oxidative stress. Acta Astronaut. 2013;91:107–14. https://doi.org/10.1016/j.actaastro.2013.05.013.
354. Esnault MA, Legue F, Chenal C. Ionizing radiation: advances in plant response. Environ Exp Bot. 2010;68(3):231–7. https://doi.org/10.1016/j.envexpbot.2010.01.007.
355. Zaka R, Vandecasteele CM, Misset MT. Effects of low chronic doses of ionizing radiation on antioxidant enzymes and G6PDH activities in Stipa capillata (Poaceae). J Exp Bot. 2002;53(376):1979–87. https://doi.org/10.1093/jxb/erf041.
356. Nagle PW, Coppes RP. Current and future perspectives of the use of organoids in radiobiology. Cells. 2020;9(12) https://doi.org/10.3390/cells9122649.
357. Schielke C, Hartel C, Durante M, Ritter S, Schroeder IS. Solving the issue of ionizing radiation induced neurotoxicity by using novel cell models and state of the art accelerator facilities [Review]. Front Phys. 2020;8(417):568027. https://doi.org/10.3389/fphy.2020.568027.
358. Białkowska K, Komorowski P, Bryszewska M, Miłowska K. Spheroids as a type of three-dimensional cell cultures—examples of methods of preparation and the most important application. Int J Mol Sci. 2020;21(17):6225. https://www.mdpi.com/1422-0067/21/17/6225.
359. Kruger M, Pietsch J, Bauer J, Kopp S, Carvalho DTO, Baatout S, Moreels M, Melnik D, Wehland M, Egli M, Jayashree S, Kobbero SD, Corydon TJ, Nebuloni S, Gass S, Evert M, Infanger M, Grimm D. Growth of endothelial cells in space and in simulated microgravity—a comparison on the secretory level. Cell Physiol Biochem. 2019;52(5):1039–60. https://doi.org/10.33594/000000071.
360. Humpel C. Organotypic brain slice cultures: a review. Neuroscience. 2015;305:86–98. https://doi.org/10.1016/j.neuroscience.2015.07.086.
361. Kloker LD, Yurttas C, Lauer UM. Three-dimensional tumor cell cultures employed in virotherapy research. Oncol Virother. 2018;7:79–93. https://doi.org/10.2147/OV.S165479.
362. Blakely EA, Chang PY. Late effects of space radiation: cataracts. In: Young LR, Sutton JP, editors. Handbook of bioastronautics. Springer International Publishing; 2021. p. 277–86. https://doi.org/10.1007/978-3-319-12191-8_87.
363. Chylack LT Jr, Peterson LE, Feiveson AH, Wear ML, Manuel FK, Tung WH, Hardy DS, Marak LJ, Cucinotta FA. NASA study of cataract in astronauts (NASCA). Report 1: cross-sectional study of the relationship of exposure to space radiation and risk of lens opacity. Radiat Res. 2009;172(1):10–20. https://doi.org/10.1667/RR1580.1.
364. Cubo-Mateo N, Podhajsky S, Knickmann D, Slenzka K, Ghidini T, Gelinsky M. Can 3D bioprinting be a key for exploratory missions and human settlements on the Moon and Mars? Biofabrication. 2020;12(4):043001. https://doi.org/10.1088/1758-5090/abb53a.
365. Ghidini T. Regenerative medicine and 3D bioprinting for human space exploration and planet colonisation. J Thorac Dis. 2018;10(Suppl 20):S2363–75. https://doi.org/10.21037/jtd.2018.03.19.
366. Milojevic T, Weckwerth W. Molecular mechanisms of microbial survivability in outer space: a systems biology approach. Front Microbiol. 2020;11:923. https://doi.org/10.3389/fmicb.2020.00923.
367. Ott E, Kawaguchi Y, Kolbl D, Rabbow E, Rettberg P, Mora M, Moissl-Eichinger C, Weckwerth W, Yamagishi A, Milojevic T. Molecular repertoire of Deinococcus radiodurans after 1 year of exposure outside the International Space Station within the Tanpopo mission. Microbiome. 2020;8(1):150. https://doi.org/10.1186/s40168-020-00927-5.
368. Mastroleo F, Van Houdt R, Leroy B, Benotmane MA, Janssen A, Mergeay M, Vanhavere F, Hendrickx L, Wattiez R, Leys N. Experimental design and environmental parameters affect Rhodospirillum rubrum S1H response to space flight. ISME J. 2009;3(12):1402–19. https://doi.org/10.1038/ismej.2009.74.

369. Wilson JW, Ott CM, Quick L, Davis R, Honer Zu Bentrup K, Crabbe A, Richter E, Sarker S, Barrila J, Porwollik S, Cheng P, McClelland M, Tsaprailis G, Radabaugh T, Hunt A, Shah M, Nelman-Gonzalez M, Hing S, Parra M, et al. Media ion composition controls regulatory and virulence response of Salmonella in spaceflight. PLoS One. 2008;3(12):e3923. https://doi.org/10.1371/journal.pone.0003923.
370. Nicholson WL, Moeller R, Team P, Horneck G. Transcriptomic responses of germinating Bacillus subtilis spores exposed to 1.5 years of space and simulated martian conditions on the EXPOSE-E experiment PROTECT. Astrobiology. 2012;12(5):469–86. https://doi.org/10.1089/ast.2011.0748.
371. Vaishampayan PA, Rabbow E, Horneck G, Venkateswaran KJ. Survival of Bacillus pumilus spores for a prolonged period of time in real space conditions. Astrobiology. 2012;12(5):487–97. https://doi.org/10.1089/ast.2011.0738.
372. Ott E, Kawaguchi Y, Kolbl D, Chaturvedi P, Nakagawa K, Yamagishi A, Weckwerth W, Milojevic T. Proteometabolomic response of Deinococcus radiodurans exposed to UVC and vacuum conditions: initial studies prior to the Tanpopo space mission. PLoS One. 2017;12(12):e0189381. https://doi.org/10.1371/journal.pone.0189381.
373. da Silveira WA, Fazelinia H, Rosenthal SB, Laiakis EC, Kim MS, Meydan C, Kidane Y, Rathi KS, Smith SM, Stear B, Ying Y, Zhang Y, Foox J, Zanello S, Crucian B, Wang D, Nugent A, Costa HA, Zwart SR, et al. Comprehensive multi-omics analysis reveals mitochondrial stress as a central biological hub for spaceflight impact. Cell. 2020;183(5):1185–1201 e1120. https://doi.org/10.1016/j.cell.2020.11.002.
374. Cortese F, Klokov D, Osipov A, Stefaniak J, Moskalev A, Schastnaya J, Cantor C, Aliper A, Mamoshina P, Ushakov I, Sapetsky A, Vanhaelen Q, Alchinova I, Karganov M, Kovalchuk O, Wilkins R, Shtemberg A, Moreels M, Baatout S, et al. Vive la radioresistance!: converging research in radiobiology and biogerontology to enhance human radioresistance for deep space exploration and colonization. Oncotarget. 2018;9(18):14692–722. https://doi.org/10.18632/oncotarget.24461.
375. Puspitasari A, Cerri M, Takahashi A, Yoshida Y, Hanamura K, Tinganelli W. Hibernation as a tool for radiation protection in space exploration. Life (Basel). 2021;11(1) https://doi.org/10.3390/life11010054.
376. Zhang X, Epperly MW, Kay MA, Chen ZY, Dixon T, Franicola D, Greenberger BA, Komanduri P, Greenberger JS. Radioprotection in vitro and in vivo by minicircle plasmid carrying the human manganese superoxide dismutase transgene. Hum Gene Ther. 2008;19(8):820–6. https://doi.org/10.1089/hum.2007.141.
377. Frosina G. Overexpression of enzymes that repair endogenous damage to DNA. Eur J Biochem. 2000;267(8):2135–49. https://doi.org/10.1046/j.1432-1327.2000.01266.x.
378. Seckbach J, Oren A, Stan-Lotter H. Polyextremophiles: life under multiple forms of stress, vol. 27. Springer Science & Business Media; 2013.
379. Baltschukat K, Horneck G. Responses to accelerated heavy ions of spores of Bacillus subtilis of different repair capacity. Radiat Environ Biophys. 1991;30(2):87–103. https://doi.org/10.1007/bf01219343.
380. Moeller R, Setlow P, Reitz G, Nicholson WL. Roles of small, acid-soluble spore proteins and core water content in survival of Bacillus subtilis spores exposed to environmental solar UV radiation. Appl Environ Microbiol. 2009;75(16):5202–8. https://doi.org/10.1128/aem.00789-09.
381. Jönsson KI, Harms-Ringdahl M, Torudd J. Radiation tolerance in the eutardigrade Richtersius coronifer. Int J Radiat Biol. 2005;81(9):649–56. https://doi.org/10.1080/09553000500368453.
382. Horneck G. Responses of Bacillus subtilis spores to space environment: results from experiments in space. Orig Life Evol Biosph. 1993;23(1):37–52. https://doi.org/10.1007/bf01581989.
383. Baqué M, Scalzi G, Rabbow E, Rettberg P, Billi D. Biofilm and planktonic lifestyles differently support the resistance of the desert cyanobacterium chroococcidiopsis under space and martian simulations. Origins Life Evol Biospheres. 2013;43(4):377–89. https://doi.org/10.1007/s11084-013-9341-6.
384. Gérard E, Jolivet E, Prieur D, Forterre P. DNA protection mechanisms are not involved in the radioresistance of the hyperthermophilic archaea Pyrococcus abyssi and P. furiosus. Mol Genet Genomics. 2001;266(1):72–8. https://doi.org/10.1007/s004380100520.
385. Daly MJ, Gaidamakova EK, Matrosova VY, Vasilenko A, Zhai M, Venkateswaran A, Hess M, Omelchenko MV, Kostandarithes HM, Makarova KS, Wackett LP, Fredrickson JK, Ghosal D. Accumulation of Mn(II) in Deinococcus radiodurans facilitates gamma-radiation resistance. Science. 2004;306(5698):1025–8. https://doi.org/10.1126/science.1103185.
386. Leuko S, Rettberg P. The effects of HZE particles, γ and X-ray radiation on the survival and genetic integrity of Halobacterium salinarum NRC-1, Halococcus hamelinensis, and Halococcus morrhuae. Astrobiology. 2017;17(2):110–7. https://doi.org/10.1089/ast.2015.1458.
387. Webb KM, DiRuggiero J. Role of Mn2+ and compatible solutes in the radiation resistance of thermophilic bacteria and archaea. Archaea. 2012;2012:845756. https://doi.org/10.1155/2012/845756.
388. Zerulla K, Soppa J. Polyploidy in haloarchaea: advantages for growth and survival [Review]. Front Microbiol. 2014;5:274. https://doi.org/10.3389/fmicb.2014.00274.
389. Kish A, Kirkali G, Robinson C, Rosenblatt R, Jaruga P, Dizdaroglu M, DiRuggiero J. Salt shield: intracellular salts provide cellular protection against ionizing radiation in the halophilic archaeon, Halobacterium salinarum NRC-1. Environ Microbiol. 2009;11(5):1066–78. https://doi.org/10.1111/j.1462-2920.2008.01828.x.
390. Pathak J, Pandey A, Maurya PK, Rajneesh R, Sinha RP, Singh SP. Cyanobacterial secondary metabolite scytonemin: a potential photoprotective and pharmaceutical compound. Proc Natl Acad Sci India B Biol Sci. 2020;90(3):467–81.
391. Shahmohammadi HR, Asgarani E, Terato H, Saito T, Ohyama Y, Gekko K, Yamamoto O, Ide H. Protective roles of bacterioruberin and intracellular KCl in the resistance of Halobacterium salinarium against DNA-damaging agents. J Radiat Res. 1998;39(4):251–62. https://doi.org/10.1269/jrr.39.251.
392. Beblo-Vranesevic K, Bohmeier M, Perras AK, Schwendner P, Rabbow E, Moissl-Eichinger C, Cockell CS, Vannier P, Marteinsson VT, Monaghan EP, Ehrenfreund P, Garcia-Descalzo L, Gómez F, Malki M, Amils R, Gaboyer F, Westall F, Cabezas P, Walter N, Rettberg P. Lack of correlation of desiccation and radiation tolerance in microorganisms from diverse extreme environments tested under anoxic conditions. FEMS Microbiol Lett. 2018;365(6) https://doi.org/10.1093/femsle/fny044.
393. Beblo-Vranesevic K, Galinski EA, Rachel R, Huber H, Rettberg P. Influence of osmotic stress on desiccation and irradiation tolerance of (hyper)-thermophilic microorganisms. Arch Microbiol. 2017;199(1):17–28. https://doi.org/10.1007/s00203-016-1269-6.
394. Beblo K, Douki T, Schmalz G, Rachel R, Wirth R, Huber H, Reitz G, Rettberg P. Survival of thermophilic and hyperthermophilic microorganisms after exposure to UV-C, ionizing radiation and desiccation. Arch Microbiol. 2011;193(11):797–809. https://doi.org/10.1007/s00203-011-0718-5.
395. Koschnitzki D, Moeller R, Leuko S, Przybyla B, Beblo-Vranesevic K, Wirth R, Huber H, Rachel R, Rettberg P. Questioning the radia-

tion limits of life: Ignicoccus hospitalis between replication and VBNC. Arch Microbiol. 2021;203(4):1299–308. https://doi.org/10.1007/s00203-020-02125-1.
396. Simonsen LC, Slaba TC, Guida P, Rusek A. NASA's first ground-based Galactic Cosmic Ray Simulator: enabling a new era in space radiobiology research. PLOS Biol. 2020;18(5):e3000669. https://doi.org/10.1371/journal.pbio.3000669.
397. ESA. Materials & Electrical Components Laboratory. ESA. 2021. Retrieved Dec 2021 from https://www.esa.int/Enabling_Support/Space_Engineering_Technology/Materials_Electrical_Components_Laboratory.
398. Takahashi A, Yamanouchi S, Takeuchi K, Takahashi S, Tashiro M, Hidema J, Higashitani A, Adachi T, Zhang S, Guirguis FNL, Yoshida Y, Nagamatsu A, Hada M, Takeuchi K, Takahashi T, Sekitomi Y. Combined environment simulator for low-dose-rate radiation and partial gravity of moon and Mars. Life (Basel). 2020;10(11):274. https://doi.org/10.3390/life10110274.
399. Durante M, Golubev A, Park W-Y, Trautmann C. Applied nuclear physics at the new high-energy particle accelerator facilities. Phys Rep. 2019;800:1–37. https://doi.org/10.1016/j.physrep.2019.01.004.
400. Michael W, Joel SB, Helle B-O, Ray FA, Paula CG, Eugene JE, Christina MF, Fitsum H, Christine LRB, Brad C, Matthew AC, Robert LU. Incidence of acute myeloid leukemia and hepatocellular carcinoma in mice irradiated with 1 GeV/nucleon ⁵⁶Fe ions. Radiat Res. 2009;172(2):213–9. https://doi.org/10.1667/RR1648.1.
401. Parihar VK, Allen BD, Caressi C, Kwok S, Chu E, Tran KK, Chmielewski NN, Giedzinski E, Acharya MM, Britten RA, Baulch JE, Limoli CL. Cosmic radiation exposure and persistent cognitive dysfunction. Sci Rep. 2016;6(1):34774. https://doi.org/10.1038/srep34774.
402. Reiser M. Theory and design of charged particle beams. John Wiley & Sons; 2008.
403. Rabbow E, Rettberg P, Barczyk S, Bohmeier M, Parpart A, Panitz C, Horneck G, von Heise-Rotenburg R, Hoppenbrouwers T, Willnecker R, Baglioni P, Demets R, Dettmann J, Reitz G. EXPOSE-E: an ESA astrobiology mission 1.5 years in space. Astrobiology. 2012;12(5):374–86. https://doi.org/10.1089/ast.2011.0760.
404. Haefer RA. Vacuum and cryotechniques in space research. Vacuum. 1972;22(8):303. https://doi.org/10.1016/0042-207x(72)93789-X.
405. Rabbow E, Parpart A, Reitz G. The planetary and space simulation facilities at DLR Cologne. Micrograv Sci Technol. 2016;28(3):215–29. https://doi.org/10.1007/s12217-015-9448-7.
406. Rabbow E, Rettberg P, Barczyk S, Bohmeier M, Parpart A, Panitz C, Horneck G, Burfeindt J, Molter F, Jaramillo E, Pereira C, Weiss P, Willnecker R, Demets R, Dettmann J, Reitz G. The astrobiological mission EXPOSE-R on board of the International Space Station. Int J Astrobiol. 2015;14(1):3–16. https://doi.org/10.1017/S1473550414000202.

Further Reading

Airbus Space Systems. University of Zurich and Airbus grow miniature human tissue on the International Space Station ISS. In: Airbus Newsroom. Aug 2021. https://www.airbus.com/en/newsroom.
Cekanaviciute E, et al. Central nervous system responses to simulated galactic cosmic rays. Int J Mol Sci. 2018;19(11):3669.
European Space Agency. 3D bioprinting for space. In: ESA media. Nov 2018. https://www.esa.int/ESA_Multimedia.
European Space Agency. Upside-down 3D-printed skin and bone, for humans to Mars. In: ESA enabling and support. Jul 2019. https://www.esa.int/Enabling_Support.
Furukawa S, et al. Space radiation biology for "Living in Space". Biomed Res Int. 2020;2020:4703286.
Gray T. A brief history of animals in space. In: NASA history archives. Aug 2004. https://history.nasa.gov/animals.html.
Hellweg CE, Berger T, Matthiä D, Baumstark-Khan C. Radiation in space: relevance and risk for human missions. Springer International Publishing; 2020.
Horneck G, et al. Space microbiology. Microbiol Mol Biol Rev. 2010;74(1):121–56.
Limoli C. Space brain: the adverse impact of deep space radiation exposure on the brain. In: Space physiology: to Mars and beyond, vol. 117. The Physiology Society; 2020.
Nelson GA. Space radiation: central nervous system risks. In: Young LR, Sutton JP, editors. Handbook of bioastronautics. Cham: Springer; 2021.
Senatore G, Mastroleo F, Leys N, Mauriello G. Effect of microgravity & space radiation on microbes. Fut Microbiol. 2018;13:831–47.
Sgobba T, Kanki B, Clervoy J-F, Sandal GM. Space safety and human performance. Butterworth-Heinemann; 2018.
Sims J. Why astronauts are printing organs in space. In: BBC Future. Jun 2021. https://www.bbc.com/future.
The Royal Museums Greenwich. What was the first animal sent into space? In: Royal Museums Greenwich Stories. 2022. https://www.rmg.co.uk/stories

Open Access This chapter is licensed under the terms of the Creative Commons Attribution 4.0 International License (http://creativecommons.org/licenses/by/4.0/), which permits use, sharing, adaptation, distribution and reproduction in any medium or format, as long as you give appropriate credit to the original author(s) and the source, provide a link to the Creative Commons license and indicate if changes were made.

The images or other third party material in this chapter are included in the chapter's Creative Commons license, unless indicated otherwise in a credit line to the material. If material is not included in the chapter's Creative Commons license and your intended use is not permitted by statutory regulation or exceeds the permitted use, you will need to obtain permission directly from the copyright holder.